POLAR TIP GROWTH OF *ASPERGILLUS NIDULANS*

by

XIAORONG LIN

(Under the direction of Michelle Momany)

ABSTRACT

Upon germination, filamentous fungi grow mainly by tip extension after brief isotropic expansion. This dissertation uses *Aspergillus nidulans* as a model organism to study genes that are involved in polar growth by a forward genetics approach. Two temperature sensitive mutants, *swoC1* and *swoH1*, defective in polarity establishment and maintenance were characterized. Both genes were genetically mapped and cloned. The *swoC* gene encodes an rRNA pseudouridine synthase (AnCBF5) and the *swoH* gene encodes a nucleoside diphosphate kinase (NDK). Null mutants of *swoC* and *swoH* genes were lethal in *A. nidulans*. Although both genes have been considered housekeeping genes, recent evidence from this and other studies suggests that they have more complex roles. Possible biological functions of SwoCp in nuclear positioning and polarity establishment, and SwoHp in stress attenuation in *Aspergillus nidulans* are discussed.

INDEX WORDS: polar growth, nuclear distribution, stress response

POLAR TIP GROWTH OF *ASPERGILLUS NIDULANS*

by

XIAORONG LIN

B.E., Dalian University of Technology, China, 1996

M.E., Dalian Institute of Chemical and Physics, China, 1999

A Dissertation Submitted to the Graduate Faculty of The University of Georgia in Partial Fulfillment of the Requirements for the Degree

DOCTOR OF PHILOSOPHY

ATHENS, GEORGIA

2003

POLAR TIP GROWTH OF *ASPERGILLUS NIDULANS*

by

XIAORONG LIN

Major Professor:	Michelle Momany
Committee:	Sarah Covert Alan Darvill Scott Gold Zheng-Hua Ye

Electronic Version Approved:

Maureen Grasso
Dean of the Graduate School
The University of Georgia
May 2003

ACKNOWLEDGMENTS

I would like to acknowledge the support of my major advisor Michelle Momany, and my committee members: Sarah Covert, Scott Gold, Alan Darvill, and Zheng-Hua Ye. I would also like to thank my friends: Brain Shaw, Suneng Fu, Patrick Westfall, Gretel Guest, Elizabeth Richardson and Glenn Freshour.

TABLE OF CONTENTS

Page

CHAPTER 1

INTRODUCTION AND LITERATURE REVIEW

A challenge in developmental biology is to understand how asymmetries are established and maintained. Asymmetric growth or polar growth is essential for all organisms from bacteria to human beings and is involved in various cellular processes such as differentiation, mating, pathogenicity, molecule transport, cell migration, and cytokinesis (Dickson 2002; Keller 2002; Pellettieri and Seydoux 2002; Shapiro *et al.* 2002). The timely expression and localization of membrane proteins, signaling molecules and cytoskeleton components responding to internal and external cues, makes cellular asymmetric growth possible (Pruyne and Bretscher 2000a; Pruyne and Bretscher 2000b; Dickson 2002; Keller 2002; Pellettieri and Seydoux 2002; Shapiro *et al.* 2002). Filamentous fungi, like nerve cells, root hairs, and pollen tubes, take polar growth to the extreme (Momany *et al.* 1999; Momany and Taylor 2000; Wendland 2001). When spores of the filamentous fungus *Aspergillus nidulans* break dormancy, they expand isotropically before switching to polar tip extension. Afterwards, new growth occurs exclusively at the hyphal tip of the germ tube. The secondary germ tube usually emerges later in a bipolar pattern in wild-type *Aspergillus nidulans* (Harris *et al.* 1999; Momany and Taylor 2000). After septation (hyphal compartmentation), only the tip cells are mitotically active and continue elongating until branch initiation generates new tip growth, which is essential for the maintenance of exponential growth in filamentous fungi (Trinci 1979).

In the work described in this dissertation, *Aspergillus nidulans* was used as a model organism to study polar growth. *Aspergillus nidulans* is a saprobic homothallic Ascomycete. It has asexual, parasexual and sexual life cycles. Asexual reproduction generates thousands of conidia on each conidiophore. Sexual reproduction occurs in a closed ascospore-bearing fruitbody called a cleistothecium. The parasexual life cycle occurs when two hyphae fuse to produce a diploid strain that then undergoes haploidization without meiosis to produce a haploid strain (Figure 1.1). These processes were utilized in mapping and generating the desired strains in the work described here. Moreover, transformation and homologous integration of foreign DNA is relatively easy in this filamentous fungus which makes *A. nidulans* tractable for molecular biology studies. The whole genome sequence of *Aspergillus nidulans* is now available to the public (http://microbial.cereon.com/) and both the genetic and physical map of all eight chromosomes are also available through the Fungal Genetics and Stock Center (http://www.fgsc.net). These factors make *Aspergillus nidulans* an ideal organism for classical genetics and modern biological study.

Polarity genes in filamentous fungi are proposed to fall into two categories (Momany *et al.* 1999): those responsible for establishing a location where a germ tube will emerge (polarity establishment genes), and those responsible for maintaining this directed polar growth (polarity maintenance genes). In this work, we use a forward genetics approach to study polar growth in *A. nidulans*. Two temperature-sensitive mutants of *A. nidulans, swoC1* and *swoH1*, were isolated based on their isotropic (swollen) phenotype in a screen to identify genes involved in polar growth (Momany *et al.* 1999).

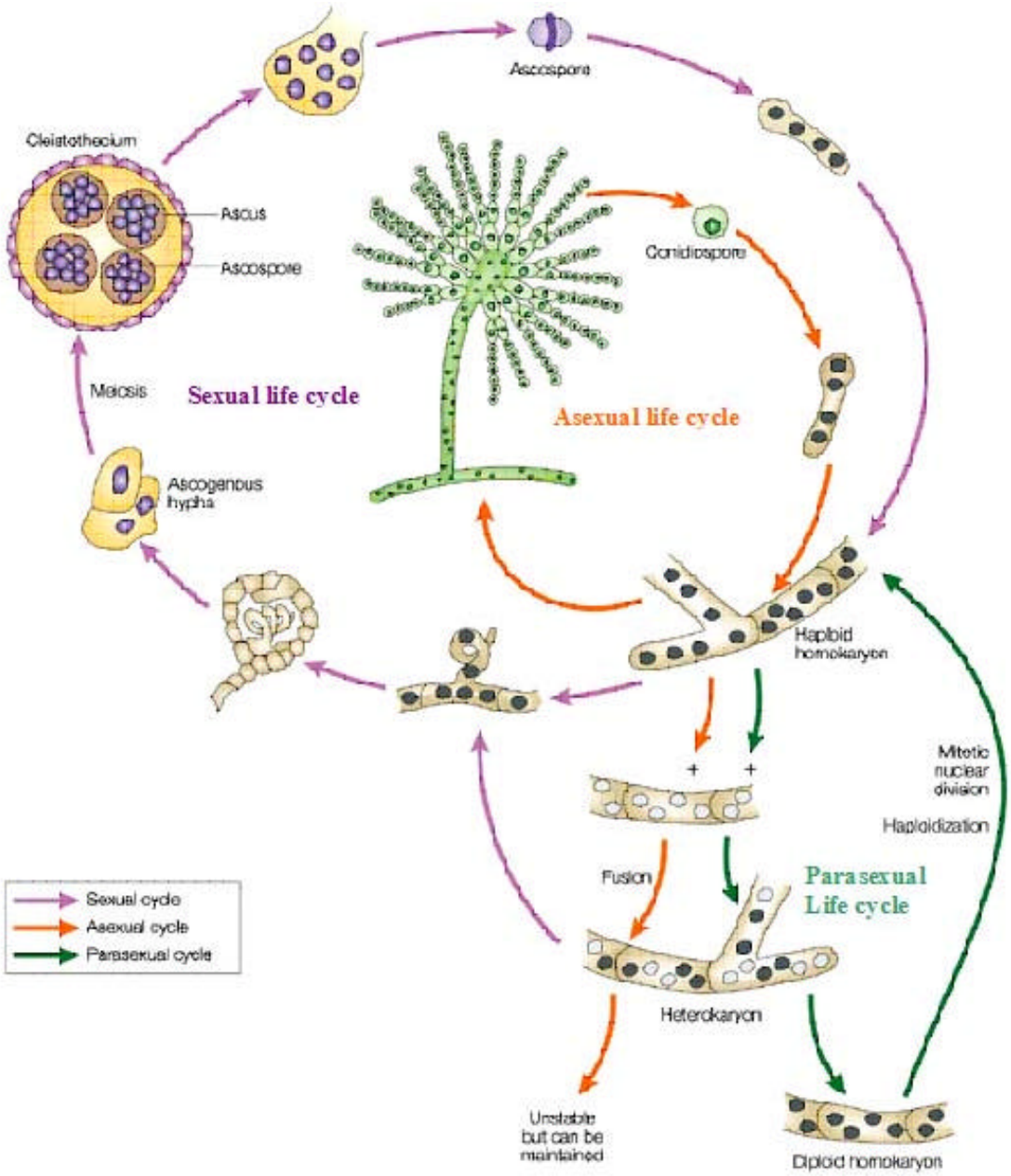

Figure 1.1. Life cycle of *Aspergillus nidulans.* Asexual cycle: vegetative mycelium is produced asexually by conidiation on a structure called a conidiophore (indicated by yellow). Sexual cycle: two haploid nuclei fuse, the diploid nucleus undergoes meiosis, and a subsequent mitosis yields eight haploid ascospores, which occur in the fruiting body called the cleistothecium (indicated by purple). Parasexual cycle: two hyphae fuse forming a heterokaryon, which is stable but can be induced to haploidize (indicated by green).
This picture is taken from
http://www.nature.com/nrg/journal/v3/n9/slideshow/nrg889_bx1.html

The *swoC1* mutant is not able to establish polarity but is able to maintain polarity at restrictive temperature (Momany *et al.* 1999). The *swoH1* mutant is not able to maintain polarity at restrictive temperature (Momany *et al.* 1999).

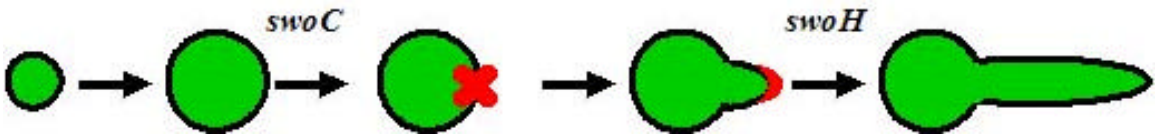

Figure 1.2. Model of polarity establishment and maintenance in *A. nidulans*. Red "x" indicates the site of germ tube emergence. Red represents areas of new growth.

In *Saccharomyces cerevisiae*, where extensive study on polarity has been done, genes responsible for polarity generation and maintenance include CDC42, cytoskeleton genes, G-protein and *BUD* genes (see review Chant 1999). To further study the *swoC1* and *swoH1* mutants, both genes were mapped to a specific chromosome by mitotic mapping and their positions on the chromosomes were refined by meiotic mapping. The genes were cloned by complementation of the temperature sensitive phenotype. Surprisingly, the *swoC* gene encodes a homologue of yeast Cbf5p, a pseudouridine synthase responsible for isomerization of uridine (U) to pseudouridine (?) in rRNA (Lafontaine *et al.* 1998; Watkins *et al.* 1998; Zebarjadian *et al.* 1999; Watanabe and Gray 2000); the *swoH* gene encodes a nucleoside diphosphate kinase responsible for making the majority of cellular nucleoside triphosphates except ATP (Agarwal *et al.* 1978).

How SwoCp, the rRNA pseudouridine synthase is involved in polar growth is still unclear. In eukaryotes, isomerization of uridine (U) to pseudouridine (?) is one of the most abundant post-transcriptional modifications of rRNA prior to production of mature 18S, 5.8S, and 28S rRNAs (reviewed by Charette and Gray 2000). The biological role of pseudouridine is not yet clear. Recent evidence suggests that ? is not essential for

ribosomal functions (Ofengand *et al.* 1995; Gutgsell *et al.* 2000; Gutgsell *et al.* 2001). Yeast depleted of virtually all ? residues in rRNA are viable (Bousquet-Antonelli *et al.* 1997). Nonetheless, deletion of *CBF5* is lethal (Ganot *et al.* 1997) suggesting that Cbf5p must have functions essential for cell survival other than pseudouridine synthesis. The human homologue Dkc1p binds hTR (the RNA component of human telomerase complex) and plays an important role in telomere maintenance (Marciniak *et al.* 2000; Dez *et al.* 2001). Mutations of *DKC1* cause X-linked recessive Dyskeratosis Congenita (Heiss *et al.* 1998) and Hoyeraal-Hreidarsson syndrome (Yaghmai *et al.* 2000).

In Chapter 2, I show that the *swoC1* mutant had defects in endocytosis, compartmentation, and conidiation. These mutant phenotypes are likely downstream of SwoCp's involvement in nuclear distribution. The *swoC1* mutant was still able to make rRNA pseudouridines and rRNA processing appeared normal. While deletion of the *swoC* gene was lethal in *A. nidulans,* the C-terminal portion was dispensable. I hypothesized that the SwoCp may function as a nuclear signal (likely by its products) for the growth switch from isotropic to polar and the PUA domain (RNA binding domain) is essential for this function.

In Chapter 3, the SwoHp is identified as the nucleoside diphosphate kinase (NDK), a homologue of yeast YNK1. NDKs catalyze the transfer of the ?-phosphate from a nucleoside triphosphate to a nucleoside diphosphate and are important in nucleotide metabolism (Agarwal *et al.* 1978). NDK null mutants of *Escherichia coli* and *Pseudomonas aeruginosa* are viable (Izumiya and Yamamoto 1995; Zaborina *et al.* 1999). Although null mutants have much lower nucleoside diphosphate kinase activity than wild type (10% and 30% for *S. cerevisiae* and *S. pombe* respectively) they are normal in

vegetative growth, sporulation, mating, and morphology (Fukuchi *et al.* 1993; Izumiya and Yamamoto 1995). In *N. crassa* an amino acid change P72H in NDK protein causes reduced NDK activity and deficient light response for perithecial polarity (Ogura *et al.* 1999; Ogura *et al.* 2001). Multiple isoforms of NDK exist in higher organisms (Gilles *et al.* 1991; Venturelli *et al.* 1995; Munier *et al.* 1998; Ouatas *et al.* 1998; Agou *et al.* 1999; Lee and Lee 1999; Milon *et al.* 2000; Barraud *et al.* 2002; Fournier *et al.* 2002a; Fournier *et al.* 2002b). In higher organisms, NDKs are involved in a variety of essential cellular processes. In mammals, NDKs are involved in differentiation, cell survival, tumor metastasis and proliferation (Lee *et al.* 1997; Nosaka *et al.* 1998; Lee and Lee 1999; Postel *et al.* 2000a; Postel *et al.* 2000b; Roymans *et al.* 2000; Amendola *et al.* 2001; Otsuki *et al.* 2001; Roymans *et al.* 2001). In *Drosophila melanogaster* and *Xenopus laevis*, NDKs are essential for development (Chiadmi *et al.* 1993; Ouatas *et al.* 1997; Ouatas *et al.* 1998). In *C. elegans,* NDK seems to be important for embryogenesis (Maeda *et al.* 2001). In plants, NDK interacts with the phytochrome molecules, sensory photoreceptors transducing environmental light signals to responsive nuclear genes (Hasunuma and Yabe 1998; Choi *et al.* 1999; Quail 2000).

The *swoH1* mutant was found to be low in NDK activity, which is consistent with the structural modeling showing that the *swoH1* mutation may distort the enzyme active sites. Purified SwoHp has phosphate transferase activity. Deletion of the *swoH* gene was lethal in *A. nidulans*, suggesting that SwoHp is essential in this filamentous fungus. The possibility that NDK plays a more important role in multicellular organisms is discussed.

In Chapter 4, the possibility that the SwoHp may be involved in stress response attenuation is explored. Several phenotypes of the *swoH1* mutant such as swollen hyphae,

cell lysis, growth restoration by salt, sensitivity to SDS, and accumulation of glycogen suggest that SwoHp may be involved in the stress response. Possible roles of SwoHp in stress adaptation/attenuation are discussed.

REFENRENCES

Agarwal, R. P., B. Robison and R. E. Parks, Jr., 1978 Nucleoside diphosphokinase from human erythrocytes. Methods Enzymol **51:** 376-386.

Agou, F., S. Raveh, S. Mesnildrey and M. Veron, 1999 Single strand DNA specificity analysis of human nucleoside diphosphate kinase B. J Biol Chem **274:** 19630-19638.

Amendola, R., R. Martinez, A. Negroni, D. Venturelli, B. Tanno *et al.*, 2001 DR-nm23 expression affects neuroblastoma cell differentiation, integrin expression, and adhesion characteristics. Med Pediatr Oncol **36:** 93-96.

Barraud, P., L. Amrein, E. Dobremez, S. Dabernat, K. Masse *et al.*, 2002 Differential expression of nm23 genes in adult mouse dorsal root ganglia. J Comp Neurol **444:** 306-323.

Bousquet-Antonelli, C., Y. Henry, P. G'Elugne J, M. Caizergues-Ferrer and T. Kiss, 1997 A small nucleolar RNP protein is required for pseudouridylation of eukaryotic ribosomal RNAs. Embo J **16:** 4770-4776.

Chant, J., 1999 Cell polarity in yeast. Annu Rev Cell Dev Biol **15:** 365-391.

Charette, M., and M. W. Gray, 2000 Pseudouridine in RNA: what, where, how, and why. IUBMB Life **49:** 341-351.

Chiadmi, M., S. Morera, I. Lascu, C. Dumas, G. Le Bras *et al.*, 1993 Crystal structure of the Awd nucleotide diphosphate kinase from Drosophila. Structure **1:** 283-293.

Choi, G., H. Yi, J. Lee, Y. K. Kwon, M. S. Soh *et al.*, 1999 Phytochrome signalling is mediated through nucleoside diphosphate kinase 2. Nature **401:** 610-613.

Dez, C., A. Henras, B. Faucon, D. Lafontaine, M. Caizergues-Ferrer *et al.*, 2001 Stable expression in yeast of the mature form of human telomerase RNA depends on its association with the box H/ACA small nucleolar RNP proteins Cbf5p, Nhp2p and Nop10p. Nucleic Acids Res **29:** 598-603.

Dickson, B. J., 2002 Molecular mechanisms of axon guidance. Science **298:** 1959-1964.

Fournier, H. N., S. Dupe-Manet, D. Bouvard, M. L. Lacombe, C. Marie *et al.*, 2002a ICAP-1alpha interacts directly with the metastasis suppressor nm23-H2 and both proteins are targeted to newly formed cell adhesion sites upon integrin engagement. J Biol Chem **27:** 27.

Fournier, H. N., S. Dupe-Manet, D. Bouvard, M. L. Lacombe, C. Marie *et al.*, 2002b Integrin cytoplasmic domain-associated protein 1alpha (ICAP-1alpha) interacts directly with the metastasis suppressor nm23-H2, and both proteins are targeted to newly formed cell adhesion sites upon integrin engagement. J Biol Chem **277:** 20895-20902.

Fukuchi, T., J. Nikawa, N. Kimura and K. Watanabe, 1993 Isolation, overexpression and disruption of a *Saccharomyces cerevisiae* YNK gene encoding nucleoside diphosphate kinase. Gene **129:** 141-146.

Ganot, P., M. L. Bortolin and T. Kiss, 1997 Site-specific pseudouridine formation in preribosomal RNA is guided by small nucleolar RNAs. Cell **89:** 799-809.

Gilles, A. M., E. Presecan, A. Vonica and I. Lascu, 1991 Nucleoside diphosphate kinase from human erythrocytes. Structural characterization of the two polypeptide chains responsible for heterogeneity of the hexameric enzyme. J Biol Chem **266:** 8784-8789.

Gutgsell, N., N. Englund, L. Niu, Y. Kaya, B. G. Lane *et al.*, 2000 Deletion of the *Escherichia coli* pseudouridine synthase gene truB blocks formation of pseudouridine 55 in tRNA in vivo, does not affect exponential growth, but confers a strong selective disadvantage in competition with wild-type cells. Rna **6:** 1870-1881.

Gutgsell, N. S., M. D. Del Campo, S. Raychaudhuri and J. Ofengand, 2001 A second function for pseudouridine synthases: A point mutant of RluD unable to form pseudouridines 1911, 1915, and 1917 in *Escherichia coli* 23S ribosomal RNA restores normal growth to an RluD-minus strain. Rna **7:** 990-998.

Harris, S. D., A. F. Hofmann, H. W. Tedford and M. P. Lee, 1999 Identification and characterization of genes required for hyphal morphogenesis in the filamentous fungus *Aspergillus nidulans*. Genetics **151:** 1015-1025.

Hasunuma, K., and N. Yabe, 1998 Early events occurring during light signal transduction in plants. Tanpakushitsu Kakusan Koso **43:** 1443-1452.

Heiss, N. S., S. W. Knight, T. J. Vulliamy, S. M. Klauck, S. Wiemann *et al.*, 1998 X-linked dyskeratosis congenita is caused by mutations in a highly conserved gene with putative nucleolar functions. Nat Genet **19:** 32-38.

Izumiya, H., and M. Yamamoto, 1995 Cloning and functional analysis of the ndk1 gene encoding nucleoside-diphosphate kinase in *Schizosaccharomyces pombe*.PG - 27859-64. J Biol Chem **270:** 27859-27864.

Keller, R., 2002 Shaping the vertebrate body plan by polarized embryonic cell movements. Science **298:** 1950-1954.

Lafontaine, D. L., C. Bousquet-Antonelli, Y. Henry, M. Caizergues-Ferrer and D. Tollervey, 1998 The box H + ACA snoRNAs carry Cbf5p, the putative rRNA pseudouridine synthase. Genes Dev **12:** 527-537.

Lee, H. Y., and H. Lee, 1999 Inhibitory activity of nm23-H1 on invasion and colonization of human prostate carcinoma cells is not mediated by its NDP kinase activity. Cancer Lett **145:** 93-99.

Lee, I. H., S. I. Chang, K. Okada, H. Baba and H. Shiku, 1997 Transcription effect of nm23-M2/NDP kinase on c-myc oncogene. Mol Cells **7:** 589-593.

Maeda, I., Y. Kohara, M. Yamamoto and A. Sugimoto, 2001 Large-scale analysis of gene function in *Caenorhabditis elegans* by high-throughput RNAi. Curr Biol **11:** 171-176.

Marciniak, R. A., F. B. Johnson and L. Guarente, 2000 Dyskeratosis congenita, telomeres and human ageing. Trends Genet **16:** 193-195.

Milon, L., P. Meyer, M. Chiadmi, A. Munier, M. Johansson *et al.*, 2000 The human nm23-H4 gene product is a mitochondrial nucleoside diphosphate kinase. J Biol Chem **275:** 14264-14272.

Momany, M., and I. Taylor, 2000 Landmarks in the early duplication cycles of *Aspergillus fumigatus* and *Aspergillus nidulans:* polarity, germ tube emergence and septation. Microbiology **146:** 3279-3284.

Momany, M., P. J. Westfall and G. Abramowsky, 1999 *Aspergillus nidulans swo* mutants show defects in polarity establishment, polarity maintenance and hyphal morphogenesis. Genetics **151:** 557-567.

Munier, A., C. Feral, L. Milon, V. P. Pinon, G. Gyapay *et al.*, 1998 A new human nm23 homologue (nm23-H5) specifically expressed in testis germinal cells. FEBS Lett **434:** 289-294.

Nosaka, K., M. Kawahara, M. Masuda, Y. Satomi and H. Nishino, 1998 Association of nucleoside diphosphate kinase nm23-H2 with human telomeres. Biochem Biophys Res Commun **243:** 342-348.

Ofengand, J., A. Bakin, J. Wrzesinski, K. Nurse and B. G. Lane, 1995 The pseudouridine residues of ribosomal RNA. Biochem Cell Biol **73:** 915-924.

Ogura, Y., Y. Yoshida, K. Ichimura, C. Aoyagi, N. Yabe *et al.*, 1999 Isolation and characterization of *Neurospora crassa* nucleoside diphosphate kinase NDK-1. Eur J Biochem **266:** 709-714.

Ogura, Y., Y. Yoshida, N. Yabe and K. Hasunuma, 2001 A point mutation in nucleoside diphosphate kinase results in a deficient light response for perithecial polarity in *Neurospora crassa*. J Biol Chem **276:** 21228-21234.

Otsuki, Y., M. Tanaka, S. Yoshii, N. Kawazoe, K. Nakaya *et al.*, 2001 Tumor metastasis suppressor nm23H1 regulates Rac1 GTPase by interaction with Tiam1. Proc Natl Acad Sci U S A **98:** 4385-4390.

Ouatas, T., B. Abdallah, L. Gasmi, J. Bourdais, E. Postel *et al.*, 1997 Three different genes encode NM23/nucleoside diphosphate kinases in *Xenopus laevis*. Gene **194:** 215-225.

Ouatas, T., M. Selo, Z. Sadji, J. Hourdry, H. Denis *et al.*, 1998 Differential expression of nucleoside diphosphate kinases (NDPK/NM23) during Xenopus early development. Int J Dev Biol **42:** 43-52.

Pellettieri, J., and G. Seydoux, 2002 Anterior-Posterior Polarity in *C. elegans* and Drosophila--PARallels and Differences. Science **298:** 1946-1950.

Postel, E. H., B. M. Abramczyk, M. N. Levit and S. Kyin, 2000a Catalysis of DNA cleavage and nucleoside triphosphate synthesis by NM23-H2/NDP kinase share an active site that implies a DNA repair function. Proc Natl Acad Sci U S A **97:** 14194-14199.

Postel, E. H., S. J. Berberich, J. W. Rooney and D. M. Kaetzel, 2000b Human NM23/nucleoside diphosphate kinase regulates gene expression through DNA binding to nuclease-hypersensitive transcriptional elements. J Bioenerg Biomembr **32:** 277-284.

Pruyne, D., and A. Bretscher, 2000a Polarization of cell growth in yeast. J Cell Sci **113:** 571-585.

Pruyne, D., and A. Bretscher, 2000b Polarization of cell growth in yeast. I. Establishment and maintenance of polarity states. J Cell Sci **113:** 365-375.

Quail, P. H., 2000 Phytochrome-interacting factors. Semin Cell Dev Biol **11:** 457-466.

Roymans, D., K. Vissenberg, C. De Jonghe, R. Willems, G. Engler *et al.*, 2001 Identification of the tumor metastasis suppressor Nm23-H1/Nm23-R1 as a constituent of the centrosome. Exp Cell Res **262:** 145-153.

Roymans, D., R. Willems, K. Vissenberg, C. De Jonghe, B. Grobben *et al.*, 2000 Nucleoside diphosphate kinase beta (Nm23-R1/NDPKbeta) is associated with intermediate filaments and becomes upregulated upon cAMP-induced differentiation of rat C6 glioma. Exp Cell Res **261:** 127-138.

Shapiro, L., H. H. McAdams and R. Losick, 2002 Generating and exploiting polarity in bacteria. Science **298:** 1942-1946.

Trinci, J. H. B. a. A. P. J. (Editor), 1979 *Fungal walls and hyphal growth.* Cambridge University Press, London.

Venturelli, D., R. Martinez, P. Melotti, I. Casella, C. Peschle *et al.*, 1995 Overexpression of DR-nm23, a protein encoded by a member of the nm23 gene family, inhibits granulocyte differentiation and induces apoptosis in 32Dc13 myeloid cells. Proc Natl Acad Sci U S A **92:** 7435-7439.

Watanabe, Y., and M. W. Gray, 2000 Evolutionary appearance of genes encoding proteins associated with box H/ACA snoRNAs: cbf5p in *Euglena gracilis*, an early diverging eukaryote, and candidate Gar1p and Nop10p homologs in archaebacteria. Nucleic Acids Res **28:** 2342-2352.

Watkins, N. J., A. Gottschalk, G. Neubauer, B. Kastner, P. Fabrizio *et al.*, 1998 Cbf5p, a potential pseudouridine synthase, and Nhp2p, a putative RNA-binding protein, are present together with Gar1p in all H BOX/ACA-motif snoRNPs and constitute a common bipartite structure. RNA **4:** 1549-1568.

Wendland, J., 2001 Comparison of morphogenetic networks of filamentous fungi and yeast. Fungal Genet Biol **34:** 63-82.

Yaghmai, R., A. Kimyai-Asadi, K. Rostamiani, N. S. Heiss, A. Poustka *et al.*, 2000 Overlap of dyskeratosis congenita with the Hoyeraal-Hreidarsson syndrome. J Pediatr **136:** 390-393.

Zaborina, O., N. Misra, J. Kostal, S. Kamath, V. Kapatral *et al.*, 1999 P2Z-Independent and P2Z receptor-mediated macrophage killing by *Pseudomonas aeruginosa* isolated from cystic fibrosis patients. Infect Immun **67:** 5231-5242.

Zebarjadian, Y., T. King, M. J. Fournier, L. Clarke and J. Carbon, 1999 Point mutations in yeast CBF5 can abolish in vivo pseudouridylation of rRNA. Mol Cell Biol **19:** 7461-7472.

CHAPTER 2

SWOCP PLAYS A ROLE IN POLAR GROWTH AND NUCLEAR DISTRIBUTION IN *ASPERGILLUS NIDULANS*[1]

[1]Lin, X. and Michelle Momany. To be submitted to *Genetics*.

ABSTRACT

Previous work identified *swoC1* as a single gene mutant with defects in polarity establishment. In the current study *swoC1* was shown to have defects in endocytosis, compartmentation, and conidiation. In wild type *Aspergillus nidulans*, after a brief period of isotropic growth, cells send out germ tubes sequentially in a bipolar pattern. After extended isotropic growth at restrictive temperature, the *swoC1* mutant cells send out multiple germ tubes at random sites simultaneously after release of the temperature block. The *swoC* gene was mapped to the centromere of chromosome III and cloned by complementation of the temperature-sensitive phenotype. The predicted SwoCp is homologous to rRNA pseudouridine synthases of yeast (Cbf5p) and human (Dkc1p). However, neither rRNA pseudouridine synthesis nor rRNA processing appear to be affected in the *swoC1* mutant. The *swoC1* mutation occurs in the putative RNA binding domain upstream of the C-terminus leaving the N-terminal TRUB catalytic domain intact. Interestingly, while deletion of the *swoC* gene was lethal in *A. nidulans*, the C-terminus, including NLS, microtubule-binding, and coiled-coil domains, was dispensable for growth. SwoCp likely plays an important role in polar growth and nuclear distribution in *A. nidulans*, functions not yet described for its homologues.

INTRODUCTION

In filamentous fungi, spores break dormancy and expand isotropically before switching to polar tip growth. Further growth occurs exclusively at the hyphal tip. Germ tube emergence in wild-type *Aspergillus nidulans* is sequential and usually occurs in a bipolar pattern (Harris *et al.* 1999; Momany and Taylor 2000). Along the hyphae, septa

are laid down at regular intervals and nuclei are evenly distributed (Fiddy and Trinci 1976; Trinci 1978). The temperature-sensitive *swoC1* mutant of *A. nidulans* was isolated based on its isotropic (swollen) phenotype in a screen to identify genes involved in polar growth (Momany *et al.* 1999).

Polarity genes in filamentous fungi are proposed to fall into two categories (Momany *et al.* 1999; Momany 2002): those responsible for establishing a location where a germ tube will emerge (polarity establishment genes), and those responsible for maintaining this directed polar growth (polarity maintenance genes). Previous work showed that the *swoC1* mutant is not able to establish polarity, but is able to maintain polarity at restrictive temperature and thus is a polarity establishment mutant (Momany *et al.* 1999). The genetic analysis of polarity in yeast and filamentous fungi has shown that the cytoskeleton, Bud proteins and members of G protein and MAP kinase signaling pathways play major roles in polarity generation (Rasmussen *et al.* 1992; Roberts and Fink 1994; Bachewich and Heath 1998; Chant 1999; Roze *et al.* 1999; Pruyne and Bretscher 2000a; Pruyne and Bretscher 2000b; Wendland and Philippsen 2001; Momany 2002).

Surprisingly, we found that *swoC* encodes a homologue of *Saccharomyces cerevisiae* Cbf5p. Originally discovered by its affinity to the yeast centromere, Cbf5p is the pseudouridine synthase responsible for isomerization of uridine to pseudouridine in rRNA (Lafontaine *et al.* 1998; Watkins *et al.* 1998; Zebarjadian *et al.* 1999; Watanabe and Gray 2000). In eukaryotes, rRNA undergoes a series of modifications and cleavages after transcription to produce 18S, 5.8S and 28S mature rRNAs. Isomerization of uridine to pseudouridine is one of the most abundant post-transcriptional modifications and

mostly occurs in the large subunit of ribosomal RNA (reviewed by (Charette and Gray 2000).

The biological role of pseudouridine is not yet clear. Recent evidence suggests that pseudouridine is not essential for ribosomal functions. Yeast depleted of virtually all pseudouridine residues in rRNA are viable (Bousquet-Antonelli *et al.* 1997). Nonetheless, deletion of *CBF5* is lethal (Ganot *et al.* 1997) suggesting that Cbf5p must have functions other than pseudouridine synthesis. Indeed, yeast Cbf5p has been shown to associate with microtubules (Jiang *et al.* 1993), Pol I transcription factor (Cadwell *et al.* 1997) and snR30, which is involved in pre-RNA endonucleolytic processing (Lafontaine *et al.* 1998). The human homologue Dkc1p, binds hTR (the RNA component of human telomerase complex) and plays an important role in telomere maintenance (Marciniak *et al.* 2000; Dez *et al.* 2001). Mutations of *DKC1* cause the X-linked recessive diseases Dyskeratosis Congenita (Heiss *et al.* 1998) and Hoyeraal-Hreidarsson syndrome (Yaghmai *et al.* 2000), and patients have a rare bone-marrow failure disorder and early mortality.

MATERIALS AND METHODS

Strains and media: Strains used in this study were: A104 (*yA2; adE20; AcrA1; phenA2; pyroA4; lysB5; sB3; nicB8; coA1*), A457 (*proA1; biA1; galE9; sC12; diA1; phenA2; choA1*), A773 (*pyrG89; wA3; pyroA4*), A852 (*biA1;_argB::trpC_B;methG1;veA1 trpC801\\pabaA1 yA2;_argB::trpC_B;veA1 trpC801*), AGA22 (*swoC1; pabaA*) and AXL8 (*swoC1; pyroG89, wA3; pyroA4*). All strains were obtained from the Fungal Genetics Stock Center (Department of

Microbiology, University of Kansas Medical Center) except AGA22 and AXL8, which were constructed for this study. Identification of the temperature-sensitive *swoC1* mutant and verification that it is a single gene mutation have been previously described (Momany *et al.* 1999). Media used was as previously reported (Harris *et al.* 1994). Strain construction and genetic analysis were by standard *A. nidulans* techniques (Kafer 1977; Harris *et al.* 1994).

Growth conditions and microscopic observations:

Vegetative growth: Conditions for vegetative growth and preparation of cells were as previously reported (Momany *et al.* 1999). Briefly, conidia were inoculated on coverslips in liquid medium and incubated in a petri dish. Cells were fixed, nuclei were stained with Hoechst 33258 (Sigma, St. Louis, MO) and septa were stained with Calcofluor (American Cyanamid, Wayne, NJ). Microscopic observations were made using a Zeiss Axioplan microscope (Thornwood, NY) and digital images were acquired using an Optronics digital imaging system (Goleta, CA). Images were prepared using Photoshop 5.5 (Adobe, Mountain View, CA).

Conidiation: Conidia were inoculated on the edges of a small square of agar medium placed on top of a coverslip, which was placed in a petri dish containing solidified agar to keep it moist. Another coverslip was placed on top of the agar square after inoculation. Plates were sealed with parafilm and incubated inverted at 42° for 9hr then shifted to 30° for 2 days. For observation of conidiophore structure, coverslips with aerial hyphae and conidiophores attached were dipped into 100% ethanol, mounted on slides, and observed microscopically. Otherwise, cells attached to coverslips were fixed and stained as described for vegetative growth.

FM4-64 staining: Complete liquid medium with proper supplements was inoculated with 1–5x10^4 conidia/ml, poured into a petri dish containing a glass coverslip, and incubated as indicated. Coverslips with adhering cells were labeled with 20 ?M FM4-64 (Molecular Probes Inc. Eugene, OR) solution for 30 min at the indicated temperature. 10 mM NaZ_3 was added to stop the labeling. A 20 ?M FM4-64 solution with 10 mM NaZ_3 was used as the control.

DNA and RNA isolation: DNA was isolated from *A. nidulans* using previously described methods (Harris *et al.* 1994). Total RNA from *A. nidulans* was extracted using Trizol Reagent according to the manufacturer's instructions (GIBCO BRL, Grand Island, NY).

Cloning by complementation and plasmid rescue: A random genomic plasmid library carrying a *pryG* marker provided by Dr. Greg May (University of Texas, M. D. Anderson Cancer Center, Houston, TX, USA) (Osherov and May 2000) was transformed into protoplasts of the *swoC1* mutant AXL8 by standard *A. nidulans* protocols (Yelton *et al.* 1984). Transformants with *pyrG* prototrophy restored to wild-type growth at restrictive temperature (42º) were selected. The complementing plasmids were rescued by transformation of *E. coli* XL1-blue with total DNA purified from the *A. nidulans* transformants. Restriction mapping showed that all the complementing plasmids contained the same fragment within overlapping genomic DNA inserts (data not shown). The smallest complementing plasmid, p8c1, was chosen for further study.

Confirmation of complementation by map-based cloning:

Mitotic mapping: *swoC1* strain AGA22 was fused with the mitotic mapping strain A104 by standard methods (Ma and Kafer 1974; Kafer 1977). Diploid conidia were

incubated on solid complete medium with 60 ? g/ml of benomyl for two days and transferred to complete medium without benomyl for two weeks. Genotypes of haploid sectors were scored.

Meiotic mapping: The *swoC1* mutant strain AGA22 was crossed with meiotic mapping strain A457. Ascospores released from individual cleistothecia were plated on selective media to test genotypes (Kafer 1977).

Cloning of swoC: The *swoC* gene is tightly linked to the *phenA* marker, which is located near the centromere of chromosome III. Based on the physical map of *A. nidulans* (http://gene.genetics.uga.edu/), twenty cosmids near the centromere from the chromosome specific genomic library (Fungal Genetics Stock Center http://www.fgsc.net/) were chosen to transform into the *swoC1* mutant. Only cosmid W21H06 restored the *swoC1* mutant to wild-type growth at restrictive temperature. Southern blotting experiments (Sambrook *et al.* 1989) showed that cosmid W21H06 contains the same fragment as p8c1 and the two other complementing plasmids (data not shown).

Identification and sequencing of the *swoC* gene by transposon tag: Transposons (GPS-1 system; New England Biolabs, Beverly, MA) were randomly inserted into the complementing plasmid p8c1. Each of the resulting plasmids contains one copy of the transposon at random sites. Forty-eight plasmids were sequenced using primers unique for the transposon ends on an ABI 3700 DNA Analyzer (Applied Biosystem, CA) according to the manufacturer's instructions.

The sequences were assembled and analyzed using the Phred (version 0.000925c), Phrap (version 0.990319), and Consed (version 11.0) computer programs

(http://depts.washington.edu/ventures/collabtr/direct/ppccombo.htm). All sequences have at least four-fold redundancy with a quality rating of at least 20. The assembled contig was used to search the NCBI databases (www.ncbi.nlm.nih.gov) using the Blast program to identify open reading frames (ORFs). Only one ORF was found. Plasmids with transposons inserted within the ORF were transformed into the *swoC1* mutant. Plasmids that failed to rescue the *swoC1* mutant at restrictive temperature were assumed to have transposon insertions disrupting the complementing gene. The genomic sequence of the *swoC* gene, its intron locations, and the predicted protein sequence are deposited in GenBank (accession no. AY057454).

Sequencing of the *swoC1* mutant allele: The *swoC1* mutant allele was amplified by three independent PCR reactions using the Expand High Fidelity PCR System (Roche Diagnostics, Indianapolis, IN, USA) and cloned into the pGEM-T Vector System (Promega, Madison, WI). Genomic DNA from *swoC1* mutant strain AXL8 was used as the template. Primers used for PCR amplifications were: 5'GAATGTTTACGCAGGTGG and 5'GTGGCTTGTGATGATGCGG. Three clones from each reaction (nine in total) were sequenced using the transposon strategy described above. All sequences showed an identical change in base 1220 (G to T) of *swoC1*. The sequences obtained were compared with the wild type allele using GeneDoc (version 2.6.001) (www.psc.edu/biomed/genedoc) with default parameters.

Protein alignment: Sequences of SwoC1p homologues were obtained from GenBank (http://www.ncbi.nlm.nih.gov/). Protein sequences were aligned using GeneDoc (version 2.6.001) with default parameters.

Pseudouridine analysis by HPLC-MS: Enzymatic digestion of 100 µg total RNA by

Nuclease P1, Phosphodiesterase I and Alkaline phosphatase was conducted as previously described (Pomerantz and McCloskey 1990). The pseudouridine level of the hydrolates was analyzed by HPLC-MS basically as previously described (Pomerantz and McCloskey 1990) by the Chemical and Biological Sciences Mass Spectrometry Facility, University of Georgia (*http://www.uga.edu/mass-spec/*). Standards (adenosine, cytidine, guanosine, pseudouridine, and uridine) were used to determine the optimal gradient conditions for separation. Peaks were identified by their retention time and mass spectrum. The experiment was repeated three times.

Northern hybridization: Total RNA was isolated from wild type A773 and *swoC1* mutant AXL8 cultured in complete medium at 42^{o}. RNA was separated on a 1.2% formaldehyde agarose gel and transferred to a nylon membrane by standard methods (Sambrook *et al.* 1989). The following probes were generated based on *A. nidulans* 18S, ITS1, ITS2, and 25S rRNA sequences, respectively. Probe 1: CTCCCCGCCGAAGCAACAGTG; Probe 2: GAGCCATTCGCAGTTTCACAG; Probe 3: GACGACGACCCAACACACAAGC; Probe 4: CACTCTACTTGTGCGCTATCGGTC. Probes were labeled at the 5'-end by T4 polynucleotide kinase (Roche, Indianapolis, IN) according to the manufacturer's instructions.

Construction of *swoC* knock out: Flanking sequences from upstream and downstream of the *swoC* gene (1.1 kb each) were amplified by high fidelity PCR. Primers used to amplify the 5'flanking sequence of *swoC* were: 5'CCGCTCGAGGGTGAATGTTTACGCAGGTGGTTTTGG (with the addition of *Xho*I restriction site) and 5'GGAATTCCGGCCATTGCGACTGTTATTGAG (with the

addition of *Eco*RI restriction site). Primers used to amplify the 3'flanking sequence of *swoC* with the addition of *Sac*II restriction sites were: 5'TCCCCGCGGCGACCAAATGGAAGTCCGAATAC and 5'CCCCGCGGGGACTAACGTCAAGTGTGGCGAGTG. After double digestion with *Eco*RI and *Xho*I, the 5' flanking sequence was inserted into pargBC-1 (Momany and Hamer 1997) bearing the *argB* gene as the selectable marker. The resulting plasmid pargBC-5F was then ligated with 3' flanking sequence after digestion with *Sac*II. Correct insert direction of the 3' flanking sequence was confirmed by restriction mapping and PCR. The plasmid pargBC-5F-3F was then digested with *Bss*HII and separated on a 1% agarose gel. The 4.2 kb fragment containing *argB* with *swoC* flanking sequences (5F-argB-3F) was purified using the Qiagen Gel purification kit (Qiagen Inc., Valencia, CA).

The linear fragment containing 5F-argB-3F was transformed into *A. nidulans* diploid strain A852. Transformants were selected for growth on minimal medium lacking arginine. Genomic DNA of 72 transformants was isolated and digested with *Kpn*I. Southern blot was performed with random labeled 3' flanking sequence as the probe. Putative homologous integrants were confirmed by Southern blot with *Bam*HI and *Kpn*I double digestion. A single heterozygous diploid transformant with *argB* replacing *swoC* on one chromosome and a wild type *swoC* on the other was treated with benomyl to induce haploidization as described for mitotic mapping. In total 206 haploid sectors were scored for genotype. None of the haploid colonies grew on minimal medium without arginine supplement.

Construction of the *swoC* C-terminal deletion allele. The construction of C-terminal deletion allele was essentially the same as the null allele except that the truncated *swoC*

gene lacking the final 294 bases was inserted into pargBC-1 (Momany and Hamer 1997) after double digestion with *Eco*RI and *Pst*I. This *swoC* C-terminal deletion fragment was amplified by high fidelity PCR using primers: 5'CTGCAGTGATGGTCAGGACTGG and 5'AACTGCAGAACCAATCCATTGGGGCTGGGGTGGCTTCGTTGG (with addition of *Pst*I site). The resulting plasmid pargBC-N-swoC was ligated with the 3' flanking sequence as described above. The linear fragment containing truncated-swoC-argB-3F was transformed into *A. nidulans* diploid strain A852. Screening and confirmation were performed essentially as described for the null mutant construct.

RESULTS

Phenotypic Characterization of the *swoC1* Mutant

Nuclear division is uncoupled from polarity establishment in the *swoC1* mutant: Previous work has shown that uninucleate spores switch from isotropic to polar growth after the first round of mitosis in wild-type *A. nidulans* (Momany and Taylor 2000) (Figure 2.1a, b). In the current study, nuclear staining showed that 80% of *swoC1* mutant spores do not switch to polar growth until the second round of mitosis at 30^{o} (Figure 2.1c, d). This observation suggests that nuclear division and polar growth are uncoupled in the *swoC1* mutant even at permissive temperature.

Previous work has shown that *swoC1* grew isotropically at restrictive temperature (42^{o}) for 13 hr and accumulated 6 nuclei on average (Momany *et al.* 1999). To determine if *swoC1* arrests isotropic growth upon extended incubation, we observed the growth of *swoC1* after 24 hr at 42^{o}. We found that *swoC1* could grow into giant, balloon-like cells and accumulate a large number of nuclei (Figure 2.2b, c). Some cells were at least 15

times larger than a wild type conidium and contained more than 30 nuclei. Even after 53 hr at restrictive temperature, about half of the population survived (data not shown), indicating that the mutant is viable and nuclear division is not blocked by the polar growth defect. This supports our previous suggestion that polar growth and nuclear division are carried out by two independent pathways in *A. nidulans* (Momany and Taylor 2000).

The *swoC1* mutant sends out multiple germ tubes simultaneously at random sites: Previous work concluded that the *swoC1* mutant does not establish polarity at restrictive temperature based on failure to send out germ tubes within one cell cycle after shift from restrictive to permissive temperature, while polarity maintenance mutant *swoA* sent out germ tube within 15 min after temperature shift (Momany *et al.* 1999). To determine if the *swoC1* mutant loses the competence for polar growth after sustained isotropic expansion, the *swoC1* mutant was incubated at restrictive temperature for 4 hr, 10 hr and 24 hr (Figure 2.3a, b, c) and then shifted to permissive temperature for 10 hr (several cell cycles). The *swoC1* mutant sent out germ tubes in all cases (Figure 2.3d, e, f). Even after 53 hr at restrictive temperature, mutant cells sent out germ tubes upon temperature shift (data not shown). This suggests that the competence for polar growth is either retained in the *swoC1* mutant at restrictive temperature or can be established after release of the temperature block. Interestingly, the longer the incubation at restrictive temperature, the more germ tubes the *swoC1* mutant sent out after shift to permissive temperature (Figure 2.3). To determine if these multiple polarity sites are activated simultaneously after the temperature block is released, we incubated the *swoC1* mutant at restrictive temperature for 20 hr and shifted to permissive temperature for 3 hr. We found that many germ tubes

emerged at random sites (Figure 2.3g). Because these germ tubes were all the same length after 3 hr growth at permissive temperature, we assume that they emerged simultaneously. In contrast, in wild-type *A. nidulans*, germ tubes emerge sequentially, usually in a bipolar pattern (Figure 2.2a) (Harris *et al.* 1999; Momany and Taylor 2000). Our results show that more than one polarity apparatus may form simultaneously in the *swoC1* mutant and suggest that polarity establishment may be tied to membrane volume.

The *swoC1* mutant is defective in endocytosis: One possible explanation for a connection between increased membrane volume and increased germ tube emergence in the *swoC1* mutant would be a failure to remove accumulated polarity establishment markers from the plasma membrane during isotropic expansion. Indeed in *S. cerevisiae*, an endocytic block causes isotropic cell growth, similar to the *swoC1* mutant swollen phenotype (reviewed by (Pruyne and Bretscher 2000a; Pruyne and Bretscher 2000b). To investigate endocytosis of the *swoC1* mutant we used FM4-64, a membrane-selective dye that is internalized from the plasma membrane to internal membranes of organelles by endocytosis (Vida and Emr 1995) and has been used to investigate endocytosis and vesicle trafficking in filamentous fungi (Fischer-Parton *et al.* 2000). Wild type and the *swoC1* mutant were incubated at restrictive temperature, and cells were labeled with FM4-64 for 30 min. Labeling was terminated by addition of NaZ_3, a strong metabolic inhibitor. In the presence of NaZ_3, FM4-64 labeled only the plasma membrane of wild type and the *swoC1* mutant (Figure 2.4b, d). In the absence of NaZ_3, FM4-64 labeled plasma membrane and internal organelles of wild type during both isotropic growth and polar growth (Figure 2.4c). Under the same conditions, FM4-64 labeled only the plasma

membrane of the *swoC1* mutant (Figure 2.4a) showing that the *swoC1* mutant is defective in endocytosis at restrictive temperature.

An early delay in polarity establishment perturbs nuclear distribution during vegetative growth and conidiation in *swoC1*: To determine whether an early delay in polarity establishment affects later vegetative growth, we incubated wild type and *swoC1* at restrictive temperature for 9 hr (the *swoC1* mutant averaged 4 nuclei) and shifted to permissive temperature for 15 hr. We measured the length and nuclear number of each subapical compartment (n=120). Compartment length and nuclear number varied greatly in the *swoC1* mutant after temperature down shift, but were relatively uniform in the wild type (Figure 2.5). The *swoC1* mutant incubated at permissive temperature showed only slight variation in subapical compartment length and nuclear number (data not shown). Occasionally, we observed compartments without nuclei in the mutant (Figure 2.5, A). Empty compartments were never observed in wild type. In wild type, majority of compartments were between 10 micrometer (?M) and 60 ?M with 60% falling between 30 ?M and 40 ?M, and 23% falling between 40 ?M and 50 ?M (Figure 2.5, B). In the *swoC1* mutant, compartment length ranged from less than 10 ?M to greater than 110 ?M with only 26% falling between 30 ?M and 40 ?M, and 20% falling between 40 ?M and 50 ?M. In wild type, nuclear number per compartment fell between 1 and 7 with 87% of compartments contained 2 to 4 nuclei (Figure 2.5, C). In *swoC1* however, nuclear number per compartment ranged from 1 and 20 with only 47% of compartments contained 2 to 4 nuclei. The compartment length variation in the *swoC1* mutant probably reflects nuclear position variation since in this filamentous fungus, the site of septation is determined by nuclear position (Wolkow *et al.* 1996).

In wild-type *A. nidulans*, asexual reproduction produces uniform uninucleate conidia on a reproductive structure called the conidiophore (Timberlake 1991; Adams *et al.* 1998). Conidiophore development starts as aerial hyphae elongate and swell at the tip to form a vesicle (Figure 2.6a). From the vesicle forms a layer of primary sterigmata called metulae (Figure 2.6b). The metulae bud twice to form a layer of uninulceate phialides (Figure 2.6c). The phialides produce chains of conidia after repeated mitotic division and cytokinesis (Figure 2.6d). Mitosis, nuclear migration and cytokinesis must be tightly coordinated to ensure normal conidiation. To determine whether an early delay in polarity establishment affects asexual reproduction in the *swoC1* mutant, we incubated wild type and the *swoC1* mutant at restrictive temperature for 9 hr and shifted to permissive temperature for 2 days and observed conidiophores. After this slight delay in polarity establishment, all mutant conidiophores (n>50) appeared to be missing cell layers (Figure 2.6g, h). About 5.5% of *swoC1* conidia contained more than one nucleus and 4.5% contained no nucleus (n=200). Mutant conidiophores incubated only at permissive temperature also showed some morphological defects with 1% of conidia containing more than one nucleus or no nucleus (data not shown).

The *swoC* Gene Encodes rRNA Pseudouridine Synthase in *A. nidulans*

The *swoC* gene maps near the centromere of chromosome III: To identify the chromosome on which the *swoC* gene lies, we took advantage of the parasexual cycle in *A. nidulans* (Kafer 1977). A heterozygous diploid was made between the *swoC1* mutant strain AGA22 and the mitotic mapping strain A104, which has a marker on each chromosome. The diploid was treated with the microtubule destabilizing drug benomyl to stimulate chromosome loss until a stable haploid state was reached. All haploid sectors

were tested for their genotypes. The remaining set of chromosomes of the haploid sectors was a random mixture derived from either the *swoC1* mutant or the mitotic mapping strain. The *phenA*$_2$ marker on chromosome III segregated 100% in repulsion to the *swoC1* temperature-sensitive phenotype in these haploid sectors (Table 2.1). Therefore the *swoC* gene is on chromosome III.

To define the position of the *swoC* gene on chromosome III, the *swoC1* mutant strain AGA22 was crossed with the meiotic mapping strain A457. The distance between the *swoC1* allele and other markers on chromosome III was determined by recombination frequency. The *swoC1* allele was tightly linked to the *phenA*$_2$ marker near the centromere of chromosome III (Table 2.2).

The *swoC* gene encodes a homologue of rRNA pseudouridine synthase: Based on the physical map of *A. nidulans* (http://gene.genetics.uga.edu/), twenty cosmids near the centromere of chromosome III were chosen from the chromosome specific library and transformed into the *swoC1* mutant. Only cosmid W21H06 complemented the *swoC1* ts-phenotype.

In a separate experiment, three autonomously replicating plasmids from a random plasmid library were also found to restore the *swoC1* mutant to wild-type growth at restrictive temperature. Restriction mapping showed that these three plasmids contained overlapping genomic DNA inserts (data not shown).

Southern blotting indicated that the three high copy plasmids shared a common fragment with the W21H06 cosmid (data not shown), showing that the plasmids contain the *swoC* gene, rather than a high copy suppressor of the *swoC1* mutation (The cosmid does not have autonomous replicating sequence). The smallest plasmid, p8c1, was chosen

for sequencing using a transposon tagging strategy. Only one ORF was identified in the 8 kb *A. nidulans* genomic DNA insert in plasmid p8c1. This is not surprising since the *swoC* gene localizes to the gene-poor centromere-proximal region. Using the NCBI Blast program, the predicted SwoCp was found to be 70% identical with *S. cerevisiae* Cbf5p, 71% identical with *K. lactis* Cbf5p and 63% identical with *H. Sapiens* Dkc1p. All are members of a highly conserved family of eukaryotic rRNA pseudouridine synthases. Like other members of this family, SwoCp contains serveral predicted domains: a pseudouridylate synthase domain (TruB), an RNA binding domain (PUA), a microtubule binding domain (MT-Binding), a nuclear localization signal (NLS) and a coiled-coil protein-protein interaction domain (Figure 2.7).

Sequencing the *swoC1* mutant allele amplified from strain AXL8 by PCR showed a G to T mutation at base 1220, which results in a valine to phenylalanine substitution at amino acid 338 in the predicted PUA domain.

Deletion of the *swoC* gene is lethal in *A. nidulans*: Even though elimination of all detectable pseudouridine residues in rRNA from *S. cerevisiae* has no phenotype (Bousquet-Antonelli *et al.* 1997), deletion of the *CBF5* gene is lethal in yeast (Ganot *et al.* 1997). rRNA pseudouridine synthase knock out mutants have not yet been described for other organisms. Because we expected that deletion of *swoC* was likely to be lethal in *A. nidulans*, we constructed a heterozygous diploid wherein one copy of the *swoC* gene was replaced with the *argB* marker by homologous integration (Figure 2.8). We induced haploidization of the heterozygous diploid and scored haploid sectors (Kafer 1977). None of the 206 haploid sectors recovered was *argB*+, indicating that only haploids with the intact *swoC* gene survived. Therefore, the *swoC* gene is essential in *A. nidulans*.

The C-terminus of SwoCp is dispensable: To determine which portion of the *swoC* gene is required, we took advantage of the transposon inserts in plasmid p8c1 created for sequencing *swoC*. Two p8c1 plasmids with transposons in the first exon (data not shown) and the third exon (p8c1-A11) (Figure 2.9c) of the gene were not able to restore the *swoC1* mutant to wild-type growth at restrictive temperature. The p8c1 plasmid with a transposon in the first intron (p8c1-H07) also did not complement the *swoC1* phenotype (Figure 2.9b) likely because *A. nidulans,* which usually has 40 bp - 100 bp introns, could not properly process the 5kb intron resulting from transposon insertion. Most interestingly, the plasmid p8c1 with a transposon in the C-terminus (p8c1-E10) complemented the *swoC1* phenotype (Figure 2.9a). The E10 insertion is predicted to remove 98 amino acids from the C-terminus of the encoded protein including the MT-binding domain, NLS and coiled-coil domain. Distribution of nuclei and compartment length were similar in *swoC1* mutant strains transformed with either the intact p8c1 or p8c1-E10 (data not shown). Two explanations are possible: either the C-terminus is not essential for SwoCp, or the truncated *swoC* gene product can function together with the *swoC1* mutated gene product to restore the wild type phenotype. To distinguish between these explanations, we constructed a heterozygous diploid wherein the C-terminus of one copy of the *swoC* gene was replaced with the *argB* marker by homologous integration (Figure 2.8). We induced haploidization of the heterozygous diploid and scored haploid sectors (Kafer 1977). Out of 380 haploid sectors recovered, 327 haploid sectors were *argB+*, indicating that the C-terminus is indeed dispensable.

The *swoC1* mutant shows no defect in pseudouridine synthesis or rRNA processing: Pseudouridination is one of the two most abundant nucleic acid

modifications and occurs predominantly in rRNA (Maden and Hughes 1997; Ofengand 2002). In eukaryotes, approximately 1% of rRNA nucleic acids are pseudouridines (reviewed by (Charette and Gray 2000; Ofengand 2002)). Evidence suggests that the box H/ACA small nuclear ribonucleoprotein particles (snRNPs) may be the universal complex responsible for all eukaryotic rRNA pseudouridine synthesis using boxH/ACA snRNAs as guide and Cbf5p is the key enzyme in the complex (Bousquet-Antonelli *et al.* 1997; Peculis 1997; Lafontaine *et al.* 1998; Watkins *et al.* 1998; Zebarjadian *et al.* 1999; Charette and Gray 2000; Watanabe and Gray 2000; Yang *et al.* 2000; Pienkowska and Szweykowska-Kulinska 2001; Ofengand 2002). To determine if *A. nidulans* uses the same box H/ACA snRNP complex for rRNA pseudouridine synthesis, we searched *A. nidulans* databases and found homologues of other genes predicted to encode box H/ACA snRNP proteins (Gar1p, Nhp2p and Nop10p) in addition to SwoCp. All these predicted proteins are highly conserved. Thus, it is very likely that *A. nidulans* uses the same mechanism for rRNA pseudouridine synthesis. Since greater than 90% of total RNA is rRNA, we expected to see a gross decrease of pseudouridine in total RNA if the *swoC1* phenotype is due to loss of pseudouridine synthesis activity. Total RNA isolated from overnight culture of wild type and the *swoC1* mutant grown at restrictive and permissive temperature was enzymatically digested. We used HPLC coupled with MS to separate and identify pseudouridine. HPLC has long been used to detect modified nucleic acids (Russo *et al.* 1984; Amuro *et al.* 1988; Pomerantz and McCloskey 1990; Umegae *et al.* 1990; Palmisano *et al.* 1995; Shingfield and Offer 1999; Patteson *et al.* 2001). Three independent experiments showed that pseudouridine levels were similar in the *swoC1* mutant and wild type at both temperatures (Figure 2.10 shows results at restrictive

temperature and results at permissive temperature are not shown). The other major modified nucleic acid, 2'-O-methylated adenosine, was also detected in both the *swoC1* mutant and wild type indicating that our analysis was sound (Figure 2.10). These results suggest that the *swoC1* mutation does not grossly affect pseudouridine synthesis *in vivo.*

In *S. cerevisiae*, certain mutations in *CBF5* cause defects in pre-rRNA processing and steady-state levels of mature cytoplasmic ribosomes (Cadwell *et al.* 1997). To determine if the *swoC1* mutant phenotype could be caused by defective rRNA processing, we isolated total RNA from the *swoC1* mutant and wild type and probed with oligonucleotides designed based on 18S, ITS1, ITS2 and 25S sequences of *A. nidulans* (Lafontaine *et al.* 1998). The *swoC1* mutant and wild type showed identical band size and intensity of mature rRNA products (data not shown) and accumulation of pre-rRNA was not detected. A northern blot probed with ITS1-5.8S-ITS2 PCR product also showed no difference between wild type and *swoC1* mutant cultured at restrictive temperature. These results suggested that rRNA processing is normal in the *swoC1* mutant consistent with our observation that at restrictive temperature the *swoC1* mutant has sustained isotropic growth. Sustained growth is unlikely to occur if there is a severe defect in rRNA processing since breaking dormancy and growing isotropically both require protein synthesis (Herman and Rine 1997; Wendland 2001).

DISCUSSION

Polarity establishment cues persist or are reinitiated in *swoC1*: In *S. cerevisiae* budding occurs once in each cell cycle. Sites for bud emergence are tagged by cortical markers laid down during the previous round of budding. Cdc42p is recruited to these sites where it drives polar growth through interactions with the cytoskeleton and polarity

maintenance apparatus (Madden and Snyder 1992; Ziman *et al.* 1993; Kron *et al.* 1994; Chant *et al.* 1995; Goodson *et al.* 1996; Shafaatian *et al.* 1996; Yabe *et al.* 1996; Santos and Snyder 1997; Madden and Snyder 1998; Shulman and St Johnston 1999; Svoboda *et al.* 2001). The identities of cortical polarity markers tagging the sites for germ tube emergence are not yet known in filamentous fungi. It is not clear whether the germ tube emergence marker is laid down during formation of the spore or after dormancy is broken (Momany 2002).

In the *swoC1* mutant, an extreme delay in polarity establishment did not cause loss of competence for polar growth, suggesting that the underlying polarity markers either persist or can be formed despite a delay. While polar growth could still occur when *swoC1* was shifted from restrictive to permissive temperature, the normal bipolar pattern of germ tube emergence was disrupted. We were especially surprised by the increase in the number of germ tubes with increased incubation time at restrictive temperature (Fig. 2.3). Given the endocytosis defect of the *swoC1* mutant, it seems likely that new polarity markers are synthesized during the incubation at restrictive temperature and that failure to remove these markers leads to the emergence of multiple germ tubes in random positions after release of the temperature block.

The *swoC1* growth pattern defect is likely caused by defective nuclear distribution: The *swoC1* mutant continues nuclear division in the absence of polar growth, consistent with previous observations that the two processes are independent (Momany and Taylor 2000). However, nuclear distribution and polar growth are likely coupled in *A. nidulans*. Indeed, the *nudC* deletion mutant, which is defective in nuclear migration, only grows isotropically (Chiu *et al.* 1997). The *swoC1* mutation likely causes

growth pattern defects by its apparent involvement in nuclear distribution. The compartmentation defect during vegetative growth in the *swoC1* mutant could be caused by the irregular nuclear distribution along the hyphae as nuclear position determines septation sites in *A. nidulans* (Wolkow *et al.* 1996). Since conidiation is a process requiring highly synchronized growth, nuclear division, nuclear distribution, and cytokinesis, conidia with varied size and abnormal nuclear number generated by the *swoC1* mutant may also result from defective nuclear distribution during conidiation.

The *swoC1* phenotype is likely related to cryptic function in the PUA domain: Surprisingly, the gene that complemented the *swoC1* ts- phenotype was more than 60% identical with rRNA pseudouridine synthases from other eukaryotes. Based on our inability to detect any change in multiple activities associated with rRNA pseudouridine synthases, it is reasonable to propose that we cloned a suppressor rather than the authentic *swoC* gene. However, we genetically mapped the *swoC1* mutation to the centromere of chromosome III. Only cosmid W21H06 from the Chromosome III centromere region complemented the *swoC1* ts- phenotype. The rRNA pseudouridine synthase gene from complementing plasmids hybridized to the W21H06 cosmid. In addition, sequencing revealed a point mutation in the PUA domain in the *swoC1* mutant allele. Thus the rRNA pseudouridine synthase gene is the authentic *swoC* gene and not a suppressor.

If *swoC* encodes a pseudouridine synthase and *A. nidulans* uses the same system for rRNA pseudouridine synthesis, why do we fail to detect any changes in pseudouridine levels or rRNA processing in the *swoC1* mutant? The most obvious explanation is that the mutation affects some other function of SwoCp. Mutations in the TruB catalytic sites

of *CBF5* inhibit pseudouridine synthesis and rRNA processing. Indeed, the TruB domain is intact in the *swoC1* mutant allele. This is consistent with work on yeast Cbf5p and *E .coli* RluD implying that the pseudouridine synthesis function of the enzyme is not critical for cell growth while the protein itself is essential (Bousquet-Antonelli *et al.* 1997; Gutgsell *et al.* 2001; Ofengand 2002).

Our results suggest that the unknown essential function of SwoCp may require the PUA domain. The *swoC1* mutation occurs in the PUA domain, a conserved RNA-binding domain found both in archaea and eukaryotes (Becker *et al.* 1997; Aravind and Koonin 1999). Interestingly, another pseudouridine synthase in yeast, which modifies cytoplasmic and mitochondrial tRNAs, does not contain a PUA domain consistent with the idea that the PUA domain may contribute to binding of a specific RNA structure (Becker *et al.* 1997). The *swoC1* V338F mutation may disrupt the ability of SwoCp to bind certain RNA substrates, while retaining the pseudouridine synthase enzyme activity. In X-linked Dysteratosis Congenita patients, many mutations of DKC1 occur in or around the PUA domain (Knight *et al.* 1999). These mutations may alter the interaction of Dkc1p with telomerase hTR, which has a box H/ACA motif (Mitchell *et al.* 1999). We did not detect any telomere length change in the *swoC1* mutant after numerous replications at restrictive temperature (unpublished observation). It is possible that *A. nidulans* telomerase RNA does not share any homology with box H/ACA snoRNAs like yeast telomerase RNA.

Asymmetric distribution of RNA is critical for development (Micklem 1995; Stephen *et al.* 1999; van Eeden and St Johnston 1999; Stebbings 2001). It is possible that an RNA

substrate of SwoCp other than box H/ACA snoRNA might be affected by the *swoC1* mutation. It is also possible that the PUA domain might serve as a DNA binding domain since yeast Cbf5p has been shown to bind centromere and kinetochore complexes *in vitro* (Jiang *et al.* 1993).

We cannot rule out the possibility that the *swoC1* mutation does not directly cause the nonpolar phenotype. Many different mutations have been reported to result in a nonpolar phenotype. In yeast, defects in a 60S ribosomal subunit protein QSR1 (Eisinger *et al.* 1997), a C53 subunit of RNA polymerase (Mann *et al.* 1992) and a ubiquitin ligase SCF (Patton *et al.* 2000) result in formation of large unbudded cells. In *A. nidulans*, two polarity-defective ts- mutants (*podG* and *podH*) have defects in the alpha subunit of mitochondrial phenylalanyl--tRNA synthase and transcription factor IIF interacting component of the CTD phosphatase, respectively (Osherov *et al.* 2000). Also protein modification is critical in polarity establishment (Shaw *et al.* 2002). This evidence suggests that polarity establishment requires coordination of multiple processes. The *swoC1* mutation may perturb one or more of the processes, which may block polarity establishment. However, based on the nuclear distribution defect of the *swoC1* mutant and that nuclear migration defect can cause isotropic growth in *A. nidulans* (Chiu *et al.* 1997), it is more likely that problems with nuclear migration and proper nuclear positioning cause the nonpolar phenotype of *swoC1*.

ACKNOWLEDGMENTS

This work was sponsored by Department of Energy Biosciences grant DE-FG02-97ER20275 to MM. We thank Dr. Brian Shaw for assistance in sequencing and

identification of complementing plasmid and valuable suggestions, Gretel Guest for AGA22 construction, and Dr. Greg May for providing the plasmid library used in this work.

Table 2.1

Mitotic mapping of the *swoC* gene[a]

CHR		I	II	III	IV	V	VI	VII
marker	*ts-*	*adE20*$^{-}$	*acrA*^{r}	*phenA*$_2^{-}$	*pyroA*$_4^{-}$	*lysB*$_5^{-}$	*sB*$_3^{-}$	*nicB*$_8^{-}$
swoC1	100	57	43	100	54	78	75	54

[a] AGA22 (*swoC1; pabaA*) and mitotic mapping strain A104 (*yA2; adE20; AcrA1; phenA2; pyroA4; lysB5; sB3; nicB8; coA1*) were fused to create a diploid. The percentage of haploid sectors with markers segregated in repulsion to the *swoC1* ts- phenotype after treatment with benomyl is shown. The chromosome VIII marker in the mitotic mapping strain A104 has a ts- phenotype (compact morphology), which makes it impossible to score at the same time as *swoC1* (ts-). Out of 300 haploid sectors, only 28 were ts-, which may be caused by reduced viability of the ts- strain.

Table 2.2

Meiotic mapping of the *swoC* gene[a]

Marker	*choA1*	*galE9*	*phenA2*	*sC12*
Map unit[b]	>50	30.5	0	25.4

[a] AGA22 (*swoC1; pabaA*) and A457 (*proA1; biA1; galE9; sC12; diA1; phenA2; choA1*) were crossed. Ascospores (n = 350) were collected and markers were scored.

[b] Map units between *swoC1* and other markers were calculated based on recombination frequency of ts- strains. Only 59 of the progeny were ts-, which may be caused by reduced viability of ts- strain.

Figure 2.1. Polarity establishment is delayed in the *swoC1* mutant. Conidia of wild type A773 and *swoC1* mutant AXL8 were incubated for 6 hr (a, b) and 8hr (c, d) respectively at permissive temperature (30?), fixed, and stained with Hoechst 33258. (a, b) wild type, (c, d) *swoC1* mutant. The upper and lower rows show D.I.C and fluorescent images of the same field. Bar, 5 ? m.

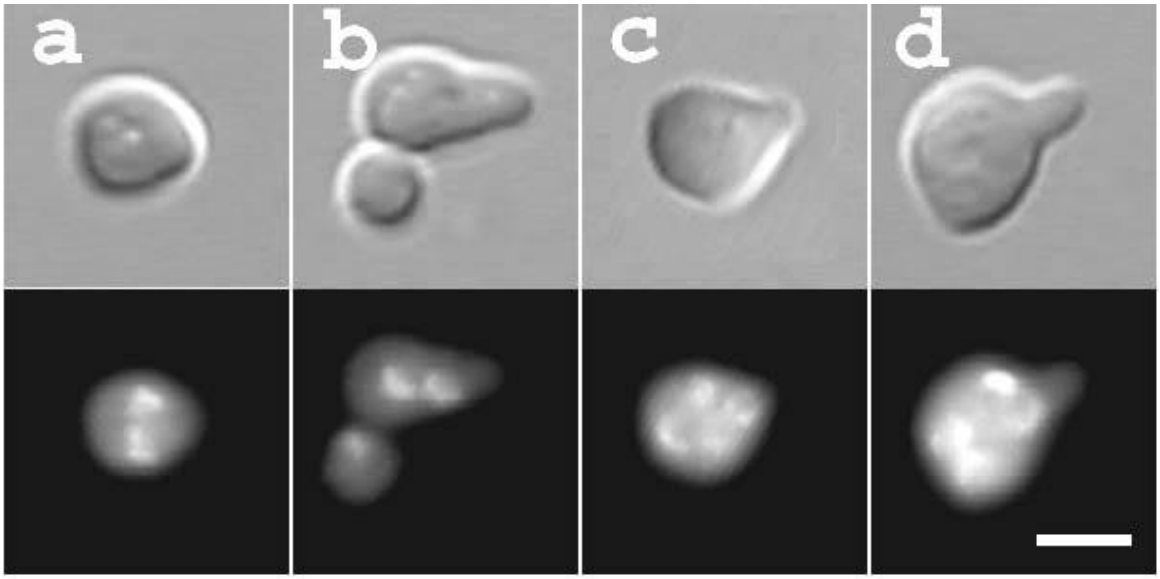
a
b
c
d

Figure 2.2. The *swoC1* mutant continues isotropic growth with extended incubation at restrictive temperature. Conidia of (a) wild type A773 and (b, c) *swoC1* mutant AXL8 were incubated at restrictive temperature (42?) for (a, b) 12 hr or (c) 24 hr, fixed, and stained with Hoechst 33258. The upper and lower rows show D.I.C. and fluorescent images of the same field. Bar, 5 ? m.

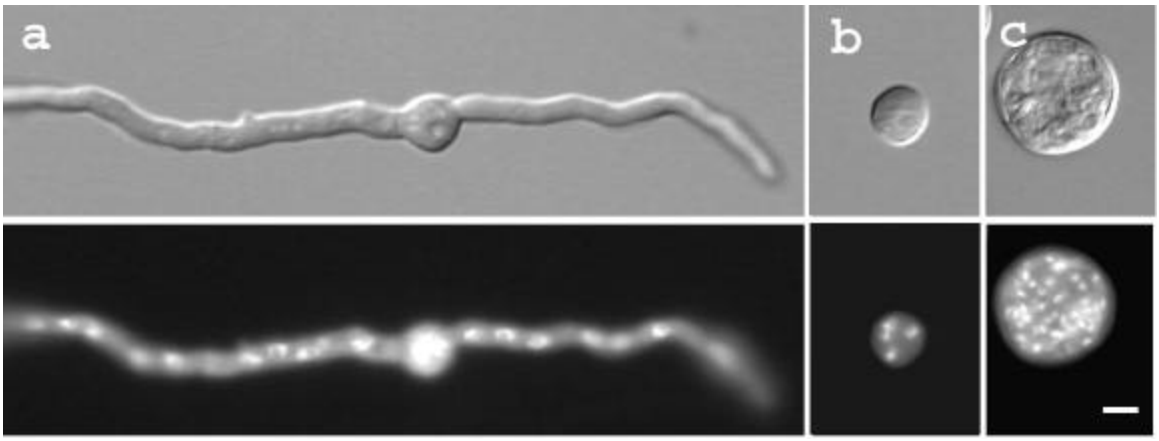
a
b
c

Figure 2.3. The *swoC1* mutant sends out multiple germ tubes after extended incubation at restrictive temperature. Conidia of *swoC1* mutant AXL8 were incubated at restrictive temperature (42 ^{o}) for (a) 4 hr, (b) 10 hr, (c) 24 hr and shifted to permissive temperature (30^{o}) for 10 hr (d, e, f, respectively). (g) Conidia of *swoC1* mutant AXL8 were incubated at restrictive temperature (42 ^{o}) for 20hr and shifted to permissive temperature (30^{o}) for 3 hr. Bars, 5 ? m.

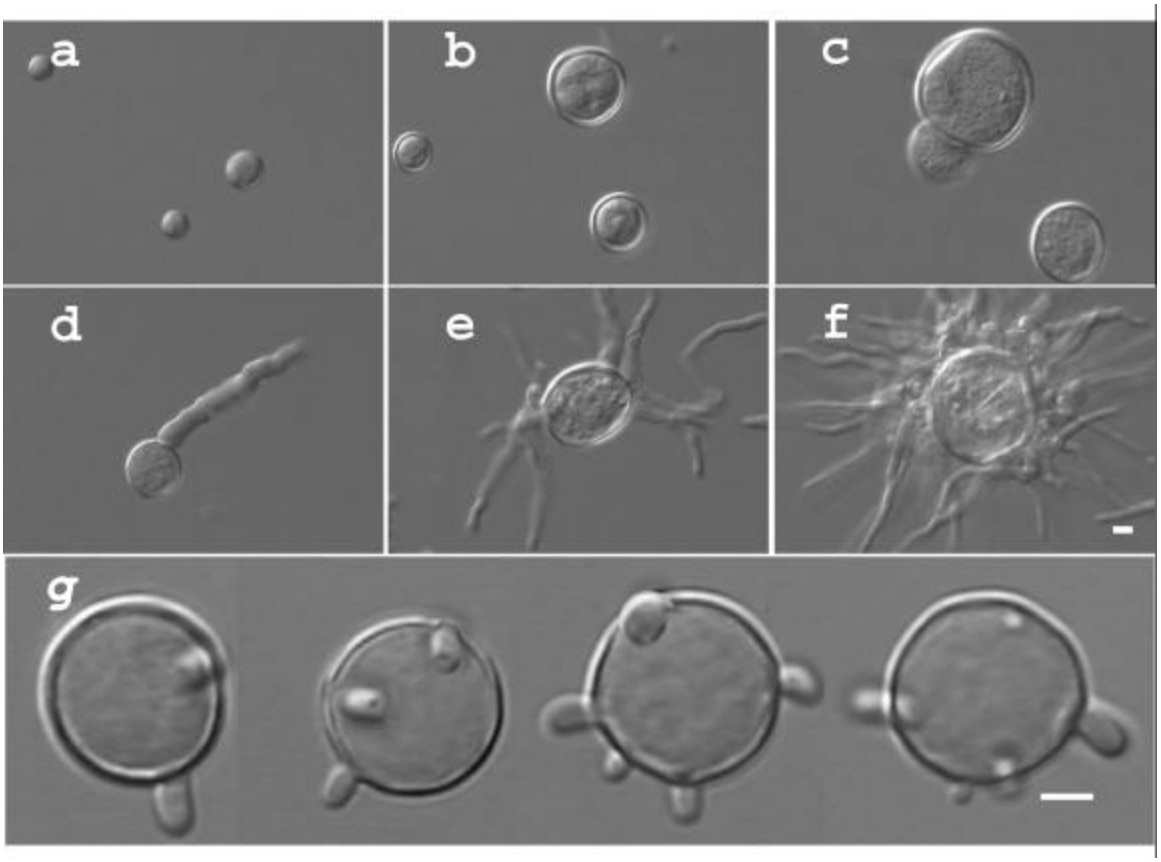
a
b
c
d
e
f
g

Figure 2.4. The *swoC1* mutant is defective in endocytosis. Conidia of wild type A773 and *swoC1* mutant AXL8 were incubated at 42^{o} for 16 hr and treated with 20 ?M FM4-64 or 20 ?M FM4-64 with 10 mMNaZ_3 for 30 min. (a) *swoC1* (b) *swoC1* with NaZ_3, (c) wild type, inset: wild type growing isotropically at 42^{o} for 4 hr, (d) wild type with NaZ_3. Bars, 5 ?m.

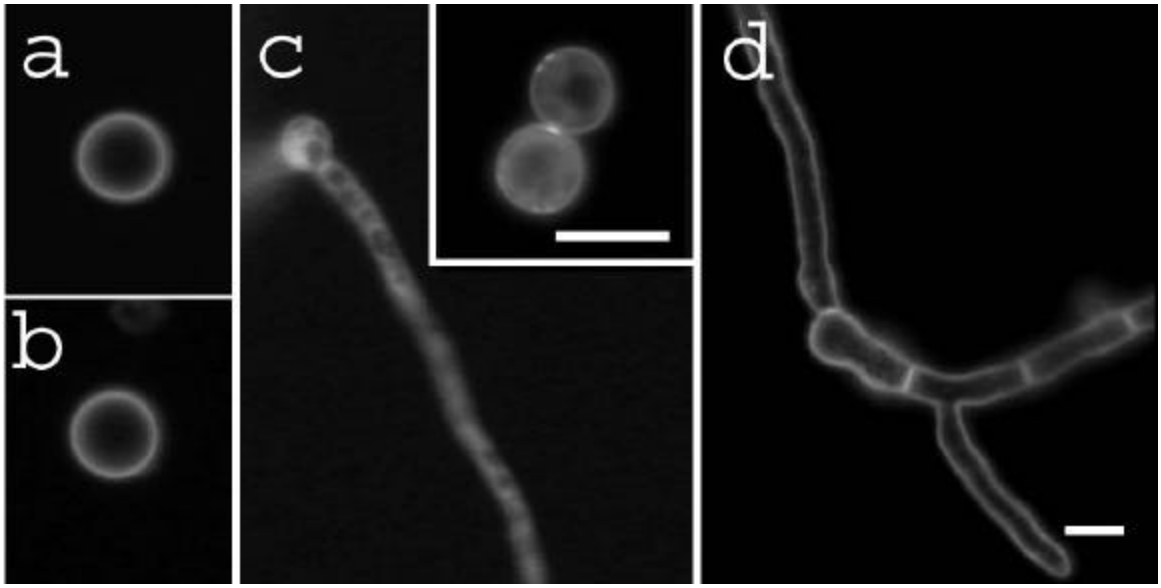
a
b
c
d

Figure 2.5. The *swoC1* mutant shows variation in compartment length and nuclear number after a delay in polarity establishment. Conidia of wild type A773 and *swoC1* mutant AXL8 were incubated at restrictive temperature (42 ^{o}) for 9 hr and shifted to permissive temperature (30^{o}) for 15 hr. Cells were fixed, stained with Hoechst 33258 and Calcolfluor and nuclear number per compartment and compartment length were measured (n=120). Panel A: micrographs of *swoC1* (a-c) and wild type (d). (a) *swoC1* compartment with crowded nuclei, (b) *swoC1* compartment with 10 nuclei, (c) *swoC1* compartment with no nuclei, (d) wild type compartments with relatively uniform length and 2-4 nuclei. Arrows point to septa. Bar, 5 ? m. Panel B: compartment length, Panel C: number of nuclei per compartment.

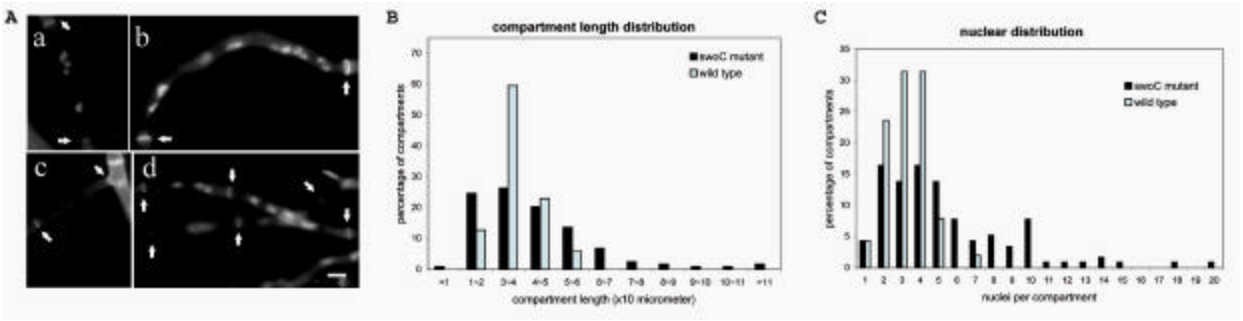
A
a
b
c
d
B
compartment length distribution
avoC mutant
wild type
percentage of compartments
compartment length (x10 micrometer)
C
nuclear distribution
avoC mutant
wild type
percentage of compartments
nuclei per compartment

Figure 2.6. The *swoC1* mutant shows abnormal conidiation after a delay in polarity establishment. (a-d) Wild type A773 and (e-h) *swoC1* mutant AXL8 were grown at 42^{o} for 9hr before shifted to 30^{o} for 2 days. Cells were fixed in 100% ethanol. (a) swollen vesicle, (b) metulae, (c) phialides, (d) chains of conidia, (e) metulae, (f-h) chains of conidia. Bar, 10 ? m.

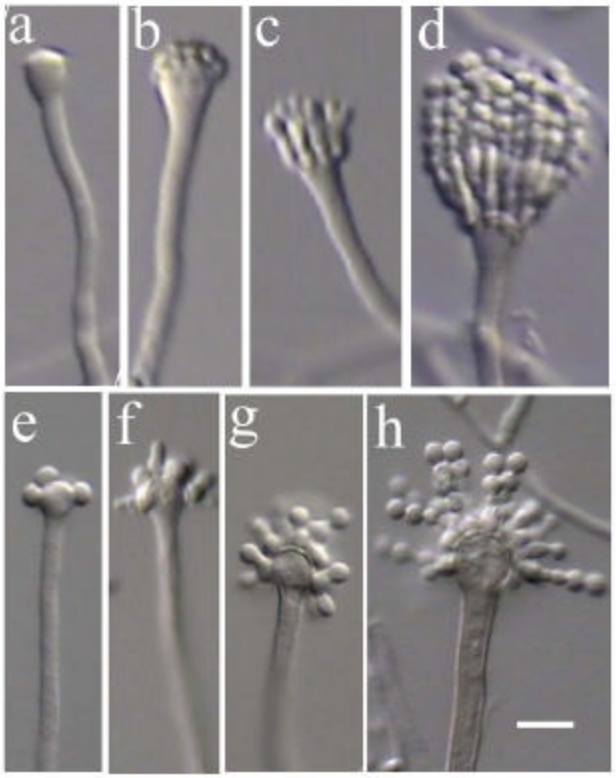
a
b
c
d
e
f
g
h

Figure 2.7. Alignment of rRNA pseudouridine synthases. SwoC1p is from *A. nidulans*, KlCbf5p from *K. lactis*, ScCbf5p from *S. cerevisiae* and Dkc1p from *H. sapiens*. Black shading indicates identical or highly similar residues. Dark and light gray indicate 75% and 50% shared similar residues, respectively. Position of E10 Tn insertion is indicated by an arrow below the sequence. The *swoC1* V338F mutation is indicated by an asterisk and an F below the sequence. The positions of predicted motifs are indicated by the broken line beneath the sequence and labeled as follows: TRUB: pseudouridylate synthase domain, PUA: RNA binding domain, MT-Binding: a microtubule binding domain, NLS: nuclear localization signal, Coiled-coil: protein-protein interaction domain.

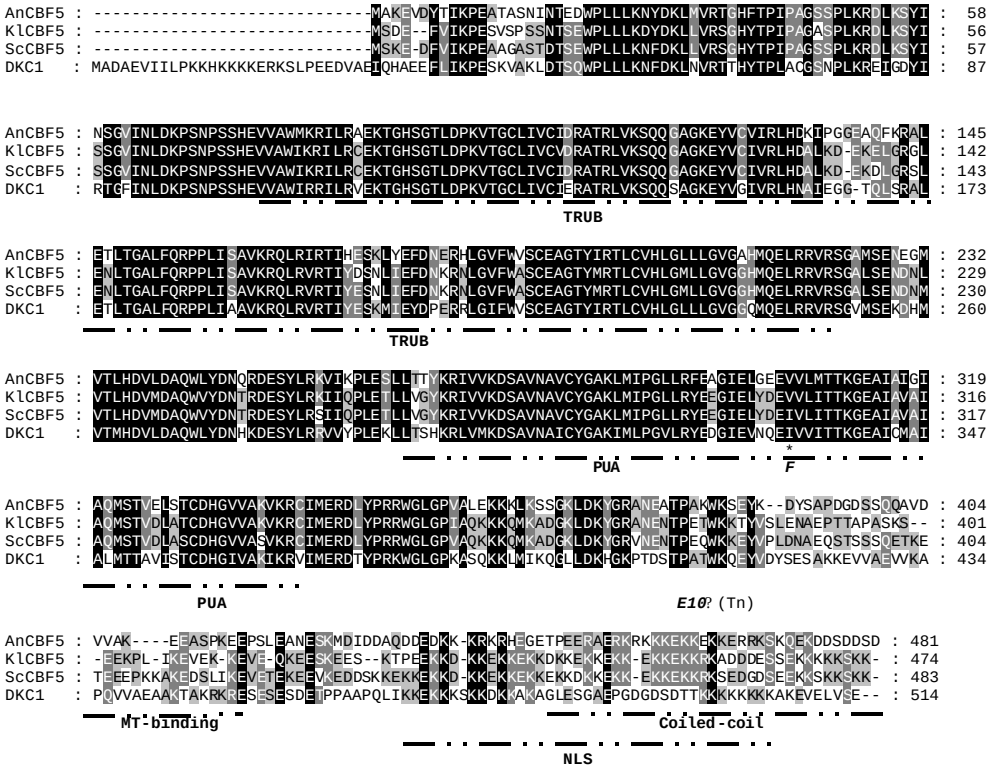
AnCBF5 : ----------MAKEVDYIIKPEATASNINTEDWPLLLKNYDKLMVRTGHFTPIPAGSSPLKRDLKSYI : 58
KlCBF5 : ----------MSDE--FVIKPESVSPSSNTSEWPLLLKDYDKLLVRSGHYTPIPAGASPLKRDLKSYI : 56
ScCBF5 : ----------MSKE-DFVIKPEAAGASTDTSEWPLLLKNFDKLLVRSGHYTPIPAGSSPLKRDLKSYI : 57
DKC1 : MADAEVIILPKKHKKKKERKSLPEEDVAEIQHAEEFLIKPESKVAKLDTSQWPLLLKNFDKLNVRTTHYTPLACGSNPLKREIGDYI : 87
AnCBF5 : NSGVINLDKPSNPSSHEVVAWMKRILRAEKTGHSGTLDPKVTGCLIVCIDRATRLVKSQQGAGKEYVCVIRLHDKIPGGEAQFKRAL : 145
KlCBF5 : SSGVINLDKPSNPSSHEVVAWIKRILRQEKTGHSGTLDPKVTGCLIVCVDRATRLVKSQQGAGKEYVCIVRLHDALKD-EKELGRGL : 142
ScCBF5 : SSGVINLDKPSNPSSHEVVAWIKRILRQEKTGHSGTLDPKVTGCLIVCIDRATRLVKSQQGAGKEYVCIVRLHDALKD-EKDLGRSL : 143
DKC1 : RTGFINLDKPSNPSSHEVVAWIRRILRVEKTGHSGTLDPKVTGCLIVCIERATRLVKSQQSAGKEYVGIVRLHNAIEGG-TQLSRAL : 173
TRUB
AnCBF5 : ETLTGALFQRPPLISAVKRQLRIRTIHESKLYEFDNERHLGVFWVSCEAGTYIRTLCVHLGLLLGVGAHMQELRRVRSGAMSENEGM : 232
KlCBF5 : ENLTGALFQRPPLISAVKRQLRVRTIYDSNLIEFDNKRNLGVFWASCEAGTYMRTLCVHLGMLLGVGGHMQELRRVRSGALSENDNL : 229
ScCBF5 : ENLTGALFQRPPLISAVKRQLRVRTIYESNLIEFDNKRNLGVFWASCEAGTYMRTLCVHLGMLLGVGGHMQELRRVRSGALSENDNM : 230
DKC1 : ETLTGALFQRPPLIAAVKRQLRVRTIYESKMIEYDPERRLGIFWVSCEAGTYIRTLCVHLGLLLGVGGQMQELRRVRSGVMSEKDHM : 260
TRUB
AnCBF5 : VTLHDVLDAQWLYDNQRDESYLRKVIKPLESLLTTYKRIVVKDSAVNAVCYGAKLMIPGLLRFEAGIELGEEVVLMTTKGEAIAIGI : 319
KlCBF5 : VTLHDVMDAQWVYDNTRDESYLRKIIQPLETLLVGYKRIVVKDSAVNAVCYGAKLMIPGLLRYEEGIELYDEVVLITTKGEAIAVAI : 316
ScCBF5 : VTLHDVMDAQWVYDNTRDESYLRSIIQPLETLLVGYKRIVVKDSAVNAVCYGAKLMIPGLLRYEEGIELYDEIVLITTKGEAIAVAI : 317
DKC1 : VTMHDVLDAQWLYDNHKDESYLRRVVYPLEKLLTSHKRLVMKDSAVNAICYGAKIMLPGVLRYEDGIEVNQEIVVITTKGEAICMAI : 347
PUA
F
AnCBF5 : AQMSTVELSTCDHGVVAKVKRCIMERDLYPRRWGLGPVALEKKKLKSSGKLDKYGRANEATPAKWKSEYK--DYSAPDGDSSQQAVD : 404
KlCBF5 : AQMSTVDLATCDHGVVAKVKRCIMERDLYPRRWGLGPIAQKKKQMKADGKLDKYGRANENTPETWKKTYVSLENAEPTTAPASKS-- : 401
ScCBF5 : AQMSTVDLASCDHGVVASVKRCIMERDLYPRRWGLGPVAQKKKQMKADGKLDKYGRVNENTPEQWKKEYVPLDNAEQSTSSSQETKE : 404
DKC1 : ALMTTAVLSTCDHGIVAKIKRVIMERDTYPRKWGLGPKASQKKLMIKQGLLDKHGKPTDSTPATWKQEYVDYSESAKKEVVAEVVKA : 434
PUA
E10? (Tn)
AnCBF5 : VVAK----EEASPKEEPSLEANESKMDIDDAQDDEDKK-KRKRHEGETPEERAERKRKKKEKKEKKERRKSKQEKDDSDDSD : 481
KlCBF5 : -EEKPL-IKEVEK-KEVE-QKEESKEES--KTPEEKKD-KKEKKEKKDKKEKKEKK-EKKEKKRKADDDESSEKKKKSKK- : 474
ScCBF5 : TEEEPKKAKEDSLIKEVETEKEEVKEDDSKKEKKEKKD-KKEKKEKKEKKDKKEKK-EKKEKKRKSEDGDSEEKKSKKSKK- : 483
DKC1 : PQVVAEAATAKRKKRESESESDEIPPAAPQLIKKEKKKSKKDKKAKAGLESGAEPGDGDSDTTKKKKKKKAKEVELVSE-- : 514
MT-binding
Coiled-coil
NLS

Figure 2.8. Heterozygous strains with *swoC* null allele and C-terminal deletion allele. Left panel shows the southern blot of the heterozygous diploid (1) with one copy of *swoC* replaced by *argB* and (2) the heterozygous diploid with *argB* replacing the C-terminus of *swoC*. Genomic DNA was digested with *Kpn*I and probed with randomly labeled 3' flanking sequence. Sizes (kb) based on molecular markers are shown at left. Right panel shows the restriction map of (a) wild type *swoC*, (b) *argB* replacement of *swoC*, (c) *argB* replacement of *swoC* C-terminus. Fragment sizes after restriction digestion are indicated below. K: *Kpn*I. 5F and 3F: 5' and 3' flanking sequences respectively.

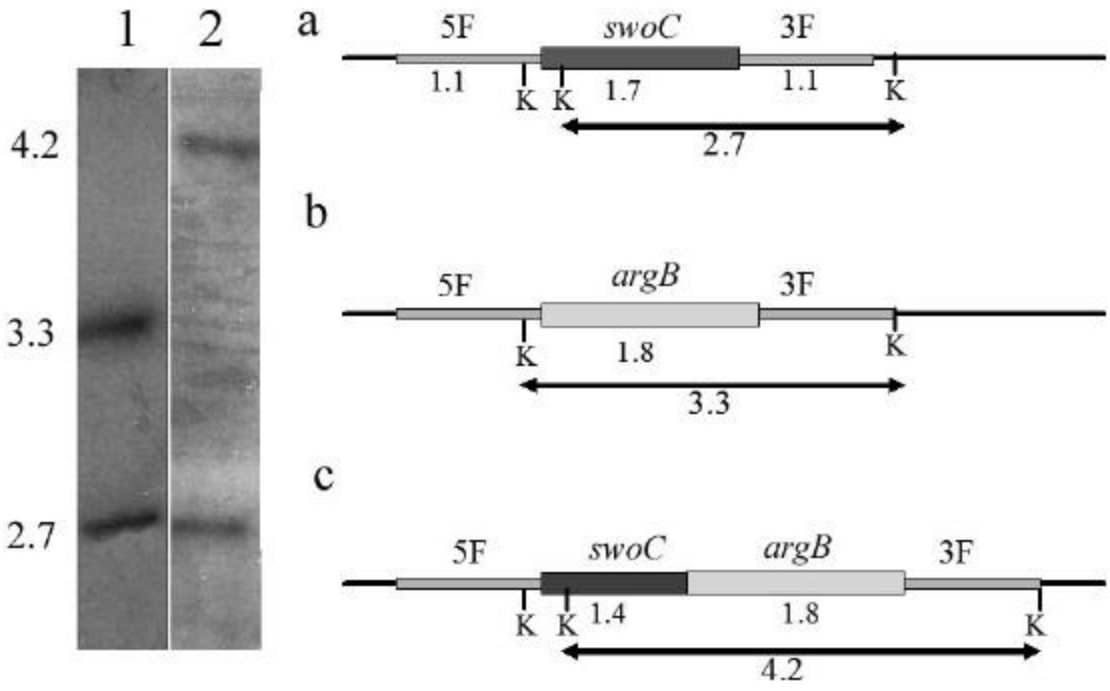
1
2
4.2
3.3
2.7
a
5F
swoC
3F
1.1
K
K
1.7
1.1
K
2.7
b
5F
argB
3F
K
1.8
K
3.3
c
5F
swoC
argB
3F
K
K
1.4
1.8
K
4.2

Figure 2.9. Transposon insertions affect the ability of p8c1 to complement *swoC1*. The *swoC1* mutant carrying p8c1 with transposon insertions was grown at restrictive temperature (42^{o}) for 2 days. The *swoC1* mutant transformed with (a) p8c1-E10, (b) p8c1-H07, (c) p8c1-A11, (d) p8c1, (e) no plasmid. Position of insertions is indicated diagrammatically at right. Grey bars: exons. Black lines: introns.

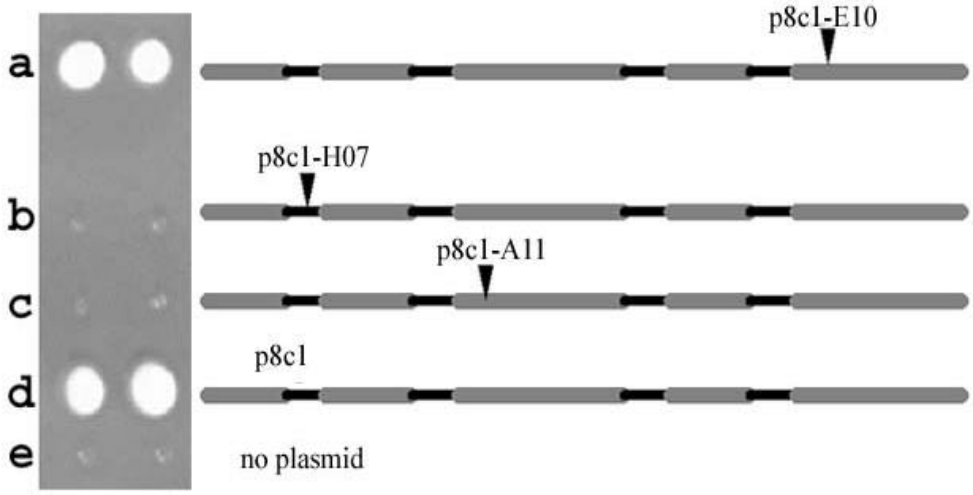
a
b
c
d
e
p8c1-E10
p8c1-H07
p8c1-A11
p8c1
no plasmid

Figure 2.10. The *swoC1* mutant shows normal level of pseudouridine. Total RNA was isolated from wild type and *swoC1* incubated at 42^{o} for 18 hr, enzymatically digested, and analyzed by HPLC-MS. Numbered peaks were identified by MS as follows: (1) pseudouridine, (2) cytidine, (3) uridine, (4) guanosine, (5) adenosine, (6) 2'-O-methylated adenosine.

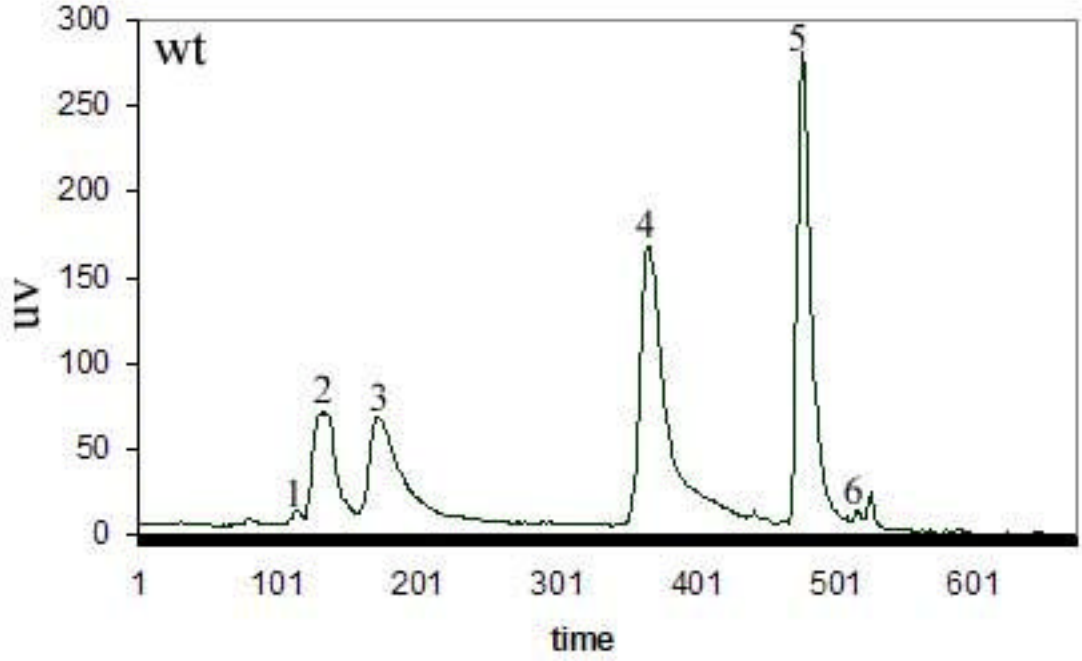
wt
uv
time
300
250
200
150
100
50
0
1
101
201
301
401
501
601
1
2
3
4
5
6

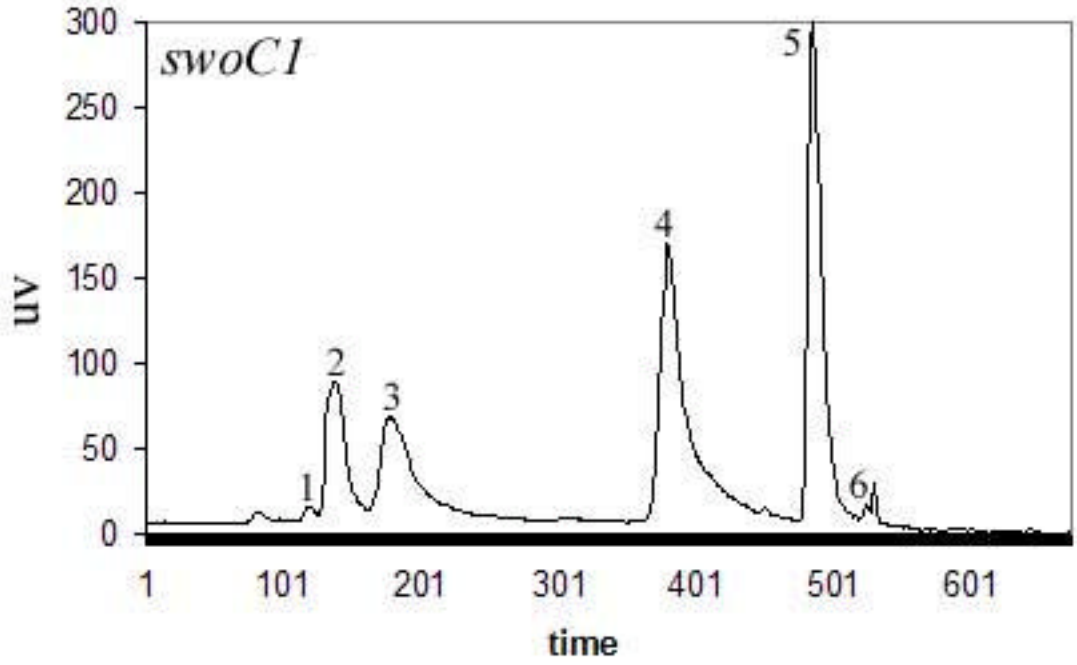
swoC1
uv
time
300
250
200
150
100
50
0
1
101
201
301
401
501
601
1
2
3
4
5
6

REFERENCES

Adams, T. H., J. K. Wieser and J. H. Yu, 1998 Asexual sporulation in *Aspergillus nidulans*. Microbiol Mol Biol Rev **62:** 35-54.

Amuro, Y., H. Nakaoka, S. Shimomura, S. Tamura, T. Hada *et al.*, 1988 Rapid high-performance liquid chromatography for pseudouridine assay in serum and urine. Clin Chim Acta **172:** 117-122.

Aravind, L., and E. V. Koonin, 1999 Novel predicted RNA-binding domains associated with the translation machinery. J Mol Evol **48:** 291-302.

Bachewich, C., and I. B. Heath, 1998 Radial F-actin arrays precede new hypha formation in Saprolegnia: implications for establishing polar growth and regulating tip morphogenesis. J Cell Sci **111 (Pt 14):** 2005-2016.

Becker, H. F., Y. Motorin, R. J. Planta and H. Grosjean, 1997 The yeast gene YNL292w encodes a pseudouridine synthase (Pus4) catalyzing the formation of psi55 in both mitochondrial and cytoplasmic tRNAs. Nucleic Acids Res **25:** 4493-4499.

Bousquet-Antonelli, C., Y. Henry, P. G'Elugne J, M. Caizergues-Ferrer and T. Kiss, 1997 A small nucleolar RNP protein is required for pseudouridylation of eukaryotic ribosomal RNAs. Embo J **16:** 4770-4776.

Cadwell, C., H. J. Yoon, Y. Zebarjadian and J. Carbon, 1997 The yeast nucleolar protein Cbf5p is involved in rRNA biosynthesis and interacts genetically with the RNA polymerase I transcription factor RRN3. Mol Cell Biol **17:** 6175-6183.

Chant, J., 1999 Cell polarity in yeast. Annu Rev Cell Dev Biol **15:** 365-391.

Chant, J., M. Mischke, E. Mitchell, I. Herskowitz and J. R. Pringle, 1995 Role of Bud3p in producing the axial budding pattern of yeast. J Cell Biol **129:** 767-778.

Charette, M., and M. W. Gray, 2000 Pseudouridine in RNA: what, where, how, and why. IUBMB Life **49:** 341-351.

Chiu, Y. H., X. Xiang, A. L. Dawe and N. R. Morris, 1997 Deletion of nudC, a nuclear migration gene of *Aspergillus nidulans*, causes morphological and cell wall abnormalities and is lethal. Mol Biol Cell **8:** 1735-1749.

Dez, C., A. Henras, B. Faucon, D. Lafontaine, M. Caizergues-Ferrer *et al.*, 2001 Stable expression in yeast of the mature form of human telomerase RNA depends on its association with the box H/ACA small nucleolar RNP proteins Cbf5p, Nhp2p and Nop10p. Nucleic Acids Res **29:** 598-603.

Eisinger, D. P., F. A. Dick and B. L. Trumpower, 1997 Qsr1p, a 60S ribosomal subunit protein, is required for joining of 40S and 60S subunits. Mol Cell Biol **17:** 5136-5145.

Fiddy, C., and A. P. Trinci, 1976 Mitosis, septation, branching and the duplication cycle in *Aspergillus nidulans.* J Gen Microbiol **97:** 169-184.

Fischer-Parton, S., R. M. Parton, P. C. Hickey, J. Dijksterhuis, H. A. Atkinson *et al.*, 2000 Confocal microscopy of FM4-64 as a tool for analysing endocytosis and vesicle trafficking in living fungal hyphae. J Microsc **198:** 246-259.

Ganot, P., M. L. Bortolin and T. Kiss, 1997 Site-specific pseudouridine formation in preribosomal RNA is guided by small nucleolar RNAs. Cell **89:** 799-809.

Goodson, H. V., B. L. Anderson, H. M. Warrick, L. A. Pon and J. A. Spudich, 1996 Synthetic lethality screen identifies a novel yeast myosin I gene (MYO5): myosin I proteins are required for polarization of the actin cytoskeleton. J Cell Biol **133:** 1277-1291.

Gutgsell, N. S., M. D. Del Campo, S. Raychaudhuri and J. Ofengand, 2001 A second function for pseudouridine synthases: A point mutant of RluD unable to form pseudouridines 1911, 1915, and 1917 in *Escherichia coli* 23S ribosomal RNA restores normal growth to an RluD-minus strain. Rna **7:** 990-998.

Harris, S. D., A. F. Hofmann, H. W. Tedford and M. P. Lee, 1999 Identification and characterization of genes required for hyphal morphogenesis in the filamentous fungus *Aspergillus nidulans.* Genetics **151:** 1015-1025.

Harris, S. D., J. L. Morrell and J. E. Hamer, 1994 Identification and characterization of *Aspergillus nidulans* mutants defective in cytokinesis. Genetics **136:** 517-532.

Heiss, N. S., S. W. Knight, T. J. Vulliamy, S. M. Klauck, S. Wiemann *et al.*, 1998 X-linked dyskeratosis congenita is caused by mutations in a highly conserved gene with putative nucleolar functions. Nat Genet **19:** 32-38.

Herman, P. K., and J. Rine, 1997 Yeast spore germination: a requirement for Ras protein activity during re-entry into the cell cycle. Embo J **16:** 6171-6181.

Jiang, W., K. Middleton, H. J. Yoon, C. Fouquet and J. Carbon, 1993 An essential yeast protein, CBF5p, binds in vitro to centromeres and microtubules. Mol Cell Biol **13:** 4884-4893.

Kafer, E., 1977 Meiotic and mitotic recombination in Aspergillus and its chromosomal aberrations. Adv Genet **19:** 33-131.

Knight, S. W., N. S. Heiss, T. J. Vulliamy, S. Greschner, G. Stavrides *et al.*, 1999 X-linked dyskeratosis congenita is predominantly caused by missense mutations in the DKC1 gene. Am J Hum Genet **65:** 50-58.

Kron, S. J., C. A. Styles and G. R. Fink, 1994 Symmetric cell division in pseudohyphae of the yeast *Saccharomyces cerevisiae*. Mol Biol Cell **5:** 1003-1022.

Lafontaine, D. L., C. Bousquet-Antonelli, Y. Henry, M. Caizergues-Ferrer and D. Tollervey, 1998 The box H + ACA snoRNAs carry Cbf5p, the putative rRNA pseudouridine synthase. Genes Dev **12:** 527-537.

Ma, G. C., and E. Kafer, 1974 Genetic analysis of the reciprocal translocation T2(I;8) of Asperigillus using the technique of mitotic mapping in homozygous translocation diploids. Genetics **77:** 11-23.

Madden, K., and M. Snyder, 1992 Specification of sites for polarized growth in *Saccharomyces cerevisiae* and the influence of external factors on site selection. Mol Biol Cell **3:** 1025-1035.

Madden, K., and M. Snyder, 1998 Cell polarity and morphogenesis in budding yeast. Annu Rev Microbiol **52:** 687-744.

Maden, B. E., and J. M. Hughes, 1997 Eukaryotic ribosomal RNA: the recent excitement in the nucleotide modification problem. Chromosoma **105:** 391-400.

Mann, C., J. Y. Micouin, N. Chiannilkulchai, I. Treich, J. M. Buhler *et al.*, 1992 RPC53 encodes a subunit of *Saccharomyces cerevisiae* RNA polymerase C (III) whose inactivation leads to a predominantly G1 arrest. Mol Cell Biol **12:** 4314-4326.

Marciniak, R. A., F. B. Johnson and L. Guarente, 2000 Dyskeratosis congenita, telomeres and human ageing. Trends Genet **16:** 193-195.

Micklem, D. R., 1995 mRNA localisation during development. Dev Biol **172:** 377-395.

Mitchell, J. R., J. Cheng and K. Collins, 1999 A box H/ACA small nucleolar RNA-like domain at the human telomerase RNA 3' end. Mol Cell Biol **19:** 567-576.

Momany, M., 2002 Polarity in filamentous fungi: establishment, maintenance and new axes. Curr Opin Microbiol **5:** 580-585.

Momany, M., and J. E. Hamer, 1997 The *Aspergillus nidulans* Septin Encoding Gene, aspB, Is Essential for Growth. Fungal Genet Biol **21:** 92-100.

Momany, M., and I. Taylor, 2000 Landmarks in the early duplication cycles of *Aspergillus fumigatus* and *Aspergillus nidulans:* polarity, germ tube emergence and septation. Microbiology **146:** 3279-3284.

Momany, M., P. J. Westfall and G. Abramowsky, 1999 *Aspergillus nidulans swo* mutants show defects in polarity establishment, polarity maintenance and hyphal morphogenesis. Genetics **151:** 557-567.

Ofengand, J., 2002 Ribosomal RNA pseudouridines and pseudouridine synthases. FEBS Lett **514:** 17-25.

Osherov, N., J. Mathew and G. S. May, 2000 Polarity-defective mutants of *Aspergillus nidulans*. Fungal Genet Biol **31:** 181-188.

Osherov, N., and G. May, 2000 Conidial germination in *Aspergillus nidulans* requires RAS signaling and protein synthesis. Genetics **155:** 647-656.

Palmisano, F., T. Rotunno, M. La Sorsa, C. G. Zambonin and I. Abbate, 1995 Simultaneous determination of pseudouridine, neopterine and creatinine in urine by ion-pair high-performance liquid chromatography with in-series ultraviolet and fluorescence detection. Analyst **120:** 2185-2189.

Patteson, K. G., L. P. Rodicio and P. A. Limbach, 2001 Identification of the mass-silent post-transcriptionally modified nucleoside pseudouridine in RNA by matrix-

assisted laser desorption/ionization mass spectrometry. Nucleic Acids Res **29:** E49-49.

Patton, E. E., C. Peyraud, A. Rouillon, Y. Surdin-Kerjan, M. Tyers *et al.*, 2000 SCF(Met30)-mediated control of the transcriptional activator Met4 is required for the G(1)-S transition. Embo J **19:** 1613-1624.

Peculis, B., 1997 RNA processing: pocket guides to ribosomal RNA. Curr Biol **7:** R480-482.

Pienkowska, J., and Z. Szweykowska-Kulinska, 2001 Pseudouridine synthases--enzymes introducing the most abundant modified nucleoside in nucleic acids--pseudouridine. Postepy Biochem **47:** 232-242.

Pomerantz, S. C., and J. A. McCloskey, 1990 Analysis of RNA hydrolyzates by liquid chromatography-mass spectrometry. Methods Enzymol **193:** 796-824.

Pruyne, D., and A. Bretscher, 2000a Polarization of cell growth in yeast. J Cell Sci **113:** 571-585.

Pruyne, D., and A. Bretscher, 2000b Polarization of cell growth in yeast. I. Establishment and maintenance of polarity states. J Cell Sci **113:** 365-375.

Rasmussen, C. D., K. P. Lu, R. L. Means and A. R. Means, 1992 Calmodulin and cell cycle control. J Physiol Paris **86:** 83-88.

Roberts, R. L., and G. R. Fink, 1994 Elements of a single MAP kinase cascade in *Saccharomyces cerevisiae* mediate two developmental programs in the same cell type: mating and invasive growth. Genes Dev **8:** 2974-2985.

Roze, L. V., N. Mahanti, R. Mehigh, D. G. McConnell and J. E. Linz, 1999 Evidence that MRas1 and MRas3 proteins are associated with distinct cellular functions during

growth and morphogenesis in the fungus *Mucor racemosus*. Fungal Genet Biol **28:** 171-189.

Russo, T., F. Salvatore and F. Cimino, 1984 Determination of pseudouridine in tRNA and in acid-soluble tissue extracts by high-performance liquid chromatography. J Chromatogr **296:** 387-393.

Sambrook, J., E. Fritsch and T. Maniatis, 1989 *Molecular Cloning, A Laboratory Manual*. Cold Spring Harbor Laboartory Press.

Santos, B., and M. Snyder, 1997 Targeting of chitin synthase 3 to polarized growth sites in yeast requires Chs5p and Myo2p. J Cell Biol **136:** 95-110.

Shafaatian, R., M. A. Payton and J. D. Reid, 1996 PWP2, a member of the WD-repeat family of proteins, is an essential *Saccharomyces cerevisiae* gene involved in cell separation. Mol Gen Genet **252:** 101-114.

Shaw, B. D., C. Momany and M. Momany, 2002 *Aspergillus nidulans swoF* encodes an N-myristoyl transferase. Eukaryot Cell **1:** 241-248.

Shingfield, K. J., and N. W. Offer, 1999 Simultaneous determination of purine metabolites, creatinine and pseudouridine in ruminant urine by reversed-phase high-performance liquid chromatography. J Chromatogr B Biomed Sci Appl **723:** 81-94.

Shulman, J. M., and D. St Johnston, 1999 Pattern formation in single cells. Trends Cell Biol **9:** M60-64.

Stebbings, H., 2001 Cytoskeleton-dependent transport and localization of mRNA. Int Rev Cytol **211:** 1-31.

Stephen, S., N. J. Talbot and H. Stebbings, 1999 Poly(A) mRNA is attached to insect ovarian microtubules in vivo in a nucleotide-sensitive manner. Cell Motil Cytoskeleton **43:** 159-166.

Svoboda, A., I. Slaninova and A. Holubarova, 2001 Cytoskeleton in regenerating protoplasts and restoration of cell polarity in the yeast *Saccharomyces cerevisiae*. Acta Biol Hung **52:** 325-333.

Timberlake, W. E., 1991 Temporal and spatial controls of Aspergillus development. Curr Opin Genet Dev **1:** 351-357.

Trinci, A. P. J., 1978 Fungal walls and hyphal growth, pp. 319-358 in *Symposium of the British Mycological Society*, edited by B. J. H. a. T. A.P.J. Cambridge University Press, Queen Elizabeth College, London.

Umegae, Y., H. Nohta and Y. Ohkura, 1990 Determination of pseudouridine in human urine and serum by high-performance liquid chromatography with post-column fluorescence derivatization. J Chromatogr **515:** 495-501.

van Eeden, F., and D. St Johnston, 1999 The polarisation of the anterior-posterior and dorsal-ventral axes during Drosophila oogenesis. Curr Opin Genet Dev **9:** 396-404.

Vida, T. A., and S. D. Emr, 1995 A new vital stain for visualizing vacuolar membrane dynamics and endocytosis in yeast. J Cell Biol **128:** 779-792.

Watanabe, Y., and M. W. Gray, 2000 Evolutionary appearance of genes encoding proteins associated with box H/ACA snoRNAs: cbf5p in *Euglena gracilis*, an early diverging eukaryote, and candidate Gar1p and Nop10p homologs in archaebacteria. Nucleic Acids Res **28:** 2342-2352.

Watkins, N. J., A. Gottschalk, G. Neubauer, B. Kastner, P. Fabrizio *et al.*, 1998 Cbf5p, a potential pseudouridine synthase, and Nhp2p, a putative RNA-binding protein, are present together with Gar1p in all H BOX/ACA-motif snoRNPs and constitute a common bipartite structure. RNA **4:** 1549-1568.

Wendland, J., 2001 Comparison of morphogenetic networks of filamentous fungi and yeast. Fungal Genet Biol **34:** 63-82.

Wendland, J., and P. Philippsen, 2001 Cell polarity and hyphal morphogenesis are controlled by multiple rho-protein modules in the filamentous ascomycete *Ashbya gossypii*. Genetics **157:** 601-610.

Wolkow, T. D., S. D. Harris and J. E. Hamer, 1996 Cytokinesis in *Aspergillus nidulans* is controlled by cell size, nuclear positioning and mitosis. J Cell Sci **109:** 2179-2188.

Yabe, T., T. Yamada-Okabe, S. Kasahara, Y. Furuichi, T. Nakajima *et al.*, 1996 HKR1 encodes a cell surface protein that regulates both cell wall beta-glucan synthesis and budding pattern in the yeast *Saccharomyces cerevisiae*. J Bacteriol **178:** 477-483.

Yaghmai, R., A. Kimyai-Asadi, K. Rostamiani, N. S. Heiss, A. Poustka *et al.*, 2000 Overlap of dyskeratosis congenita with the Hoyeraal-Hreidarsson syndrome. J Pediatr **136:** 390-393.

Yang, Y., C. Isaac, C. Wang, F. Dragon, V. Pogacic *et al.*, 2000 Conserved composition of mammalian box H/ACA and box C/D small nucleolar ribonucleoprotein particles and their interaction with the common factor Nopp140. Mol Biol Cell **11:** 567-577.

Yelton, M. M., J. E. Hamer and W. E. Timberlake, 1984 Transformation of *Aspergillus nidulans* by using a trpC plasmid. Proc Natl Acad Sci U S A **81:** 1470-1474.

Zebarjadian, Y., T. King, M. J. Fournier, L. Clarke and J. Carbon, 1999 Point mutations in yeast CBF5 can abolish in vivo pseudouridylation of rRNA. Mol Cell Biol **19:** 7461-7472.

Ziman, M., D. Preuss, J. Mulholland, J. M. O'Brien, D. Botstein *et al.*, 1993 Subcellular localization of Cdc42p, a *Saccharomyces cerevisiae* GTP-binding protein involved in the control of cell polarity. Mol Biol Cell **4:** 1307-1316.

CHAPTER 3

SWOHP, A NUCLEOSIDE DIPHOSPHATE KINASE, IS ESSENTIAL IN *ASPERGILLUS NIDULANS*[1]

[1]Lin, X., Momany, C., and Michelle Momany. To be submitted to *Eukaryotic Cell.*

ABSTRACT

The temperature sensitive *swoH1* mutant of *Aspergillus nidulans* was swollen and lysed during vegetative growth and did not produce conidia at restrictive temperature. The *swoH* gene was mapped to chromosome II and cloned by complementation of the temperature-sensitive phenotype. The sequence showed that the *swoH* gene encodes a homologue of nucleoside diphosphate kinases (NDKs) from other organisms. Crude cell extracts from the *swoH1* mutant have about 20% of the nucleoside diphosphate kinase activity seen in wild type. Sequencing of the mutant allele showed a predicted V83F change and structural modeling suggested that the *swoH1* mutation would lead to perturbation of the NDK active site, consistent with the observed lower NDK activity in the mutant. An HA-SwoHp fusion complemented the mutant phenotype and the fusion protein possessed phosphate transferase activity in thin layer chromatography assays. Similar to other eukaryotes, *A. nidulans* SwoHp likely forms a hexamer based on protein modeling. Although NDK has been considered a housekeeping enzyme in nucleotide metabolism, recent evidence suggests that it is also an important regulatory protein for many cellular processes in higher organisms. While NDK null mutants of *E. coli*, *P. aeruginosa*, *S. cerevisiae* and *S. pombe* are viable, deletion of the *swoH* gene was lethal in *A. nidulans*, suggesting that NDK plays a more important role in this filamentous fungus.

Index descriptors: *swoH1* mutant, polarity

INTRODUCTION

Spores of the filamentous fungus *Aspergillus nidulans* break dormancy and expand isotropically before switching to polar tip growth. Further growth occurs exclusively at the hyphal tip (Momany and Taylor 2000). The temperature sensitive *swoH1* mutant of *A. nidulans* swells shortly after switching to tip growth at restrictive temperature, and was originally isolated in a screen for polarity maintenance defects (Momany *et al.* 1999).

The sequence of the *swoH* gene reveals that it encodes a homologue of yeast YNK1, a nucleoside diphosphate kinase (NDK). NDKs catalyze the transfer of the ?-phosphate from a nucleoside triphosphate to a nucleoside diphosphate via autophosphorylated enzyme intermediate and are important in nucleotide metabolism (Agarwal *et al.* 1978; Janin and Deville-Bonne 2002). All known eukaryotic and prokaryotic NDKs form oligomers (Dumas *et al.* 1992; Almaula *et al.* 1995; Mesnildrey *et al.* 1998; Polosina *et al.* 1998; Uno *et al.* 2002). Subunit oligomerization has been correlated with the ability of this enzyme to interact with other molecules and is tightly related to its functions (Mesnildrey *et al.* 1997; Mesnildrey *et al.* 1998; Galvis *et al.* 2001).

NDK null mutants of *Escherichia coli* and *Pseudomonas aeruginosa* are viable (Izumiya and Yamamoto 1995; Zaborina *et al.* 1999). Although NDK null mutants of *S. cerevisiae* and *S. pombe* have much lower nucleoside diphosphate kinase activity than wild type (10% and 30% respectively for *S. cerevisiae* and *S. pombe*), they are normal in vegetative growth, sporulation, mating, and morphology (Fukuchi *et al.* 1993; Izumiya and Yamamoto 1995). The only reported NDK mutation in *N. crassa* P72H, causes reduced NDK activity and deficient light response for perithecial polarity (Ogura *et al.* 1999; Ogura *et al.* 2001). Higher organisms contain multiple isoforms of NDK and they

are expressed in a tissue-specific manner and have different subcellular localizations (Gilles *et al.* 1991; Venturelli *et al.* 1995; Munier *et al.* 1998; Ouatas *et al.* 1998; Agou *et al.* 1999; Lee and Lee 1999; Milon *et al.* 2000; Barraud *et al.* 2002; Fournier *et al.* 2002a; Fournier *et al.* 2002b). NDKs are involved in a variety of essential cellular processes in higher organisms. In mammals, NDKs are involved in differentiation, cell survival, tumor metastasis and proliferation (Lee *et al.* 1997; Nosaka *et al.* 1998; Lee and Lee 1999; Postel *et al.* 2000a; Postel *et al.* 2000b; Roymans *et al.* 2000; Amendola *et al.* 2001; Otsuki *et al.* 2001; Roymans *et al.* 2001). In *Drosophila melanogaster* and *Xenopus laevis*, NDKs are essential for development (Chiadmi *et al.* 1993; Ouatas *et al.* 1997; Ouatas *et al.* 1998). In *C. elegans*, NDK seems to be important for embryogenesis (Maeda *et al.* 2001). In plants, NDK interacts with the phytochrome molecules, sensory photoreceptors transducing environmental light signals to responsive nuclear genes (Hasunuma and Yabe 1998; Choi *et al.* 1999; Quail 2000).

MATERIALS AND METHODS

Strains and media. Strains used in this study are listed in Table 3.1. Identification of the temperature sensitive *swoH1* mutant has been previously described (Momany *et al.* 1999). Media used were as previously reported (Momany *et al.* 1999). Strain construction and genetic analysis used standard *A. nidulans* techniques (Ma and Kafer 1974; Kafer 1977; Harris *et al.* 1994).

Growth conditions and microscopic observation. Conditions for growth and preparation of cells were as previously reported (Harris *et al.* 1994). Briefly, spores were inoculated on coverslips in liquid medium in a petri dish. After incubation, cells adhering

to the coverslips were fixed and nuclei were stained with Hoechst 33258 (Sigma, St. Louis). Microscopic observations were made using a Zeiss Axioplan microscope (Thornwood, NY, USA) and digital images were acquired using an Optronics digital imaging system (Goleta, CA, USA). Images were prepared using Photoshop 5.5 (Adobe, Mountain View, CA, USA).

DNA isolation: DNA was isolated from *A. nidulans* using previously described methods (Harris *et al.* 1994).

Cloning by complementation and plasmid rescue. A random genomic autonomously replicating plasmid library carrying the *pyr4* marker provided by Dr. Greg May (University of Texas, M. D. Anderson Cancer Center, Houston, TX, USA) (Osherov and May 2000) was transformed into the *swoH1* mutant AXL20 by protoplasting according to standard *A. nidulans* protocols (Yelton *et al.* 1984). DNA was purified from the *A. nidulans* transformants with *pyrG* prototrophy restored to wild-type growth at restrictive temperature (42ºC). Three plasmids were rescued by transformation of *E. coli* XL1-blue with total DNA from *A. nidulans* transformants. Restriction mapping showed that these plasmids contained the same genomic DNA inserts (data not shown).

Identification and sequencing of the complementing gene by transposon tagging. Transposons were randomly inserted into the complementing plasmid using the GPS-1 system (New England Biolabs, Beverly, MA). The resulting plasmids, each containing one copy of the transposon at random sites, were sequenced using primers unique for the transposon ends on an ABI 3700 DNA Analyzer (Applied Biosystem, CA) according to the manufacturer's instructions. The sequences were assembled and analyzed using Phred (version 0.000925c), Phrap (version 0.990319) and Consed (version 11.0) computer

programs (http://depts.washington.edu/ventures/collabtr/direct/ppccombo.htm) as previously described (Shaw *et al.* 2002). The assembled contig was used to search the NCBI databases (www.ncbi.nlm.nih.gov) using the Blast program to identify open reading frames (ORFs). Plasmids with transposons inserted within the ORFs were transformed into the *swoH1* mutant. Plasmids that failed to rescue the *swoH1* mutant at restrictive temperature were assumed to have transposon insertions disrupting the complementing gene. The genomic sequence of this complementing gene, its intron locations based on protein alignment and consensus splice sequences and the predicted protein sequence are deposited in GenBank (accession no. AY057453).

Mitotic mapping. The *swoH1* mutant strain APW13 was fused with mitotic mapping strain A104 by standard methods (Ma and Kafer 1974). Conidia of the heterozygous diploid were plated in complete medium with proper supplements containing 60 ? g/ml benomyl for two days and transferred to complete medium with supplements for 2 weeks. Genotypes of the resulting haploid sectors were scored.

Meiotic mapping. The *swoH1* mutant strain APW13 was crossed with chromosome II meiotic mapping strain A254. Individual cleistothecia were isolated under a stereomicroscope. Genotypes of ascospores released from cleaned cleistothecia were scored.

Southern Blot. The NDK gene was randomly labeled using the Redi-prime II DNA Labeling System (Amersham Biosciences, NJ) according to the manufacturer's instructions and was used to probe a chromosome specific genomic library (Brody *et al.* 1991) (available from Fungal Genetics Stock Center, http://www.fgsc.net/). Four cosmids

from chromosome II hybridized to the NDK gene: W3A06, W12E04, W14F07 and W3C12.

Sequencing of the *swoH1* mutant allele. The *swoH1* mutant allele was amplified from AXL20 genomic DNA by three independent PCR reactions using the Expand High Fidelity PCR System (Roche Diagnostics, IN, USA). Primers used for PCR amplifications were: 5'CGTACTAGATTGACTTCCCTGTC and 5'GTGACGCAGTTTCCTAGAGATG. After purification with Qiagen PCR clean up kit (Qiagen Inc., Valencia, CA), the PCR products were sequenced on both strands by primer walking using an ABI310 sequencer (Applied Biosystem, CA) according to the manufacturer's instructions. The sequences obtained were compared with the wild type allele using GeneDoc (version 2.6.001) (www.psc.edu/biomed/genedoc) with default parameters. All three reactions gave the same G561T mutation.

Protein sequence alignment. Sequences of NDKs from different organisms were obtained from GenBank (http://www.ncbi.nlm.nih.gov/) and were aligned using GeneDoc (version 2.6.001) with default parameters.

Homology modeling. The SwoHp model was prepared by homology modeling using Swiss PDB Viewer version 3.7b2 (http://www.expasy.ch/spdbv/). The template used was X-ray crystallography determined atomic structure of the bovine NDK. Loops were built using the Swiss PDB viewer, in some cases, the program O was used because of its ability to merge coordinates and slightly better modeling capabilities. Poor side chain orientations were identified by their high energies and corrected using the optimize function in Swiss-PDB viewer. Finally, the model was energy minimized using steepest descent and conjugate gradients until the change in energy between steps was < 0.05

kJ/mol and no locally poor energies remained. The model has similar threading energies, conformational energies and phi-psi plots as the original crystal structure. Thus, no attempt was made to correct geometric or energetic problem areas that appeared to carry over from the atomic structures. No energy minimization was required.

Coupled enzyme assay of NDK activity. About 10^7 conidia were inoculated to 100 ml complete media with proper supplements at 30^{o}C and incubated for 24 hr with shaking. Hyphae were harvested by filtering through two layers of cheese-cloth, and washed with cold ddH_2O. Cells were ground with a mortar and pestle in liquid nitrogen. The powder was suspended in 2 volumes of buffer A. The suspension was centrifuged at 10,000xg for 10 min and again at 18,000xg for 30 min. The ammonium sulfate precipitated fraction between 45% -70% was isolated by centrifugation at 40,000xg for 40 min. The pellet was dissolved in buffer B and dialyzed against the same buffer overnight, aliquoted into small tubes, quickly frozen in liquid nitrogen, and stored at -80 ^{o}C. Protein concentration was quantified using the Biorad protein calibration kit, using BSA as a standard. Buffer A: 50 mM Tris/HCl pH 7.5, 1mM EDTA, 5% glycerol, 0.02% NaZ_3, 0.1M $(NH_4)_2SO_4$, 1mM DTT, 3µg/ml leupeptine, 1µg/ml aprotinin, 1mM PMSF (phenylmethylsulfony fluoride). Buffer B: 50 mM Tris/HC1 pH 7.5, 0.02% NaZ_3, 5 mM $MgC1_2$, 1mM DTT, 0.2 mM PMSF, 5 mM 2-mercaptoethanol.

NDK activity was determined using a modification of the continuous spectrophotometric assay of Mourad and Parks (Mourad and Parks 1966a; Mourad and Parks 1966b). ATP (2 mM) and TDP (0.6 mM) were added to 0.75ml of buffer C and pre-incubated at assay temperature. The reaction was initiated by addition of cell extract containing 15ug of total proteins. The reaction was terminated after 10 min by rapidly

heating to 100^{o}C for 5 min. Tubes were cooled by plunging into ice. Precipitated protein was removed by centrifugation at 14,000xg for 4 min. The supernatant (0.6 ml) was taken into tubes containing phosphoenolpyruvate (2.5 mM), NADH (1 mM), pyruvate kinase (10 unit/ml)/lactate dehydrogenase (20.5 units/ml) in 0.4 ml buffer C. The absorbance was measured at 340 nm at room temperature in a spectrophotometer DU640B (Beckman, USA). TDP was converted to TTP at the expense of ATP, and ADP formed was estimated by measuring NADH disappearance. Assay negative controls without TDP and without enzyme NDK were always performed. Assay was performed three times and the average was considered as the NDK activity. Buffer C: 100 mM Tris/HCl pH 7.5, 2.5 mM $MgCl_2$.

Generation of 3xHA-tagged SwoHp. To construct the 3xHA-tagged SwoHp, the *swoH* gene was modified to contain a NotI restriction site at the N-terminus by High Fidelity PCR amplification. Primers used were: 5'CGGGATCCCGATGACTAAGGAAAAAAGCGGCCGCAAAACTAATTCTGAGC AGACGTAAGTGCAT and 5'ACATGCATGCATGTTTATTCCTTCTCATAGATCCAGCCG. The product (*swoH*-NotI) was inserted into the pGR3-AMA1-Not1 vector behind the bidirectional NiiA-niaD promoter (provided by Dr. Greg May) (Osherov *et al.* 2000) creating the pGR3-AMA1-*swoH*-NotI plasmid. The 3xHA tag was obtained by digesting plasmid pBSE66 (provided by Dr. Scott Erdman, Department of Biology, Syracuse University) with NotI and the 100bp fragment was gel purified with the Qiagen gel purification kit (Qiagen Inc., Valencia, CA). The 3xHA fragment was ligated into the pGR3-AMA1-*swoH*-NotI. The resulting plasmid pGR3-AMA1-HA-*swoH* that has correct 3xHA insertion site and

direction was confirmed by sequencing using primers 5'CGGGATCCCGATGACT and 5'GTTGGGAAACTGTGCTGC.

Purification of 3xHA-tagged SwoHp. About 10^7 conidia were inoculated in 100 ml complete medium with proper supplements at 30^{o}C overnight with shaking. Hyphae were harvested by filtering through two layers of cheese-cloth, and washed with cold ddH_2O. Cells were ground with mortar and pestle in liquid nitrogen. The powder was suspended in 2 volumes of lysis buffer containing a Complete Protease Inhibitor Cocktail Tablet (Roche, USA). The suspension was centrifuged at 14,000xg for 30 min. This crude cell extract of the supernatant was used for affinity purification on an anti-HA affinity matrix (Roche, USA) according to the manufacturer's instructions. Purification was monitored by SDS-PAGE. The final purified HA-SwoHp was confirmed by silver staining and western blot. Lysis buffer: 50mM Tris, pH7.5; 150mM NaCl; 0.1% Nonidet P40.

Western blot. Crude cell extract or purified protein obtained as previously described was separated on two 8-25% gradient gels on the PhastGel system (Amersham Biosciences, NJ). One gel was silver-stained, and the other one was transferred to a membrane for western blot and probed with anti-HA monoclonal antibody (Abcam Limited, Cambridge, UK). Western analysis was performed by enhanced chemiluminescence (ECL; Amersham Life Sciences) according to the manufacturer's instructions.

Phosphate transferase activity by TLC assay. Reactions were carried out essentially as previously described (Leung and Hightower 1997), except buffer D was used. ATP (1.8mM) and GDP (1.8mM) were added as substrates. The purified fusion protein was added to start the reaction, which was incubated at 37C for 30 min. An identical control

with the addition of EDTA was always performed. An aliquot from each reaction was spotted onto a 20x20 cm polyethyleneimine-cellulose-F TLC plate, and was developed in a saturated tank containing 0.75M KH_2PO_4 (pH3.6). The TLC plate was air-dried, and the nucleotides were visualized under UV light at a wavelength of 254 nm and photographed. Buffer D: 25mM HEPES (pH7.0), 50 mM NaCl, 10 mM $MgCl_2$, 10uM DTT.

Construction of the *swoH* null allele. Flanking sequences from upstream and downstream of the *swoH* gene (1.3 kb each) were amplified by high fidelity PCR. Primers used to amplify 5'flanking sequence of *swoH* with the addition of *Pst*I restriction sites were: 5'GAATTCCGAAATAGAAGCCGAGCAG and 5'AACTGCAGAACCAATCCATTGGGTACGTTTGAGAAGAGGG. Primers used to amplify 3'flanking sequence of *swoH* with the addition of *Sac*II restriction sites were: 5'ACCCCGCGGGGACCCTCAGAGTTCATCTCTAG and 5'ACCCCGCGGGGAGCTGGTGGGTTTTTGTTCGG. After double digestion with *Eco*RI and *Pst*I, the 5' flanking sequence was inserted into pargBC-1 (Momany and Hamer 1997) bearing the *argB* gene as the selectable marker. The resulting plasmid pargBC-5F was then ligated with 3' flanking sequence after digestion with *Sac*II. Correct insert direction of the 3' flanking sequence was confirmed by restriction mapping and PCR using primers: 5'CGCCAGCTCAACATCAGC and 5'CTCTGCATCTGTGCGGTC. The plasmid pargBC-5F-3F was then digested with *Kpn*I and separated on a 1% agarose gel. The 4.4 kb size fragment containing *argB* with *swoH* gene flanking sequences on both sides (5F-argB-3F) was purified using the Qiagen Gel purification kit (Qiagen Inc., Valencia, CA).

A linear fragment containing 5F-argB-3F was transformed into *A. nidulans* strain A850 (*argB?*) and transformants were selected for growth on minimal medium lacking arginine. All transformants were screened by PCR and verified by Southern blot to distinguish ectopic integration from homologous integration events. Of 72 transformants screened, none had homologous integration (data not shown). Therefore the fragment 5F-argB-3F was transformed *A. nidulans* diploid strain A852 (*argB?*). Transformants were selected for arginine prototrophy. Genomic DNA from 72 transformants was isolated and digested with *Bam*H1. A Southern blot was performed with 5' flanking sequence of *swoH* as the probe. Only one transformant was confirmed to have a homologous integration on one chromosome and a wild type copy on the other. The transformant was then treated with benomyl to induce haploidization as described for mitotic mapping. In total 315 haploid sectors were scored for genotype. None of the haploid sectors grew on minimal medium without arginine supplement.

Phylogenic tree building. ClustalX was used to build the phylogeny as previously described (Shaw *et al.* 2002), except that 2000 replicates were used for bootstrap values.

RESULTS

The *swoH1* mutant swells and lyses at restrictive temperature. In wild type *A. nidulans*, spores break dormancy and grow isotropically, then send out a germ tube and grow by tip extension (Momany and Taylor 2000). Previous work showed that the *swoH1* mutant cells swell and stop tip elongation shortly after germ tube emergence at restrictive temperature (Momany and Taylor 2000). To determine the phenotype with longer incubation at restrictive temperature, we cultured the *swoH1* mutant cells for up to three

days. As shown in Figure 3.1A, at restrictive tempature the *swoH1* mutant cells began to swell at 10 hr (Figure 3.1Ac) and lyse at 12 hr (Figure 3.1Ad). By 38 hr, more than 90% of the cells had lysed leaving ghost cells without nuclei (Figure 3.1Af). The *swoH1* mutant cells branched randomly at restrictive temperature (Figure 3.1B), suggesting that *swoH* gene might be important for both survival and hyphal morphology during vegetative growth.

SwoHp is necessary for hyphal growth. Previous studies showed that the *swoH1* mutant maintains polar growth for at least one cell cycle after shift from permissive to restrictive temperature (Momany *et al.* 1999). This could mean that SwoHp is not needed for hyphal extension. However, if SwoHp protein were very stable then the same phenotype would be expected. To determine which explanation is correct and to find the critical stage for SwoHp function, the growth pattern of the *swoH1* mutant was observed under extended incubation at restrictive temperature after initial incubation at permissive temperature. Conidia of the *swoH1* mutant were incubated at permissive temperature for 2 hr, 4 hr, 6 hr and 8 hr and then shifted to restrictive temperature for 12 hr (several cell cycles). The *swoH1* mutant cells swelled in all cases (Figure 3.2). Longer growth at permissive temperature before shift to restrictive gave similar results (data not shown). However, swollen hyphae were not obvious when the *swoH1* mutant was shifted to restrictive temperature for less than 8 hr (data not shown). This observation suggests that SwoHp is needed for hyphal growth and that a reservoir of functional SwoHp produced at permissive temperature can support normal growth for several hours. This explanation is consistent with our observation that at restrictive temperature, the *swoH1* conidia

germinated and sent out short germ tubes, but eventually became swollen and lysed after extended incubation.

SwoHp is necessary for conidiation. *A. nidulans* produces asexual spores (conidia) on special aerial hyphae called conidiophores. To determine if SwoHp is needed for asexual reproduction, we tested the ability of the *swoH1* mutant to produce conidia at restrictive temperature. Since the *swoH1* mutant stopped growing during early vegetative growth at restrictive temperature, we cultured the *swoH1* mutant at permissive temperature in liquid media with shaking for 8 hr, 12 hr and 20 hr, then plated hyphae on solid medium to induce conidiation at restrictive temperature. Plates were examined by stereoscope after incubation for 1 day, 2 days, 3 days and 4 days. No conidia were formed, indicating that SwoHp is necessary for conidiation.

An NDK gene complements the *swoH1* mutant. A genomic plasmid library carrying a *pyr4* marker was transformed into *swoH1* mutant protoplasts. Transformants were selected by restoration of *pyrG* prototroph. Plasmids from the transformants were rescued into *E. coli* and then restriction mapped to contain the same genomic DNA insert. The plasmid pH42 was sequenced using a transposon tag strategy and the complementing gene was identified based on the fact that two transposon insertions in this ORF (Open Reading Frame) disrupted the plasmid's ability to complement the *swoH1* mutant, while transposons inserted into other ORFs had no effect (data not shown). Searching against the NCBI database showed that the ORF encodes a homologue of yeast YNK1, a nucleoside diphosphate kinase (NDK), which converts nucleoside diphosphates to nucleoside triphosphates. NDKs are a highly conserved family across prokaryotes and eukaryotes (Figure 3.3).

The NDK gene hybridizes to *swoH* cosmids. Mitotic mapping was used to identify the chromosome on which the *swoH* gene lies. A heterozygous diploid was made by fusing APW13 with the mitotic mapping strain A104, which has a marker on each chromosome. Chromosome loss was induced by benomyl treatment of the heterozygous diploid. The resulting haploid sectors have a set of chromosomes that are a random mixture from either parent. The genotypes of these haploid sectors were scored. The *acrA*^{r} marker segregated in repulsion to *swoH1* ts- phenotype indicating that *swoH* is on chromosome II (Table 3.2).

The location of the *swoH* gene on chromosome II was determined by meiotic mapping. The *swoH1* mutant strain APW13 was crossed with the meiotic mapping strain A254. Genotypes of the progeny ascospores were scored (n= 315) and the distances between *swoH* gene and other markers on chromosome II were determined by recombination frequencies. Based on the genetic map of chromosome II (available from Fungal Genetics Stock Center, http://www.fgsc.net/) and the recombination frequency of *swoH* with the markers, the *swoH* gene is located on the left arm of chromosome II (Figure 3.4).

Southern blotting experiments showed that the NDK which complemented the *swoH1* mutant phenotype hybridized to four cosmids from a chromosome II specific library (Brody *et al.* 1991). The positions of these cosmids on the *A. nidulans* physical map are consistent with our genetic mapping of the *swoH* gene (Clutterbuck 1997) (http://www.gla.ac.uk/Acad/IBLS/molgen/aspergillus/maps.html). These results showed that this NDK gene is the authentic *swoH* gene and not a high copy suppressor.

SwoHp has phosphate transferase activity. A 3xHA N-terminal tagged *swoH* gene was constructed behind the bidirectional NiiA-niaD promoter in the pGR3-AMA1-Not1

vector (Osherov *et al.* 2000). When the resulting vector was transformed into the *swoH1* mutant, it complemented the mutant phenotype at restrictive temperature in the inductive medium containing $NaNO_3$ (Punt *et al.* 1995) (Figure 3.5f) but not in the repressive medium containing ammonion tartrate (Figure 3.5e) indicating the functional integrity of the tagged protein. Empty vector had no effect on growth (data not shown). The fusion protein HA-SwoHp was purified on an anti-HA affinity matrix. Only one band was detected on SDS-PAGE by silver stain after affinity column purification suggesting that the protein obtained was fairly pure (Figure 3.6A). The purified fusion protein was used for phosphate transferase activity assay by TLC. Figure 3.6B showed that HA-SwoHp transferred the ?-phosphate from ATP to GDP and produced ADP and GTP (Figure 3.6B column 3, 4 and 5). EDTA inhibited the phosphate transferase activity (Figure 3.6B column 2). This result proved that the SwoHp has the phosphate transferase activity.

The *swoH1* mutant cell extract has lower nucleoside diphosphate kinase activity. Since the *swoH* gene encodes a nucleoside diphosphate kinase, it is possible that decreased NDK activity may directly cause the *swoH1* mutant phenotype. A coupled enzyme assay was used to measure the NDK activity of cell extract from wild type and the *swoH1* mutant grown overnight at permissive temperature (30^{o}C). To determine if temperature affects the NDK activity, the assay was carried out at 25^{o}C, 42^{o}C and 54^{o}C. Average of results from three independent experiments is shown in Table 3.3. The results showed that the crude cell extract from *swoH1* mutant had about 20% of the NDK activity compared with wild type at room temperature. Surprisingly, higher NDK activity was observed in the mutant cell extract at higher temperature. The *swoH1* mutant phenotype was observed at 42 ^{o}C, but not at temperature lower than 37 ^{o}C suggesting that

much higher NDK activity may be necessary for survival at higher temperature. Since proteins other than NDK were assumed to be responsible for the some nucleoside diphosphate kinase activity (Fukuchi *et al.* 1993; Lu and Inouye 1996; Wheeler *et al.* 1996; Kuroda and Kornberg 1997; Noguchi and Shiba 1998; Shiba *et al.* 2000), it is unclear whether the *swoH1* mutation caused loss of part or total NDK activity.

The *swoH1* mutation likely disturbs the NDK active site. Sequencing in the NDK region from the *swoH1* mutant AXL20 revealed one G561T mutation in the exon, which is predicted to change a conserved valine to phenylalanine at position 83 of the protein (Figure 3.3). Since the NDK family is highly conserved both at the primary protein sequence level (Figure 3.3) and also at the protein structure level (Gilles *et al.* 1991; Dumas *et al.* 1992; Chiadmi *et al.* 1993; Almaula *et al.* 1995; Morera *et al.* 1995; Postel 1998; Ladner *et al.* 1999; Milon *et al.* 2000; Erent *et al.* 2001; Postel *et al.* 2002), we were able to predict the protein structure of SwoHp using homology modeling. The *swoH1* mutation (V83F) at the beginning of a helix 5 is not likely to cause any dramatic overall structural change but may change the relative position of a helix 5 and the ? strand 3 where the conserved active enzyme sites such as arginine87 and histidine117 are located. This change may draw a helix 5 and the ? strand 3 closer to each other while may create extra space between the substrate and the enzyme active site, leading to the reduced NDK activity in the mutant. However, this does not exclude the possibility that other proteins may provide some NDK like activity in *A. nidulans*. Based on subunit interaction and the protein structural modeling, SwoHp, like other members of eukaryotic NDK, likely forms homohexamer in native form.

Deletion of the *swoH* gene is lethal in *A. nidulans*. To make a knock out strain, the 5' and 3' flanking sequences of the *swoH* gene were ligated on each side of the *argB* selective marker and transformed into *A. nidulans* haploid strain A850 (*argB?*). Only ectopic integrations were found from 72 transformants screened. Two explanations are possible: the *swoH* locus may be inefficient for targeting, since gene targeting is locus dependent in *A. nidulans* (Bird and Bradshaw 1997), or the *swoH* gene is essential and null mutants do not survive. To determine which explanation is correct, the disruption construct was transformed into *A. nidulans* diploid stain A852 (*argB?*). Transformants that grew on medium without arginine were tested by Southern blot. Only one diploid transformant of 72 screened was a heterozygous with one chromosome retaining the wild type copy of *swoH* and one with the homologous integrated *argB* (Figure 3.8). This transformant was induced to haploidize and the genotypes of resulting haploid sectors were scored. None of the 315 haploid sectors scored were *argB+*, indicating that only those haploid sectors with the intact *swoH* gene survived. This result showed that the *swoH* gene is essential in *A. nidulans*. The lethality of the null mutant is consistent with the phenotype of *swoH1* mutant, but contrasts with findings in yeasts, where NDK is dispensable for growth, sporulation, mating and morphology (Fukuchi *et al.* 1993; Izumiya and Yamamoto 1995).

Phylogenetic tree of NDK sequences. Higher organisms contain several isoforms of NDK, while yeasts and *E. coli* each contain only one copy. Southern blots of the *A. nidulans* genomic DNA with the *swoH* gene showed only one band (data not shown). A BLAST search of the Cereon *A. nidulans* genome database (Cereon Genomics,

http://www.cereon.com/) with the *swoH* gene sequence yielded no additional hits suggesting that there is only one NDK gene in *A. nidulans*.

To see the relationship between NDKs from different organisms, we constructed a phylogenic tree based on NDK protein sequences. Not surprisingly, SwoHp in *A. nidulans* was closest to NDK from another filamentous fungus *N. crassa*, and both split early from yeasts (Figure 3.9). NDKs from animals, plants and prokaryotes were clustered in kingdom specific clades.

DISCUSSION

In work described in this paper, we found that the ts- *swoH1* mutant was defective in vegetative growth and conidiation at restrictive temperature. The responsible gene was mapped, cloned and sequenced. The *swoH* gene encodes the nucleoside diphosphate kinase in *A. nidulans* and the *swoH1* mutant cell extract had only about 20% NDK activity compared with that of wild type. Based on structural modeling, the *swoH1* mutation might disturb the enzyme active site causing decreased enzyme activity. The purified fusion protein HA-SwoHp showed phosphate transferase activity, further proving that SwoHp is the functional NDK in *A. nidulans*.

Prediction of SwoHp stability by ProtParam Tool (http://ca.expasy.org/cgi-bin/protparam) suggested that SwoHp was stable. Studies on NDKs from other organisms also support this idea (Polosina *et al.* 1998; Ishibashi *et al.* 2001; Polosina *et al.* 2002). The structural modeling predicted that the *swoH1* mutation was unlikely to cause any dramatic overall structural change or to alter the oligomeric status. This is consistent with the delayed phenotype of the *swoH1* mutant shown at elevated temperature.

Surprisingly, deletion of the *swoH* gene was lethal in *A. nidulans*, indicating that SwoHp is essential for cell survival in this filamentous fungus. This contrasts to results in *E. coli*, *P. aeruginosa*, *S. cerevisiae* and *S. pombe* where NDK is dispensable, but is consistent with the essentiality of NDKs in animals and plants. There is an intriguing correlation between the multicellular life form and essentiality of NDKs. An interesting example is *Myxococcus xanthus*, a bacterium that undergoes complex morphological and biochemical changes to form the fruiting body with aggregation of about 100,000 cells under starvation and coordinates complicated cell motility during vegetative growth (Kuner and Kaiser 1982; Shimkets and Kaiser 1982; LaRossa *et al.* 1983; Spormann and Kaiser 1999). Consistent with its multicellular life style, NDK in this bacterium has been found to be essential (Munoz-Dorado *et al.* 1990a; Munoz-Dorado *et al.* 1990b; Harvey and French 2000). It seems that NDK might play more important roles in more complex organisms.

The exact mechanism of how the *swoH1* mutation affects protein function is still unclear, even less clear is how this mutation causes the phenotype we observed. Many molecules have been found interacting with NDKs genetically and physically (Zhang and Chang 1995; Leung and Hightower 1997; Orlov and Kimura 1998; Choi *et al.* 1999; Reymond *et al.* 1999; Agou *et al.* 2000; Postel *et al.* 2000b; Roymans *et al.* 2000; Galvis *et al.* 2001; Ohkura *et al.* 2001; Otsuki *et al.* 2001; Fournier *et al.* 2002a; Fournier *et al.* 2002b). NDK is a kinase, and itself could be phosphorylated (Almaula *et al.* 1995; Struglics and Hakansson 1999; Negroni *et al.* 2000; Uno *et al.* 2002). In addition to possibly disturbing the enzyme active site, the *swoH1* mutation lies close to Ser119, which has been shown to be phosphorylated in other organisms (Webb *et al.* 1995; Freije

et al. 1997; Struglics and Hakansson 1999) and is implied to be involved in motility-suppressing function of nm23-H1 in mammals (Chang *et al.* 1996; MacDonald *et al.* 1996). It is likely that the *swoH1* phenotype could result from changes in SwoHp functions other than the nucleoside diphosphate kinase activity.

In addition to the housekeeping function of NDK, studies in other organisms suggest that NDK may be involved in stress responses (Tsuchiya *et al.* 1993; Orlov and Kimura 1998; Zaborina *et al.* 1999; Harvey and French 2000; Song *et al.* 2000; Galvis *et al.* 2001). In yeast, NDK transcription level was upregulated under various cell damaging conditions (Ito *et al.* 2001). Evidence shows that NDK may serve as a target for protons and salts (Orlov *et al.* 1997). The NDK from Neurospora and Arabidopsis are involved in light signal transduction pathways (Tanaka *et al.* 1998; Choi *et al.* 1999; Quail 2000; Ogura *et al.* 2001) and may also be involved in additional signal transduction pathways (Zimmermann *et al.* 1999; Cuello *et al.* 2002; Hippe *et al.* 2002; Ho *et al.* 2002). It could be that the NDK may serve as a component in various signal transduction pathways, which are connected with stress responses (Barraud *et al.* 2002). The *swoH1* mutant was restored to wild-type growth by addition of salt in the medium at restrictive temperature (unpublished observation) suggesting that SwoHp might serve in the protons and salts transportation pathway in *A. nidulans.*

ACKNOWLEDGEMENTS

This work was sponsored by Department of Energy Biosciences grant DE-FG02-97ER20275. We thank Dr. Brian Shaw for assistance in sequencing and identification of complementing plasmid, Dr. Patrick Westfall for APW13 strain construction, and Dr.

Greg May for providing the plasmid library and pGR3-AMA1-Not1 plasmid with niiA-niaD promoter used in this work.

Table 3.1. Strains used in this paper

Strain	Genotype
A104[a]	*yA2; adE20; acrA1; phenA2; pyroA4; lysB5; sB3; nicB8; coA1*
A254[a]	*biA1; AcrA1; wA3; ileA3; cnxE16; adD3*
A773[a]	*pyrG89; wA3; pyroA4*
A850[a]	*biA1;_argB::trpC_B; methG1; veA1; trpC801*
A852[a]	*biA1;_argB::trpC_B; methG1; veA1; trpC801; pabaA1; yA2;_argB::trpC_B; veA1; trpC801*
APW13 [b]	*swoH1 (ts-); pabaA; char*
AXL20[c]	*swoH1 (ts-); pyroG89; pyroA4*

[a] Available from Fungal Genetics Stock Center, Department of Microbiology, University of Kansas Medical Center (Kansas City, KS).

[b] Isolated by Dr. Patrick Westfall.

[c] Isolated by crossing APW13 with A773.

Table 3.2. Mitotic mapping of the *swoH* gene[a]

CHR[b]		I	II	III	IV	V	VI	VII
marker	*ts-*	*adE20*$^{-}$	*acrA*^{r}	*phenA*$_2$$^{-}$	*pyroA*$_4$$^{-}$	*lysB*$_5$$^{-}$	*$_S$B*$_3$$^{-}$	*nicB*$_8$$^{-}$
Percent of colonies in linkage[c]	100	35	96	71	63	60	57	59

[a] : Diploid generated by crossing *swoH1* mutant with mitotic mapping A104 and was treated with benomyl to induce haploidization. Haploid sectors were scored for their genotypes.

[b] : the chromosome on which these markers are located

[c]: The percentage of conidia that have markers segregated in repulsion to *swoH1* ts- phenotype. The marker of chromosome VIII in the mitotic mapping strain A104 is also a ts- phenotype (compact morphology), which makes it impossible to score at the same time as *swoH1* (ts-). Out of 350 haploid sectors, 99 were ts-, which may be caused by reduced viability of the ts- strain.

Table 3.3. The *swoH1 mutant* crude cell extract is low in NDK activity[a]

assay temperature	25°C	42°C	54°C
swoH1 mutant	0.18?0.03	0.24?0.02	0.31?0.03
wild type	0.93?0.04	0.98?0.08	1.05?0.09
swoH1 mutant / wild type	19.3%	24.2%	29.5%

[a]: Same amount of protein was added to each reaction. Results from three independent experiments were averaged.

Figure 3.1. The *swoH1* mutant cells showed swelling, lysing and abnormal branching at restrictive temperature. A. Conidia of *swoH1* mutant AXL20 were inoculated onto coverslips in complete liquid medium and incubated at restrictive temperature (42^{o}C). Cells were fixed and stained with Hoechst 33258 to visualize nuclei. The upper and lower rows show DIC and fluorescent images of the same field. All micrographs are at the same magnification. (a) 6h, (b) 8h, (c) 10h, (d) 12h, (e) 24h, (f) 38h.

B. The *swoH1* mutant cells showed random branching and irregular growth at restrictive temperature. Conidia of *swoH1* mutant AXL20 were inoculated onto coverslips in complete liquid media and incubated at restrictive temperature (42^{o}C) for 16hr. Scale, 5?M.

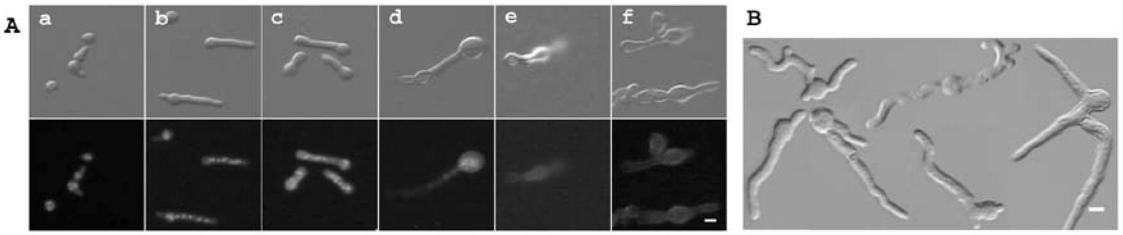
A
a
b
c
d
e
f
B

Figure 3.2. The *swoH1* mutant cannot maintain polar growth upon shift from permissive to restrictive temperature. Conidia of the *swoH1* mutant AXL20 were grown in liquid complete medium at permissive temperature (30 ^{o}C) for 2 hr, 4 hr, 6 hr and 8 hr and then shifted to restrictive temperature for 12 hr (a, b, c, and d, respectively). Cells were fixed and stained with Hoechst33258 to visualize nuclei. The upper row and lower row show DIC and fluorescent images of the same field respectively. All micrographs are at the same magnification. Scale, 5?M.

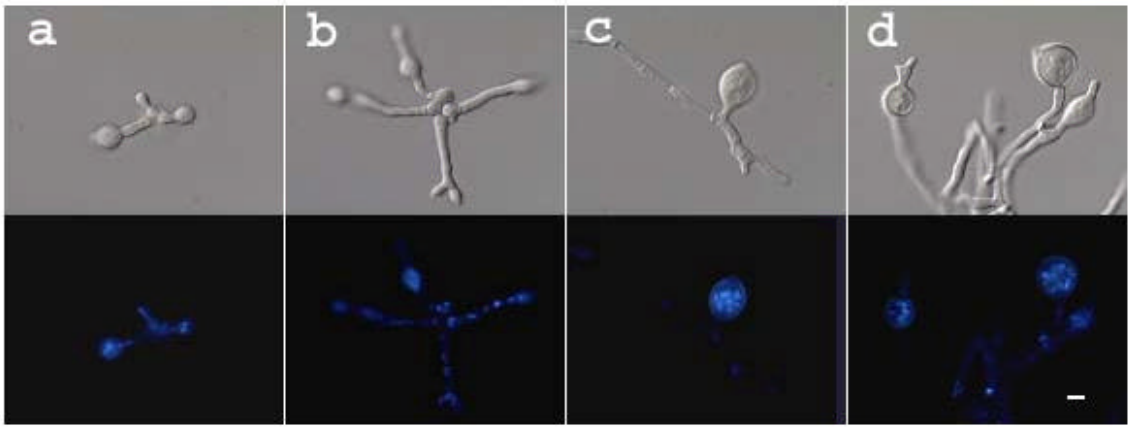
a
b
c
d

Figure 3.3. Multiple alignment of NDK sequences from different organisms. Black shading indicates identical or highly similar residues. Dark and light gray indicate 75% and 50% similar residues, respectively. The *swoH1* V83F mutation is indicated by a purple circle below the sequence. Amino acids important for catalytic phosphate transferase activity are indicated below the sequence. Symbol ? indicates the amino acid needed for DNA binding and ? indicates the amino acid needed for DNA cleavage based on results from (Postel *et al.* 2002). Color bars above the sequence show the secondary structure of SwoHp.

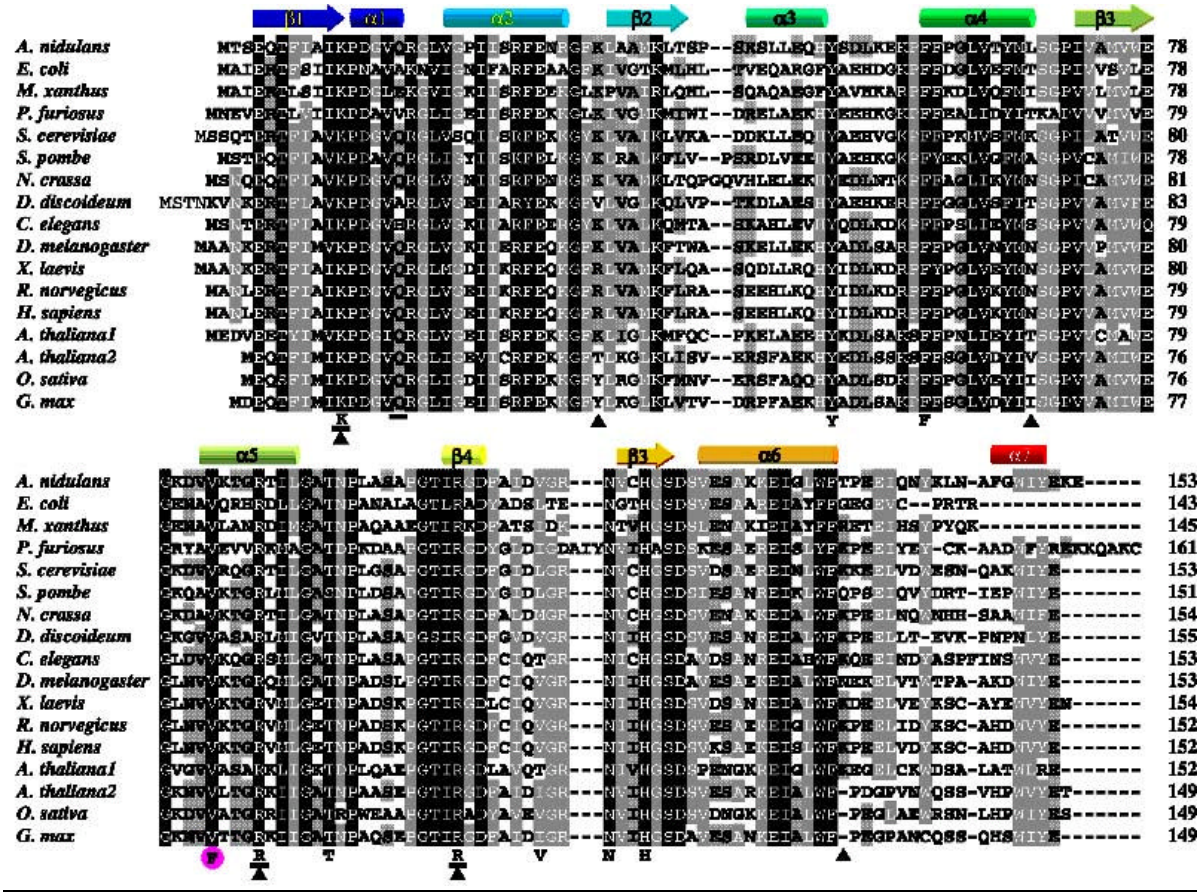
β1 α1 α2 β2 α3 α4 β3
A. nidulans
E. coli
M. xanthus
P. furiosus
S. cerevisiae
S. pombe
N. crassa
D. discoideum
C. elegans
D. melanogaster
X. laevis
R. norvegicus
H. sapiens
A. thaliana1
A. thaliana2
O. sativa
G. max
α5 β4 β3 α6
153
143
145
161
153
151
154
155
153
153
154
152
152
152
149
149
149

Figure 3.4. Genetic position of *swoH* on chromosome II. CEN stands for centromere, which is located close to the left arm of the chromosome. The numbers underneath the line are the map units between *swoH* and markers. Genetic map is based on the linkage map provided by Fungal Genetics Stock Center (http://www.fgsc.net/mirror/www.gla.ac.uk/Acad/IBLS/molgen/aspergillus/maps.html). Only relevant markers are shown.


AcrA
swoH
wA
CEN
ileA
cnxE
adD
23 28
43 45
51

Figure 3.5. HA-tagged *swoH* gene complemented *swoH1* mutant. Spores of wild type (a, b), *swoH1* mutant (c, d), *swoH1* mutant transformed with HA-tagged *swoH* gene (e, f) under inducible promoter niiA-niaD were inoculated on repressive media containing ammonium tartrate (a, c, e) and inductive media containing $NaNO_3$ (b, d, f) and incubated at indicated temperatures for two days.

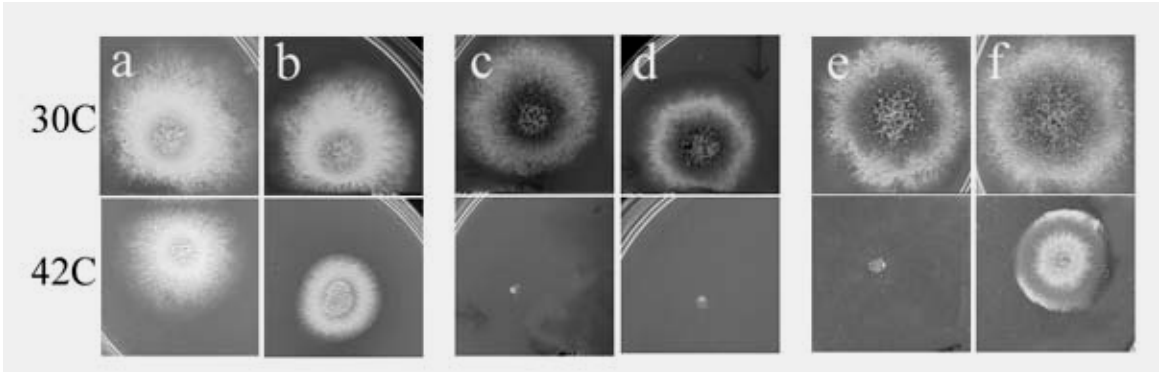
30C
42C
a
b
c
d
e
f

Figure 3.6. SwoHp processes phosphate transferase activity. A: protein purified from the anti-HA affinity column was separated on SDS PAGE gel and then silver stained. B: HA-SwoHp shows phosphate transferase activity. (1) Reaction without HA-SwoHp, (2) Reaction with 100 ng HA-SwoHp plus 100 mM EDTA, (3) Reaction with 40 ng HA-SwoHp, (4) Reaction with 100 ng HA-SwoHp, (5) Reaction with 140 ng SwoHp-HA. Standards were (6) ADP, (7) GTP, (8) GDP, (9) ATP, (10) mixture of ATP and GDP (10). All these standards were treated identically as the reaction except without HA-SwoHp.

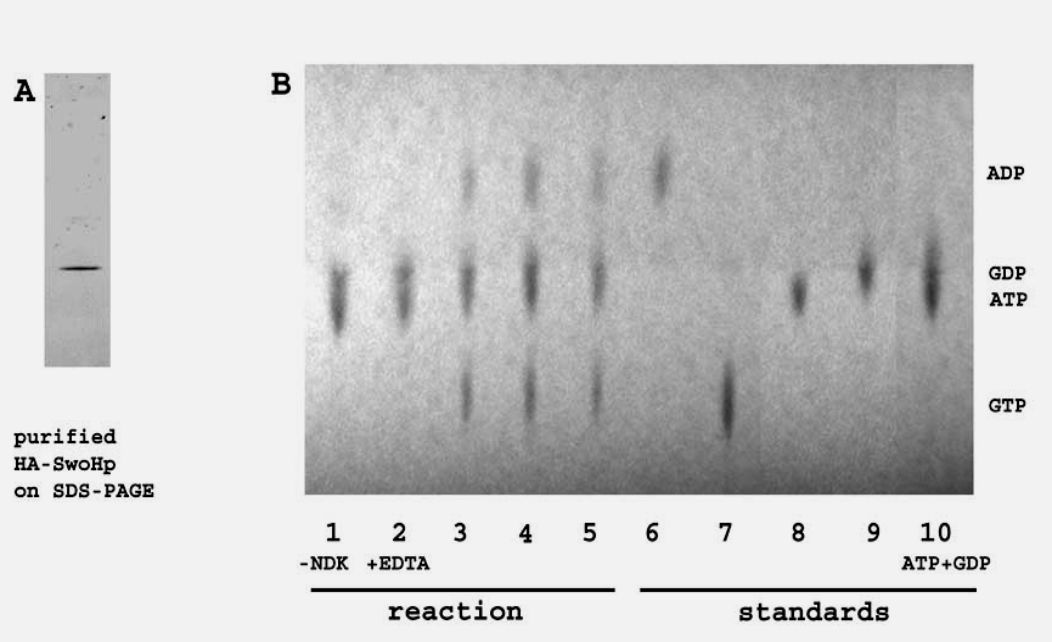
A
purified
HA-SwoHp
on SDS-PAGE
B
ADP
GDP
ATP
GTP
1 2 3 4 5 6 7 8 9 10
-NDK +EDTA
ATP+GDP
reaction
standards

Figure 3.7. Structure of NDK. One subunit of SwoHp was shown in the left. The *swoH1* mutation V83F occurs on helix 5. The original valine is shown in gray and phenylalanine is shown in purple. Active sites R87 on a helix 5 and H117 on ß strand 3 are also shown. Substrate is shown in ball and stick. The color scheme usage is same as for the structure modeling in Figure 3.3.

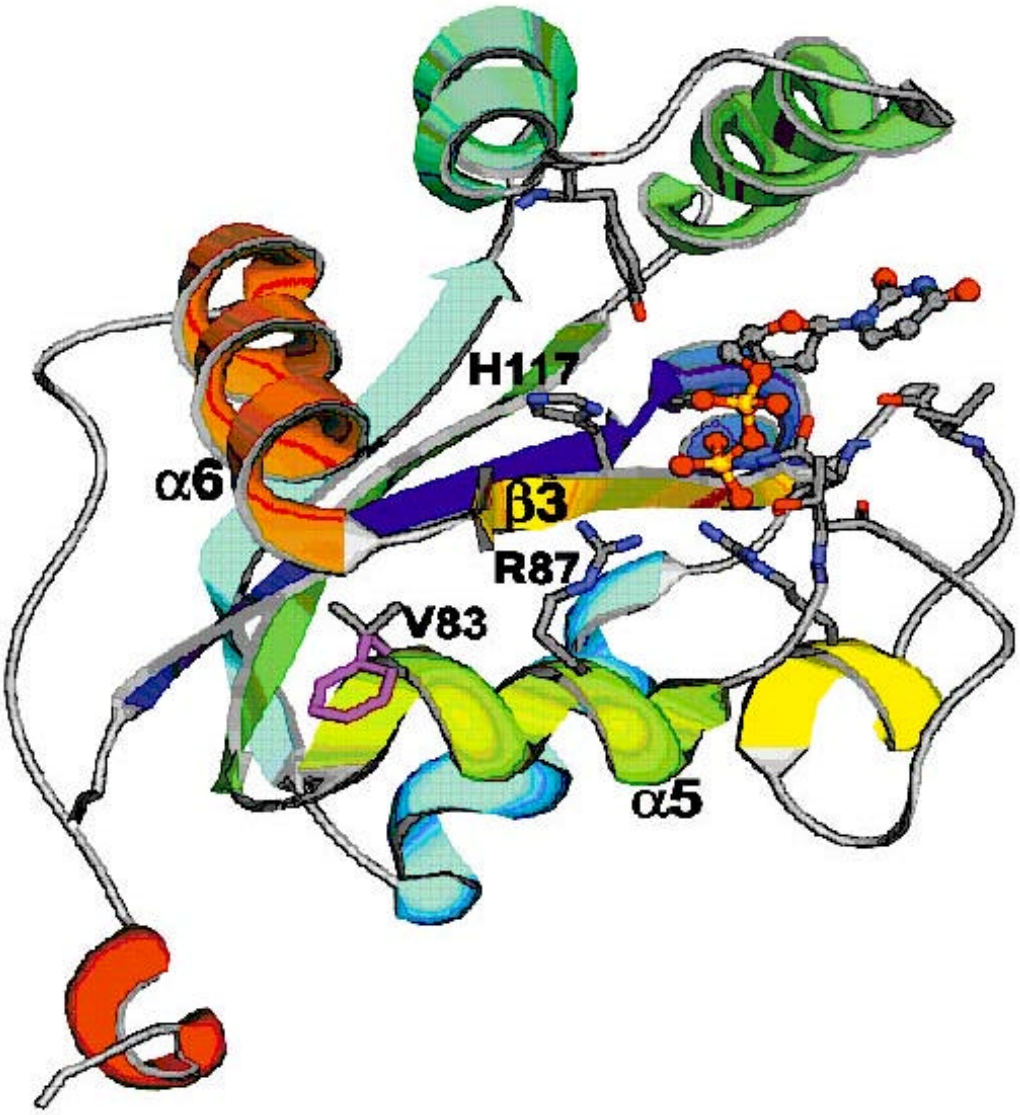
H117
α6
β3
R87
V83
α5

Figure 3.8. Homologous replacement of *swoH* gene with *argB* in A852. *Bam*H1 sites are shown in the wild type copy of the genomic DNA at original *swoH* locus and after the original *swoH* gene was replaced by the *argB* marker. The genomic DNA of the heterozygous diploid transformant was digested with *Bam*H1. The Southern blot was probed with random-labeled 5' flanking sequence of the *swoH* gene. Col-30 showed one wild type copy of *swoH* (the band above 4 kb) and one homologous replacement copy (the band at 1.4kb). These two lanes were photographed from the same gel (others are not shown).

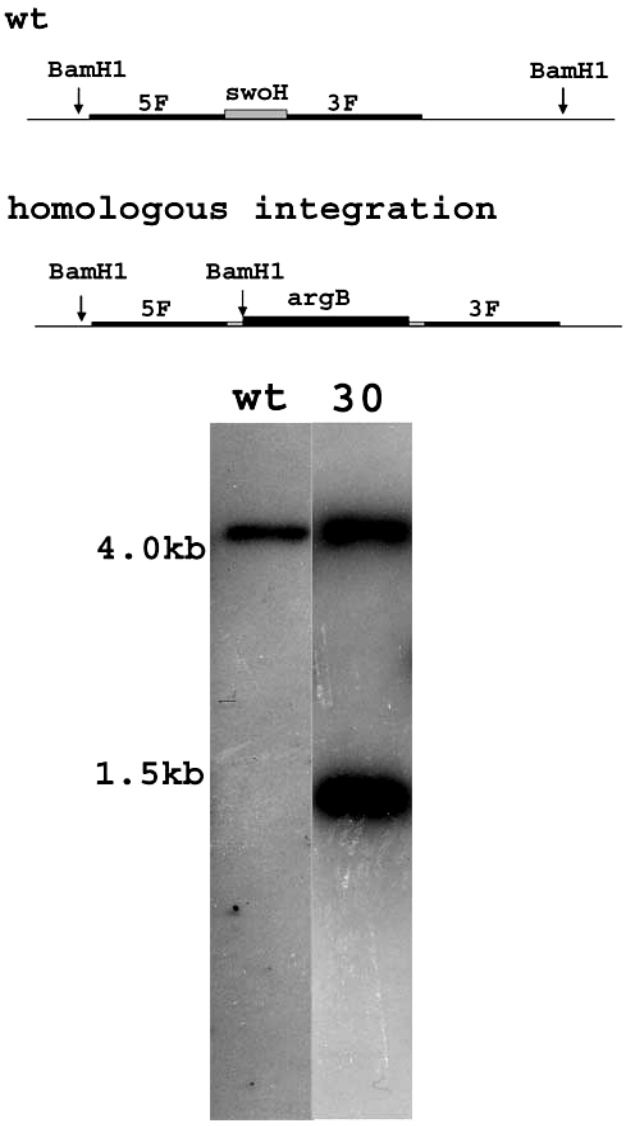
wt
BamH1
5F
swoH
3F
BamH1
homologous integration
BamH1
BamH1
5F
argB
3F
wt
30
4.0kb
1.5kb

Figure 3.9. Phylogenetic tree of NDKs. Protein sequences of NDK from different organisms were obtained from GenBank. Accession numbers are: AAL23684 (NDK from *Emericella nidulans*), NP_417013 (NDK from *Escherichia coli*), A35539 (NDK from *Myxococcus xanthus*), Q8U2A8 (NDK from *Pyrococcus furiosus*), NP_012856 (Ynk1p from *Saccharomyces cerevisiae*), P49740 (NDK from *Schizosaccharomyces pombe*), CAD37041 (NDK from *Neurospora crassa*), P22887 (NDK from *Dictyostelium discoideum*), NP_492761 (NDK from *Caenorhabditis elegans*), P08879 (NDK from *Drosophila melanogaster*), P19804 (NDK B from *Rattus norvegicus*), P22392 (NDK B from *Homo sapiens*), T51612 (NDK Ia from *Arabidopsis thaliana*), P39207 (NDK I from *Arabidopsis thaliana*), S43330 (NDK from *Oryza sativa*), T07042 (NDK from *Glycine max*), P70011 (NDK A2 from *Xenopus laevis*). ClustalX was used to build the phylogeny.

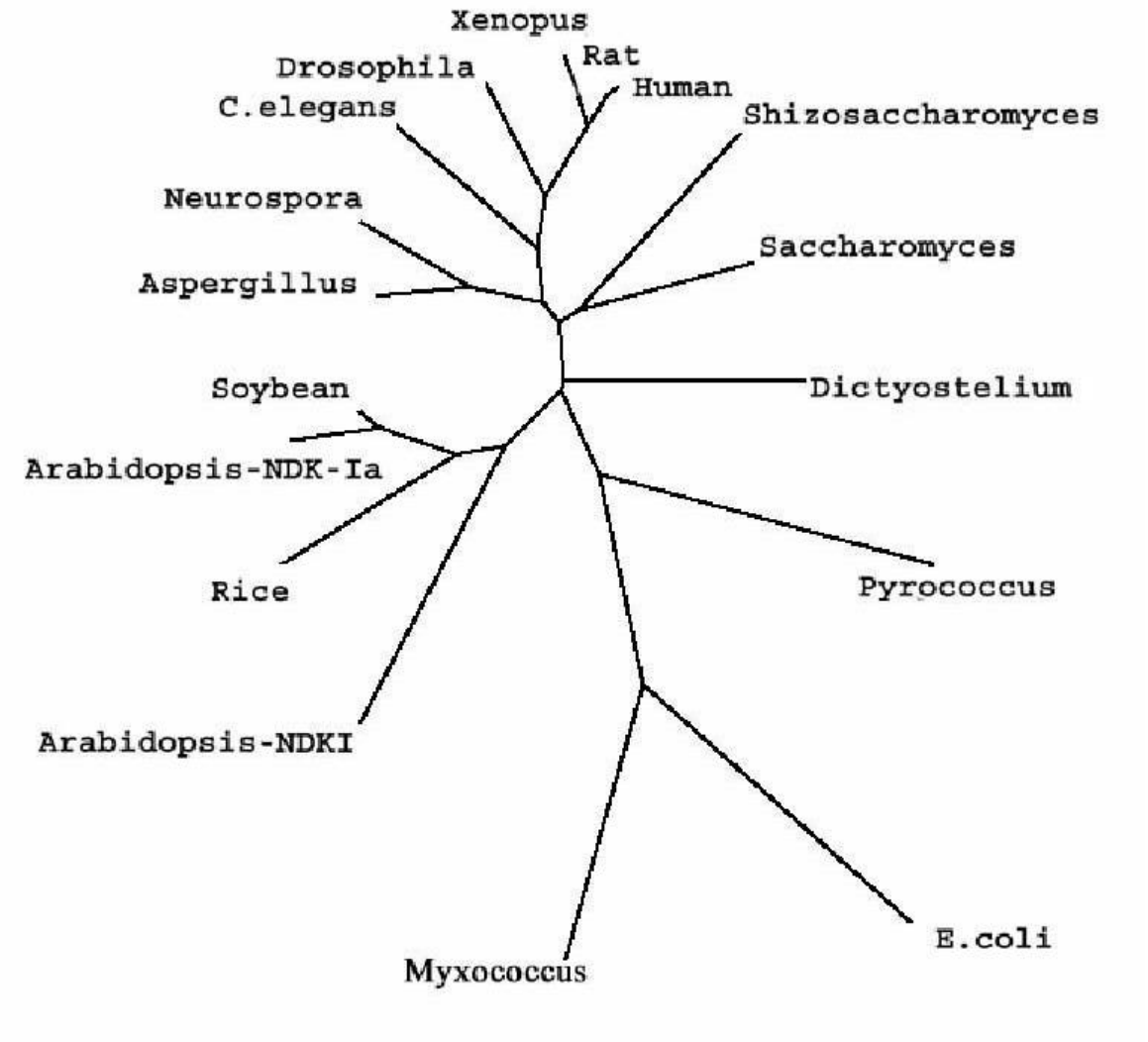
Xenopus
Rat
Drosophila
Human
C.elegans
Shizosaccharomyces
Neurospora
Saccharomyces
Aspergillus
Soybean
Dictyostelium
Arabidopsis-NDK-Ia
Rice
Pyrococcus
Arabidopsis-NDKI
E.coli
Myxococcus

REFERENCES

Agarwal, R. P., B. Robison and R. E. Parks, Jr., 1978 Nucleoside diphosphokinase from human erythrocytes. Methods Enzymol **51:** 376-386.

Agou, F., S. Raveh, S. Mesnildrey and M. Veron, 1999 Single strand DNA specificity analysis of human nucleoside diphosphate kinase B. J Biol Chem **274:** 19630-19638.

Agou, F., S. Raveh and M. Veron, 2000 The binding mode of human nucleoside diphosphate kinase B to single-strand DNA. J Bioenerg Biomembr **32:** 285-292.

Almaula, N., Q. Lu, J. Delgado, S. Belkin and M. Inouye, 1995 Nucleoside diphosphate kinase from *Escherichia coli*. J Bacteriol **177:** 2524-2529.

Amendola, R., R. Martinez, A. Negroni, D. Venturelli, B. Tanno *et al.*, 2001 DR-nm23 expression affects neuroblastoma cell differentiation, integrin expression, and adhesion characteristics. Med Pediatr Oncol **36:** 93-96.

Barraud, P., L. Amrein, E. Dobremez, S. Dabernat, K. Masse *et al.*, 2002 Differential expression of nm23 genes in adult mouse dorsal root ganglia. J Comp Neurol **444:** 306-323.

Bird, D., and R. Bradshaw, 1997 Gene targeting is locus dependent in the filamentous fungus *Aspergillus nidulans*. Mol Gen Genet **255:** 219-225.

Brody, H., J. Griffith, A. J. Cuticchia, J. Arnold and W. E. Timberlake, 1991 Chromosome-specific recombinant DNA libraries from the fungus *Aspergillus nidulans*. Nucleic Acids Res **19:** 3105-3109.

Chang, C. L., J. R. Strahler, D. H. Thoraval, M. G. Qian, R. Hinderer *et al.*, 1996 A nucleoside diphosphate kinase A (nm23-H1) serine 120-->glycine substitution in

advanced stage neuroblastoma affects enzyme stability and alters protein-protein interaction. Oncogene **12:** 659-667.

Chiadmi, M., S. Morera, I. Lascu, C. Dumas, G. Le Bras *et al.*, 1993 Crystal structure of the Awd nucleotide diphosphate kinase from Drosophila. Structure **1:** 283-293.

Choi, G., H. Yi, J. Lee, Y. K. Kwon, M. S. Soh *et al.*, 1999 Phytochrome signalling is mediated through nucleoside diphosphate kinase 2. Nature **401:** 610-613.

Clutterbuck, A. J., 1997 The validity of the *Aspergillus nidulans* linkage map. Fungal Genet Biol **21:** 267-277.

Cuello, F., R. A. Schulze, F. Heemeyer, H. E. Meyer, S. Lutz *et al.*, 2002 Activation of heterotrimeric G proteins by a high-energy phosphate transfer via nucleoside diphosphate kinase (NDPK) B and Gbeta subunits I. Complex formation of NDPK B with Gbeta gamma dimers and phosphorylation of His266 in Gbeta. J Biol Chem.

Dumas, C., I. Lascu, S. Morera, P. Glaser, R. Fourme *et al.*, 1992 X-ray structure of nucleoside diphosphate kinase. Embo J **11:** 3203-3208.

Erent, M., P. Gonin, J. Cherfils, P. Tissier, G. Raschella *et al.*, 2001 Structural and catalytic properties and homology modelling of the human nucleoside diphosphate kinase C, product of the DRnm23 gene. Eur J Biochem **268:** 1972-1981.

Fournier, H. N., S. Dupe-Manet, D. Bouvard, M. L. Lacombe, C. Marie *et al.*, 2002a ICAP-1alpha interacts directly with the metastasis suppressor nm23-H2 and both proteins are targeted to newly formed cell adhesion sites upon integrin engagement. J Biol Chem **27:** 27.

Fournier, H. N., S. Dupe-Manet, D. Bouvard, M. L. Lacombe, C. Marie *et al.*, 2002b Integrin cytoplasmic domain-associated protein 1alpha (ICAP-1alpha) interacts directly with the metastasis suppressor nm23-H2, and both proteins are targeted to newly formed cell adhesion sites upon integrin engagement. J Biol Chem **277:** 20895-20902.

Freije, J. M., P. Blay, N. J. MacDonald, R. E. Manrow and P. S. Steeg, 1997 Site-directed mutation of Nm23-H1. Mutations lacking motility suppressive capacity upon transfection are deficient in histidine-dependent protein phosphotransferase pathways in vitro. J Biol Chem **272:** 5525-5532.

Fukuchi, T., J. Nikawa, N. Kimura and K. Watanabe, 1993 Isolation, overexpression and disruption of a *Saccharomyces cerevisiae* YNK gene encoding nucleoside diphosphate kinase. Gene **129:** 141-146.

Galvis, M. L., S. Marttila, G. Hakansson, J. Forsberg and C. Knorpp, 2001 Heat stress response in pea involves interaction of mitochondrial nucleoside diphosphate kinase with a novel 86-kilodalton protein. Plant Physiol **126:** 69-77.

Gilles, A. M., E. Presecan, A. Vonica and I. Lascu, 1991 Nucleoside diphosphate kinase from human erythrocytes. Structural characterization of the two polypeptide chains responsible for heterogeneity of the hexameric enzyme. J Biol Chem **266:** 8784-8789.

Harris, S. D., J. L. Morrell and J. E. Hamer, 1994 Identification and characterization of *Aspergillus nidulans* mutants defective in cytokinesis. Genetics **136:** 517-532.

Harvey, C., and P. W. French, 2000 Effects on protein kinase C and gene expression in a human mast cell line, HMC-1, following microwave exposure. Cell Biol Int **23:** 739-748.

Hasunuma, K., and N. Yabe, 1998 Early events occurring during light signal transduction in plants. Tanpakushitsu Kakusan Koso **43:** 1443-1452.

Hippe, H. J., S. Lutz, F. Cuello, K. Knorr, A. Vogt *et al.*, 2002 Activation of heterotrimeric G proteins by a high-energy phosphate transfer via nucleoside diphosphate kinase (NDPK) B and Gbeta subunits II. Specific activation of Gsalpha by a NDPK B-Gbeta gamma complex in H10 cells. J Biol Chem.

Ho, Y., A. Gruhler, A. Heilbut, G. D. Bader, L. Moore *et al.*, 2002 Systematic identification of protein complexes in *Saccharomyces cerevisiae* by mass spectrometry. Nature **415:** 180-183.

Ishibashi, M., H. Tokunaga, K. Hiratsuka, Y. Yonezawa, H. Tsurumaru *et al.*, 2001 NaCl-activated nucleoside diphosphate kinase from extremely halophilic archaeon, *Halobacterium salinarum*, maintains native conformation without salt. FEBS Lett **493:** 134-138.

Ito, T., T. Chiba, R. Ozawa, M. Yoshida, M. Hattori *et al.*, 2001 A comprehensive two-hybrid analysis to explore the yeast protein interactome. Proc Natl Acad Sci U S A **98:** 4569-4574.

Izumiya, H., and M. Yamamoto, 1995 Cloning and functional analysis of the ndk1 gene encoding nucleoside-diphosphate kinase in *Schizosaccharomyces pombe.*PG - 27859-64. J Biol Chem **270:** 27859-27864.

Janin, J., and D. Deville-Bonne, 2002 Nucleoside-diphosphate kinase: structural and kinetic analysis of reaction pathway and phosphohistidine intermediate. Methods Enzymol **354:** 118-134.

Kafer, E., 1977 Meiotic and mitotic recombination in Aspergillus and its chromosomal aberrations. Adv Genet **19:** 33-131.

Kuner, J. M., and D. Kaiser, 1982 Fruiting body morphogenesis in submerged cultures of *Myxococcus xanthus*. J Bacteriol **151:** 458-461.

Kuroda, A., and A. Kornberg, 1997 Polyphosphate kinase as a nucleoside diphosphate kinase in *Escherichia coli* and *Pseudomonas aeruginosa*. Proc Natl Acad Sci U S A **94:** 439-442.

Ladner, J. E., N. G. Abdulaev, D. L. Kakuev, M. Tordova, K. D. Ridge *et al.*, 1999 The three-dimensional structures of two isoforms of nucleoside diphosphate kinase from bovine retina. Acta Crystallogr D Biol Crystallogr **55:** 1127-1135.

LaRossa, R., J. Kuner, D. Hagen, C. Manoil and D. Kaiser, 1983 Developmental cell interactions of *Myxococcus xanthus*: analysis of mutants. J Bacteriol **153:** 1394-1404.

Lee, H. Y., and H. Lee, 1999 Inhibitory activity of nm23-H1 on invasion and colonization of human prostate carcinoma cells is not mediated by its NDP kinase activity. Cancer Lett **145:** 93-99.

Lee, I. H., S. I. Chang, K. Okada, H. Baba and H. Shiku, 1997 Transcription effect of nm23-M2/NDP kinase on c-myc oncogene. Mol Cells **7:** 589-593.

Leung, S. M., and L. E. Hightower, 1997 A 16-kDa protein functions as a new regulatory protein for Hsc70 molecular chaperone and is identified as a member of the Nm23/nucleoside diphosphate kinase family. J Biol Chem **272:** 2607-2614.

Lu, Q., and M. Inouye, 1996 Adenylate kinase complements nucleoside diphosphate kinase deficiency in nucleotide metabolism. Proc Natl Acad Sci U S A **93:** 5720-5725.

Ma, G. C., and E. Kafer, 1974 Genetic analysis of the reciprocal translocation T2(I;8) of Asperigillus using the technique of mitotic mapping in homozygous translocation diploids. Genetics **77:** 11-23.

MacDonald, N. J., J. M. Freije, M. L. Stracke, R. E. Manrow and P. S. Steeg, 1996 Site-directed mutagenesis of nm23-H1. Mutation of proline 96 or serine 120 abrogates its motility inhibitory activity upon transfection into human breast carcinoma cells. J Biol Chem **271:** 25107-25116.

Maeda, I., Y. Kohara, M. Yamamoto and A. Sugimoto, 2001 Large-scale analysis of gene function in *Caenorhabditis elegans* by high-throughput RNAi. Curr Biol **11:** 171-176.

Mesnildrey, S., F. Agou, A. Karlsson, D. D. Bonne and M. Veron, 1998 Coupling between catalysis and oligomeric structure in nucleoside diphosphate kinase. J Biol Chem **273:** 4436-4442.

Mesnildrey, S., F. Agou and M. Veron, 1997 The in vitro DNA binding properties of NDP kinase are related to its oligomeric state. FEBS Lett **418:** 53-57.

Milon, L., P. Meyer, M. Chiadmi, A. Munier, M. Johansson *et al.*, 2000 The human nm23-H4 gene product is a mitochondrial nucleoside diphosphate kinase. J Biol Chem **275:** 14264-14272.

Momany, M., and J. E. Hamer, 1997 The *Aspergillus nidulans* Septin Encoding Gene, aspB, Is Essential for Growth. Fungal Genet Biol **21:** 92-100.

Momany, M., and I. Taylor, 2000 Landmarks in the early duplication cycles of *Aspergillus fumigatus* and *Aspergillus nidulans:* polarity, germ tube emergence and septation. Microbiology **146:** 3279-3284.

Momany, M., P. J. Westfall and G. Abramowsky, 1999 *Aspergillus nidulans swo* mutants show defects in polarity establishment, polarity maintenance and hyphal morphogenesis. Genetics **151:** 557-567.

Morera, S., M. Chiadmi, G. LeBras, I. Lascu and J. Janin, 1995 Mechanism of phosphate transfer by nucleoside diphosphate kinase: X-ray structures of the phosphohistidine intermediate of the enzymes from Drosophila and Dictyostelium. Biochemistry **34:** 11062-11070.

Mourad, N., and R. E. Parks, Jr., 1966a Erythrocytic nucleoside diphosphokinase. 3. Studies with free and phosphorylated enzyme and evidence for an essential thiol group. J Biol Chem **241:** 3838-3844.

Mourad, N., and R. E. Parks, Jr., 1966b Erythrocytic nucleoside diphosphokinase. II. Isolation and kinetics. J Biol Chem **241:** 271-278.

Munier, A., C. Feral, L. Milon, V. P. Pinon, G. Gyapay *et al.*, 1998 A new human nm23 homologue (nm23-H5) specifically expressed in testis germinal cells. FEBS Lett **434:** 289-294.

Munoz-Dorado, J., M. Inouye and S. Inouye, 1990a Nucleoside diphosphate kinase from *Myxococcus xanthus*. I. Cloning and sequencing of the gene. J Biol Chem **265:** 2702-2706.

Munoz-Dorado, J., S. Inouye and M. Inouye, 1990b Nucleoside diphosphate kinase from *Myxococcus xanthus*. II. Biochemical characterization. J Biol Chem **265:** 2707-2712.

Negroni, A., D. Venturelli, B. Tanno, R. Amendola, S. Ransac *et al.*, 2000 Neuroblastoma specific effects of DR-nm23 and its mutant forms on differentiation and apoptosis. Cell Death Differ **7:** 843-850.

Noguchi, T., and T. Shiba, 1998 Use of *Escherichia coli* polyphosphate kinase for oligosaccharide synthesis. Biosci Biotechnol Biochem **62:** 1594-1596.

Nosaka, K., M. Kawahara, M. Masuda, Y. Satomi and H. Nishino, 1998 Association of nucleoside diphosphate kinase nm23-H2 with human telomeres. Biochem Biophys Res Commun **243:** 342-348.

Ogura, Y., Y. Yoshida, K. Ichimura, C. Aoyagi, N. Yabe *et al.*, 1999 Isolation and characterization of *Neurospora crassa* nucleoside diphosphate kinase NDK-1. Eur J Biochem **266:** 709-714.

Ogura, Y., Y. Yoshida, N. Yabe and K. Hasunuma, 2001 A point mutation in nucleoside diphosphate kinase results in a deficient light response for perithecial polarity in *Neurospora crassa*. J Biol Chem **276:** 21228-21234.

Ohkura, N., M. Kishi, T. Tsukada and K. Yamaguchi, 2001 Menin, a gene product responsible for multiple endocrine neoplasia type 1, interacts with the putative

tumor metastasis suppressor nm23. Biochem Biophys Res Commun **282:** 1206-1210.

Orlov, N., T. G. Orlova, Y. K. Reshetnyak, E. A. Burstein and N. Kimura, 1997 Interaction of recombinant rat nucleoside diphosphate kinase alpha with bleached bovine retinal rod outer segment membranes: a possible mode of pH and salt effects. Biochem Mol Biol Int **41:** 189-198.

Orlov, N. Y., and N. Kimura, 1998 Interaction of nucleoside diphosphate kinase with membranes of bleached bovine retinal rod outer segments. Effects of pH, salts, and guanine nucleotides. Biochemistry (Mosc) **63:** 171-179.

Osherov, N., J. Mathew and G. S. May, 2000 Polarity-defective mutants of *Aspergillus nidulans*. Fungal Genet Biol **31:** 181-188.

Osherov, N., and G. May, 2000 Conidial germination in *Aspergillus nidulans* requires RAS signaling and protein synthesis. Genetics **155:** 647-656.

Otsuki, Y., M. Tanaka, S. Yoshii, N. Kawazoe, K. Nakaya *et al.*, 2001 Tumor metastasis suppressor nm23H1 regulates Rac1 GTPase by interaction with Tiam1. Proc Natl Acad Sci U S A **98:** 4385-4390.

Ouatas, T., B. Abdallah, L. Gasmi, J. Bourdais, E. Postel *et al.*, 1997 Three different genes encode NM23/nucleoside diphosphate kinases in *Xenopus laevis*. Gene **194:** 215-225.

Ouatas, T., M. Selo, Z. Sadji, J. Hourdry, H. Denis *et al.*, 1998 Differential expression of nucleoside diphosphate kinases (NDPK/NM23) during Xenopus early development. Int J Dev Biol **42:** 43-52.

Polosina, Y., K. F. Jarrell, O. V. Fedorov and A. S. Kostyukova, 1998 Nucleoside diphosphate kinase from haloalkaliphilic archaeon *Natronobacterium magadii*: purification and characterization. Extremophiles **2:** 333-338.

Polosina, Y. Y., D. F. Zamyatkin, A. S. Kostyukova, V. V. Filimonov and O. V. Fedorov, 2002 Stability of *Natrialba magadii* NDP kinase: comparisons with other halophilic proteins. Extremophiles **6:** 135-142.

Postel, E. H., 1998 NM23-NDP kinase. Int J Biochem Cell Biol **30:** 1291-1295.

Postel, E. H., B. A. Abramczyk, S. K. Gursky and Y. Xu, 2002 Structure-based mutational and functional analysis identify human NM23-H2 as a multifunctional enzyme. Biochemistry **41:** 6330-6337.

Postel, E. H., B. M. Abramczyk, M. N. Levit and S. Kyin, 2000a Catalysis of DNA cleavage and nucleoside triphosphate synthesis by NM23-H2/NDP kinase share an active site that implies a DNA repair function. Proc Natl Acad Sci U S A **97:** 14194-14199.

Postel, E. H., S. J. Berberich, J. W. Rooney and D. M. Kaetzel, 2000b Human NM23/nucleoside diphosphate kinase regulates gene expression through DNA binding to nuclease-hypersensitive transcriptional elements. J Bioenerg Biomembr **32:** 277-284.

Punt, P. J., J. Strauss, R. Smit, J. R. Kinghorn, C. A. van den Hondel *et al.*, 1995 The intergenic region between the divergently transcribed niiA and niaD genes of *Aspergillus nidulans* contains multiple NirA binding sites which act bidirectionally. Mol Cell Biol **15:** 5688-5699.

Quail, P. H., 2000 Phytochrome-interacting factors. Semin Cell Dev Biol **11:** 457-466.

Reymond, A., S. Volorio, G. Merla, M. Al-Maghtheh, O. Zuffardi *et al.*, 1999 Evidence for interaction between human PRUNE and nm23-H1 NDPKinase. Oncogene **18:** 7244-7252.

Roymans, D., K. Vissenberg, C. De Jonghe, R. Willems, G. Engler *et al.*, 2001 Identification of the tumor metastasis suppressor Nm23-H1/Nm23-R1 as a constituent of the centrosome. Exp Cell Res **262:** 145-153.

Roymans, D., R. Willems, K. Vissenberg, C. De Jonghe, B. Grobben *et al.*, 2000 Nucleoside diphosphate kinase beta (Nm23-R1/NDPKbeta) is associated with intermediate filaments and becomes upregulated upon cAMP-induced differentiation of rat C6 glioma. Exp Cell Res **261:** 127-138.

Shaw, B. D., C. Momany and M. Momany, 2002 *Aspergillus nidulans swoF* encodes an N-myristoyl transferase. Eukaryot Cell **1:** 241-248.

Shiba, T., K. Tsutsumi, K. Ishige and T. Noguchi, 2000 Inorganic polyphosphate and polyphosphate kinase: their novel biological functions and applications. Biochemistry (Mosc) **65:** 315-323.

Shimkets, L. J., and D. Kaiser, 1982 Induction of coordinated movement of *Myxococcus xanthus* cells. J Bacteriol **152:** 451-461.

Song, E. J., Y. S. Kim, J. Y. Chung, E. Kim, S. K. Chae *et al.*, 2000 Oxidative modification of nucleoside diphosphate kinase and its identification by matrix-assisted laser desorption/ionization time-of-flight mass spectrometry. Biochemistry **39:** 10090-10097.

Spormann, A. M., and D. Kaiser, 1999 Gliding mutants of *Myxococcus xanthus* with high reversal frequencies and small displacements. J Bacteriol **181:** 2593-2601.

Struglics, A., and G. Hakansson, 1999 Purification of a serine and histidine phosphorylated mitochondrial nucleoside diphosphate kinase from *Pisum sativum*. Eur J Biochem **262:** 765-773.

Tanaka, N., T. Ogura, T. Noguchi, H. Hirano, N. Yabe *et al.*, 1998 Phytochrome-mediated light signals are transduced to nucleoside diphosphate kinase in *Pisum sativum* L. cv. Alaska. J Photochem Photobiol B **45:** 113-121.

Tsuchiya, K. S., T. Kanbe, M. Hori, Y. Uehara, Y. Takahashi *et al.*, 1993 Distinct effects of clinically used anthracycline antibiotics on ras oncogene-expressed cells. Biol Pharm Bull **16:** 908-911.

Uno, T., M. Ueno, M. Kikuchi and Y. Aizono, 2002 Purification and characterization of nucleoside diphosphate kinase from the brain of *Bombyx mori*. Arch Insect Biochem Physiol **50:** 147-155.

Venturelli, D., R. Martinez, P. Melotti, I. Casella, C. Peschle *et al.*, 1995 Overexpression of DR-nm23, a protein encoded by a member of the nm23 gene family, inhibits granulocyte differentiation and induces apoptosis in 32Dc13 myeloid cells. Proc Natl Acad Sci U S A **92:** 7435-7439.

Webb, P. A., O. Perisic, C. E. Mendola, J. M. Backer and R. L. Williams, 1995 The crystal structure of a human nucleoside diphosphate kinase, NM23-H2. J Mol Biol **251:** 574-587.

Wheeler, L. J., N. B. Ray, C. Ungermann, S. P. Hendricks, M. A. Bernard *et al.*, 1996 T4 phage gene 32 protein as a candidate organizing factor for the deoxyribonucleoside triphosphate synthetase complex. J Biol Chem **271:** 11156-11162.

Yelton, M. M., J. E. Hamer and W. E. Timberlake, 1984 Transformation of *Aspergillus nidulans* by using a trpC plasmid. Proc Natl Acad Sci U S A **81:** 1470-1474.

Zaborina, O., N. Misra, J. Kostal, S. Kamath, V. Kapatral *et al.*, 1999 P2Z-Independent and P2Z receptor-mediated macrophage killing by *Pseudomonas aeruginosa* isolated from cystic fibrosis patients. Infect Immun **67:** 5231-5242.

Zhang, D., and K. Chang, 1995 The regulatory effect of nucleoside diphosphate kinase on G-protein and G-protein mediated phospholipase C. Chin Med Sci J **10:** 25-29.

Zimmermann, S., A. Baumann, K. Jaekel, I. Marbach, D. Engelberg *et al.*, 1999 UV-responsive genes of arabidopsis revealed by similarity to the Gcn4-mediated UV response in yeast. J Biol Chem **274:** 17017-17024.

CHAPTER 4

SWOHP IS INVOLVED IN SPECIFIC STRESS RESPONSE ATTENUATION IN *ASPERGILLUS NIDULANS*

ABSTRACT

The *swoH1* mutant exhibited some phenotypes similar to *A. nidulans* glycerol 3-phosphate dehydrogenase null mutant *?gfdA*. The glycerol 3-phosphate dehydrogenase is one of the key enzymes involved in stress responses in fungi. We found that the *swoH1* mutant accumulated glycogen, deposited more cell wall material at the swollen part of mutant hyphae and was sensitive to SDS. SwoHp is not likely to be involved in the general stress response based on observations that the *swoH1* mutant was not sensitive to several other stresses including oxidative stress, reductive stress and inhibition of DNA synthesis, cell wall, and microtubule functions. Unlike the Arabidopsis NDK Ia, SwoHp may not act through the GCN4 pathway in its regulation of stress response. The *swoH1* mutant was salt remedial but not osmotically remedial, suggesting that SwoHp might be involved specifically in saline stress response attenuation.

INTRODUCTION

The *swoH* gene encodes the nucleoside diphosphate kinase (NDK) in *Aspergillus nidulans*, which catalyzes the transfer of the ?-phosphate from a nucleoside triphosphate (NTP) to a nucleoside diphosphate (NDP) and is responsible for the maintenance of an appropriate energy state of the cell (Agarwal *et al.* 1978). As described in previous chapter, NDK is dispensable in yeast but is lethal in *A. nidulans*, so there might be other unknown important biological roles of NDK.

Indeed, besides the housekeeping function providing NTPs, NDKs are likely involved in many cellular processes. Many molecules have been found to interact with NDKs genetically and physically (Zhang and Chang 1995; Leung and Hightower 1997;

Orlov and Kimura 1998; Choi *et al.* 1999; Reymond *et al.* 1999; Agou *et al.* 2000; Postel *et al.* 2000; Roymans *et al.* 2000; Galvis *et al.* 2001; Ohkura *et al.* 2001; Otsuki *et al.* 2001; Cuello *et al.* 2002; Fournier *et al.* 2002a; Fournier *et al.* 2002b; Roymans *et al.* 2002). NDKs have been shown to be components in signal transduction pathways (Orlov and Kimura 1998; Tanaka *et al.* 1998; Choi *et al.* 1999; Zhang *et al.* 1999; Zimmermann *et al.* 1999; Quail 2000; Ogura *et al.* 2001; Cuello *et al.* 2002; Hippe *et al.* 2002; Ho *et al.* 2002). NDKs may also be involved in certain stress responses (Tsuchiya *et al.* 1993; Orlov and Kimura 1998; Zaborina *et al.* 1999; Harvey and French 2000; Song *et al.* 2000; Galvis *et al.* 2001) and may serve as a target for protons and salts (Orlov *et al.* 1997). Yeast NDK shows upregulated transcription under various cell damaging conditions (Ito *et al.* 2001).

Adaptation to changes in the environment and resumption of growth is critical for cell survival. Regulation of stress adaptation genes allows the cell to sense, respond to, and adapt to changing extracellular environmental conditions. Stress responses are classified into two categories: specific and general. The specific response changes only when challenged with specific stresses such as heat shock, oxidative stress, nutrient limitation, or osmostress (Mager and De Kruijff 1995). During the specific stress response, the general response will also be induced. Most responsive genes show a very transient expression pattern and then fall to the normal expression level in the presence of stress (Posas *et al.* 2000). The attenuation is important for resumption of normal growth. We found that SwoHp may be involved in specific stress attenuation in *A. nidulans.*

MATERIALS AND METHODS

Strains and media. Strains used in this study are: A773 (*pyrG89; wA3; pyroA4*); AGB52 (*cpcA?::phleR; pyrG89; pabaA1; yA2; veA1*); AXL20 (*swoH (ts-); pyroG89; pyroA4*). A773 was purchased from the Fungal Genetics Stock Center (Department of Microbiology, University of Kansas Medical Center). Isolation of the temperature sensitive *swoH1* mutant has been previously described (Momany *et al.* 1999). AGB52 was kindly provided by Dr. Sven Krappmann (Institute of Microbiology & Genetics, Germany). Strain construction and genetic analysis used standard *A. nidulans* techniques (Kafer 1977; Harris *et al.* 1994). Media used were as previously reported (Momany *et al.* 1999). For chemical sensitivity test, the conidia were inoculated in the medium with addition of agents such as 1M NaCl, 0.005% SDS, or 10mM histidine analog 3-amino-1,2,4-trizaole (3-AT) and incubated at indicated temperatures for two days.

Growth conditions and light microscopic observation. Conditions for growth and preparation of cells were as previously reported (Momany *et al.* 1999). Briefly, spores were inoculated on coverslips in liquid medium in a petri dish. After incubation, cells were fixed and nuclei were stained with Hoechst 33258 (Sigma, St. Louis), septa were stained with Calcofluor (American Cyanamid, Wayne, NJ) , and glycogen was stained with IKI solution (60mg/ml KI and 10mg/ml I_2) as previously described(Weber *et al.* 1998; Thines *et al.* 2000). Microscopic observations were made using a Zeiss Axioplan microscope (Thornwood, NY, USA) and digital images were acquired using an Optronics digital imaging system (Goleta, CA, USA). Images were prepared using Photoshop 5.5 (Adobe, Mountain View, CA, USA).

Transmission electron microscope observation. Spores were inoculated on dialysis membrane on minimal medium with proper supplements and were grown at 30°C for 14 hours. Preparation of cells for TEM was as previously reported (Momany *et al.* 2002). Briefly, the dialysis membrane with adhering hyphae was fixed by dip freezing and followed by freeze substitution. Samples were flat embedded in Embed/Araldite resin (Electron Microscopy Sciences, Ft. Washington, Pennsylvania) and sectioned using an RMC 6000XL ultramicrotome. Sections on gold grids were post-stained with uranyl acetate and lead citrate and was examined in a Zeiss EM 902A TEM.

Cell wall analysis. Cell wall from wild type A773, *swoH1* mutant AXL20 was isolated from an overnight culture at 42C and analyzed as previously described (Guest and Momany 2000). Briefly, cell wall samples were prepared, trimethysilylated (TMS), resolved, and analyzed using gas chromatography and mass spectroscopy (GC/MS) at the Complex Carbohydrate Research Center at the University of Georgia (http://www.ccrc.uga.edu/).

RESULTS

Stress Related Phenotype of The *swoH1* Mutant.

The *swoH1* mutant shares a similar phenotype to the *A. nidulans* glycerol 3-phosphate dehydrogenase null mutant *?gfdA*. In previous studies, it was shown that at restrictive temperature the *swoH1* mutant stopped tip growth shortly after germ tube emergence and that the mutant cells had varied but not extended swollen hyphae. This phenotype is similar to the *A. nidulans* glycerol 3-phosphate dehydrogenase null mutant *?gfdA* (Blomberg 1997; Fillinger *et al.* 2001). Glycerol 3-phosphate dehydrogenase is

one of the key enzymes in the production of glycerol (Blomberg 1997), the main osmolyte used by many fungi in response to increased external osmotic potential due to its compatibility with cellular processes at high concentrations. This suggests that there might be a connection between SwoHp and osmostress response.

The *swoH1* mutant accumulates glycogen along the hyphae. Since the *swoH1* mutant at restrictive temperature looks like the *?gfdA* mutant, then it is possible that concentration of glycerol or its polymerization product, glycogen, may change levels in the mutant cells. To observe glycogen, we used the IKI dye, which stains starch in plant cells and glycogen in fungi. We stained the *swoH1* mutant and wild type after overnight growth at restrictive temperature and found that the *swoH1* mutant showed stained brownish spots along the hyphae (Figure 4.1b), while the wild type growing under the same conditions stained only at the original conidium (Figure 4.1a). This suggests that the mutant cells accumulate glycogen along the hyphae. To make sure that what we observed was indeed glycogen, we imaged the wild type and mutant under transmission electronic microscope and found glycogen bodies in the hyphae of the mutant even at permissive temperature although fewer than at restrictive temperature (Figure 4.1c). Glycogen body was not observed in the wild type hyphae. One possible explanation for the accumulation of glycogen is that the mutant cells have a high concentration of glycerol, which converts to glycogen in the absence of high osmolarity outside of the cell.

The *swoH1* mutant is SDS sensitive. If the *swoH1* mutant has a high intracellular osmotic potential, the overstretched plasma membrane is likely to be fragile. To test if the mutant is sensitive to agents detrimental to the plasma membrane, we grew the wild type A773 and the *swoH1* mutant AXL20 in medium containing 0.005% SDS, a

detergent that can penetrate the plasma membrane. We found that indeed the *swoH1* mutant showed elevated sensitivity to SDS at permissive temperature (Figure 4.2), suggesting that the plasma membrane of the *swoH1* mutant is fragile.

The *swoH1* mutant deposits more cell wall material at the swollen part of the hyphae and showed no defect in cell wall synthesis. In the presence of higher inner pressure, cell wall synthesis pathways will be activated to strengthen the cell wall. To see if the *swoH1* mutant deposits more cell wall, we used the dye Calcofluor, which binds to ß-linked glucans and chitin, components of the fungal cell wall. In *A. nidulans* chitin is concentrated at the septa compared with other parts of the cell wall, thus Calcofluor stained septa brightly in wild type and the *swoH1* mutant grown at permissive temperature (Figure 4.3b). However, the *swoH1* mutant stained extremely brightly with Calcofluor at the swollen part of the hyphae as well as septa when grown at restrictive temperature (Figure 4.3a), which again resembles the phenotype of the *?gfdA* mutant (Blomberg 1997; Fillinger *et al.* 2001). Since the *?gfdA* mutant has a defect in cell wall integrity and mutants with cell wall defects usually have altered sensitivity to cell wall disrupting drugs (Garcia-Rodriguez *et al.* 2000; Rodriguez-Pena *et al.* 2000; Santos and Snyder 2000; Fillinger *et al.* 2001; Martin-Yken *et al.* 2001; Tanaka *et al.* 2001; Richard *et al.* 2002), we tested the sensitivity of the *swoH1* mutant to Calcofluor, which inhibits chitin synthesis, and Caspofungin acetate, an inhibitor of ß(1-3)?D-glucan synthase (CANCIDAS, Merck, Whitehouse Station, NJ)(Georgopapadakou 2001). However, the *swoH1* mutant did not show any changed sensitivity to Calcofluor (Momany *et al.* 1999) nor caspofungin acetate (data not shown) compared with wild type grown under the same condition, which is different from the *?gfdA* mutant (Fillinger *et al.* 2001).

To further analyze the cell wall composition of the mutant, we isolated cell walls from the wild type and the *swoH1* mutant culture at restrictive temperature and analyzed by Gas Chromatography coupled with Mass spectrometer (GC/MS) to see if the cell wall changed in the mutant, since cell wall defect mutants usually have different cell wall components from the wild type (personal communication with Dr. Guest) (da-Silva *et al.* 1994). As shown by Table 4.1, the *swoH1* mutant had similar cell wall composition to wild type and contained only a slightly higher ratio of carbohydrate in the cell wall, suggesting that the cell wall synthetic pathway may still be functional and that there may simply be more cell wall material produced in response to weak cell wall. (Rhamnose is a minor component in *A. nidulans* cell wall and its concentration varies a lot under different conditions).

The SwoHp is not involved in general stress response. To determine whether SwoHp is involved in a specific or general stress response, we tested the sensitivity of the *swoH1* mutant in several other stress conditions (Mager and De Kruijff 1995; Chatterjee *et al.* 2000). The following drugs were tested: (1) Anti-microtubule drugs: Microtubules are essential for tip growth in filamentous fungi and it has been shown that some NDKs can bind microtubules (Nickerson and Wells 1984). To see if a defect in microtubule function caused the *swoH1* mutant nonpolar phenotype, several drugs that affect microtubule functions were used: benomyl (breaks down microtubules), nocadazole (breaks down microtubules), taxol (stabilizes microtubules), and D_2O (stabilizes microtubules). The *swoH1* mutant did not show any changes in sensitivity to these drugs compared with wild type (data not shown). (2) DNA synthesis inhibitor. Since SwoHp is the major enzyme to provide NTP and dNTP, the *swoH1* mutation may disturb the

nucleotide triphosphate pool and could result in changed sensitivity to anti-DNA synthesis drugs. However, the *swoH1* mutant is as sensitive as wild type to hydroxyurea, which inhibits DNA synthesis by depleting nucleotide triphosphates (data not shown). (3) Oxidative stress: The *swoH1* mutant showed similar sensitivity as did wild type to Menadione bisulfate (superoxide stress), Diamide (sulfhydryl ozidizing agent), and H_2O_2 (data not shown). (4) Reductive stress: There was no difference in the sensitivity between wild type and the mutant to dithiothreitol (DTT, disulfide reducing agent) (data not shown). This evidence suggests that SwoHp is unlikely to be involved in the general stress response.

SwoHp involvement in stress response is not related to the GCN4 stress response pathway. Arabidopsis NDK Ia can complement the yeast *gcn4* null mutant (Zimmermann *et al.* 1999). GCN4 is the general transcription factor which activates enzymes involved in amino acid synthetic pathways during amino acid starvation (Natarajan *et al.* 2001). In addition, GCN4 is also a regulator in some stress responses (Zimmermann *et al.* 1999; Goossens *et al.* 2001; Marbach *et al.* 2001; Pascual-Ahuir *et al.* 2001; Hinnebusch and Natarajan 2002; Talloczy *et al.* 2002). Arabidopsis NDK Ia has been shown to bind the HIS4 promoter specifically and induces HIS4 (HIS4 encodes a protein involved in histidine synthesis) transcription in yeast (Zimmermann *et al.* 1999). Some NDKs are transcription factors and have been shown to have nuclease activity (Lee *et al.* 1997; Postel 1999; Agou *et al.* 2000; Postel *et al.* 2000; Levit *et al.* 2002; Postel *et al.* 2002). So it is possible that Arabidopsis NDK Ia might serve as a transcription factor and have overlapping function with yeast GCN4. To see if SwoHp also conserves this function, we tested the sensitivity of *swoH1* mutant to the histidine analogue 3AT and

found that the *swoH1* mutant is indeed as sensitive to histidine starvation as the the ?*cpcA* mutant (*gcn4* null mutant in *A. nidulans*) (Hoffmann *et al.* 2001) (Figure 4.4). However, multiple copies of the *swoH* gene did not complement the *A. nidulans* ?*cpcA* mutant AGB52 (*cpcA* is *A. nidulans* homologue of yeast GCN4) in the sensitivity to amino acid starvation, nor did the *swoH* cDNA complement the yeast *?gcn4* mutant (data not shown). This suggests that even though NDKs are highly conserved across kingdoms, they may have different functions in different organisms. Since amino acid and nucleotide synthesis are highly intertwined (Serre *et al.* 1999) and amino acid starvation causes derepression of both certain amino acid biosynthetic enzymes and nucleotide biosynthetic enzymes (Carsiotis and Jones 1974; Carsiotis *et al.* 1974; Schurch *et al.* 1974; Wolfner *et al.* 1975; Jia *et al.* 2000), it is very likely that the sensitivity of the *swoH1* mutant to hisitidine starvation is an indirect effect of reduced NDK activity in the *swoH1* mutant, particularly since the histidine synthesis pathway starts with condensation of ATP (Barbosa *et al.* 2002). Indeed the *swoH1* mutant is not sensitive to the analogue of tryptophan, 5-methyl-tryptophan (data not shown).

The *swoH1* mutant is salt remedial. The *swoH1* mutant may have higher than normal intracellular tugor pressure, therefore, an increase of extracellular osmotic potential may restore the swollen phenotype. Indeed, like the *?gfdA* mutant (Fillinger *et al.* 2001), the *swoH1* mutant was restored to wild type growth in media containing 1M NaCl/KCl with various carbon sources at restrictive temperature (Figure 4.5). However, unlike the *?gfdA* mutant, the *swoH1* mutant is not sorbitol (Momany *et al.* 1999) or sucrose remedial (data not shown), suggesting that SwoHp is involved specifically in salt stress rather than the general hyperosmotic stress. The cellular stress responses to the

saline condition include active exclusion of the extracellular salt in addition to intracellular accumulation of glycerol as occurred in hyperosmotic stress.

DISCUSSION

Working model for the SwoHp: higher tugor pressure caused by inability to attenuate certain stress responses is responsible for the *swoH1* mutant phenotype. Fillinger *et al* proposed that glycerol 3-phosphate dehydrogenase links with the cell wall integrity pathway (Fillinger *et al.* 2001). Since the *swoH1* mutant shared some phenotypes with the *?gfdA* mutant, it is possible that the *swoH1* mutant phenotype could also be caused by a defect in cell wall synthesis. We think, however, that the cell wall synthetic pathway is functional in the *swoH1* mutant based on the following: (1) Many cell wall defect mutants have changed sensitivity to cell wall disrupting drugs such as Calcofluor and Caspofungin acetate, but the *swoH1* mutant was not sensitive to them. (2) It is common that mutants with cell wall defects have different cell wall compositions from wild type (da-Silva *et al.* 1994)(Guest, Lin and Momany, unpublished), but cell wall isolated from the *swoH1* mutant culture grown at restrictive temperature showed a similar profile to wild type. (3) If the *swoH1* mutant phenotype is caused by a weak cell wall, then we would expect that both neutral and charged osmolytes should rescue the mutant at restrictive temperature as in the *?gfdA* mutant. However, the *swoH1* mutant is only salt remedial.

Our working model (Figure 4.6) is: At restrictive temperature, when the mutated SwoHp is not fully functional, certain stress responses cannot be attenuated in *swoH1*, and initial temporary changes in the wild type are persistent in *swoH1*. The production of

glycerol continues and leads to accumulation of glycogen in the absence of extracellular high osmolarity. The generated high inner pressure in turn caused the hypersensitivity of the *swoH1* mutant to SDS. The inability to reduce turgor pressure encourages cell expansion and results in swollen hyphae, which signals the cell to deposit more cell wall material in the weak areas. Eventually, lysis occurs. This inability of the *swoH1* mutant to attenuate certain stress responses at restrictive temperature is lethal in most situations.

Exposure to high salt causes both ionic and hyperosmotic stresses (Nakamura *et al.* 1993; Mendoza *et al.* 1994; Han and Prade 2002; Matsumoto *et al.* 2002). In conditions like this, part of the stress response will not relax after initial changes since salts have to actively be kept out of the cell to mediate ion homeostasis, which could not be accomplished only by glycerol accumulation. This saline condition provides high extracellular osmolarity and requires certain stress responses to be constantly on, which compensates for the inability of the *swoH1* mutant to survive certain stresses.

The fact that the *swoH1* mutant did not show altered sensitivity to agents affecting cell wall integrity, microtubules, DNA synthesis, oxidative stress and reductive stress suggests that SwoHp is involved in saline stress response, not the general stress response. The sensitivity to histidine starvation but not tryptophan starvation suggests that SwoHp and GCN4p are in different pathways. Comparing transcription profiles of wild type in saline stress and in hyperosmostic stress to those of the *swoH1* mutant in saline stress and without stress using microarrays will be helpful to define the role of SwoHp in stress attenuation in *A. nidulans.*

ACKNOWLEDGEMENT

I would like to thank Elizabeth Richardson for teaching me the TEM techniques.

Table 4.1. Carbohydrate composition in wild type and mutant cell walls[a]

Strain	Carb[b]/CW	Glucose	Galactose	Mannose	Rhamnose	GlcNac[c]
Wt (A28)	61	71.3	9.1	8.6	1.9	9.1
swoH1 (AXL20)	69	78.0	7.7	7.4	0.6	6.3

[a] Average percent of individual sugar present in total carbohydrate based on GC/MS chromatographic area. Analysis was repeated two times with essentially identical results.

[b] Carbohydrate

[c] N-acetylglucosamine.

Figure 4.1. The *swoH1* mutant cells accumulate glycogen along the hyphae. Wild type (a) and *swoH1* mutant cells (b) were cultured at 42C for 16 hours and stained with IKI. (c) Glycogen body shown by TEM in the *swoH1* mutant hyphae grown at 30C for 14 hours. Arrows point to glycogen bodies.

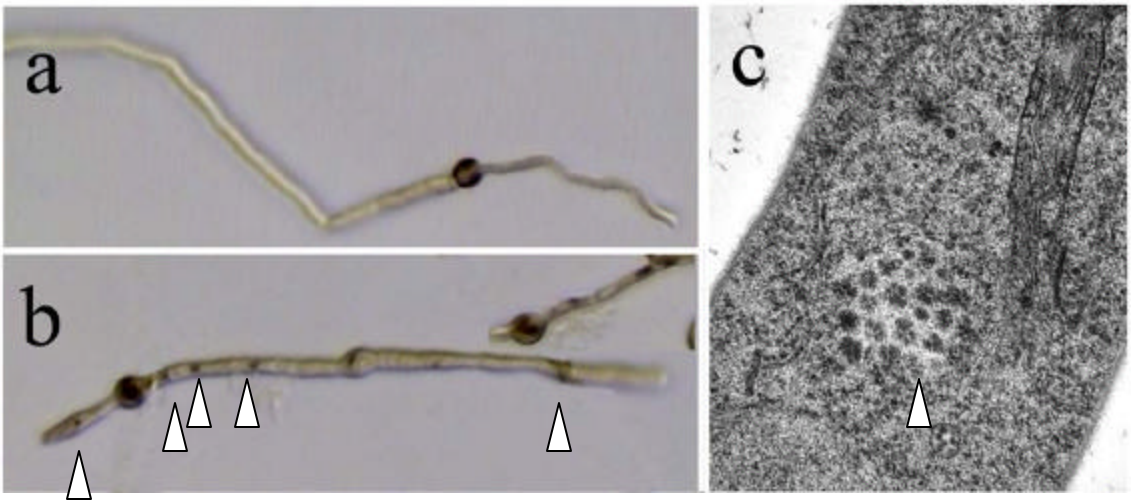
a
b
c

Figure 4.2. The *swoH1* mutant is hypersensitive to SDS. Conidia of wild type and the *swoH1* mutant were inoculated and grown at 37C for 2 days on media with different carbon sources. The lower row shows growth on media containing 0.005% SDS.

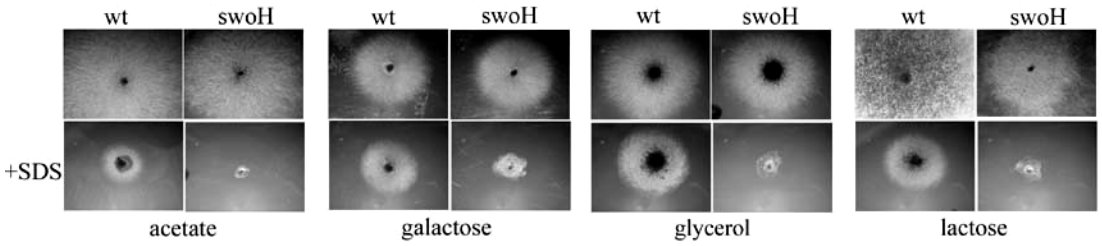
wt
swoH
wt
swoH
wt
swoH
wt
swoH
+SDS
acetate
galactose
glycerol
lactose

Figure 4.3. The *swoH1* mutant is Calcofluor bright at restrictive temperature. Wild type (b) and *swoH1* mutant (a) were grown at 42C for 16 hrs. Cells were fixed and stained with Calcofluor.

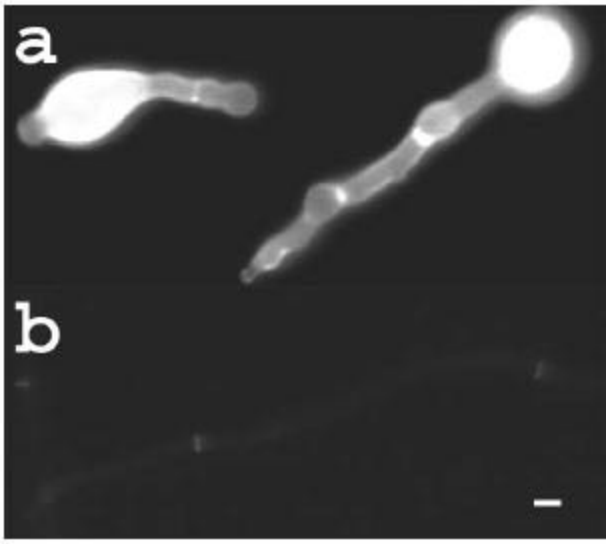
a
b

Figure 4.4. The *swoH1* mutant is sensitive to histidine starvation. Spores of wild type (lower row) and the *swoH1* mutant (upper row) were grown at 37C for 2 days in media with 0 mM 3-AT, 3 mM 3-AT, and 5 mM 3-AT.

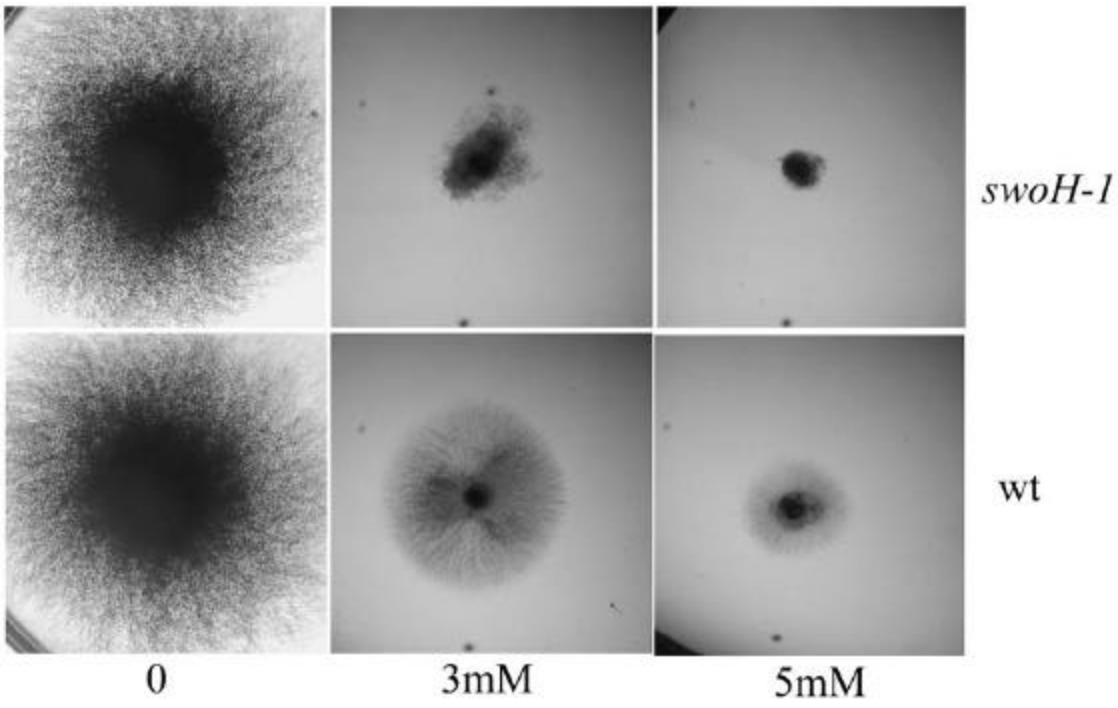
swoH-1
wt
0
3mM
5mM

Figure 4.5. The *swoH1* mutant is salt remedial. Conidia of wild type and *swoH1* mutant were inoculated and grown at 42C for 2 days on media with different carbon sources. The lower row shows growth on media with 1M NaCl.

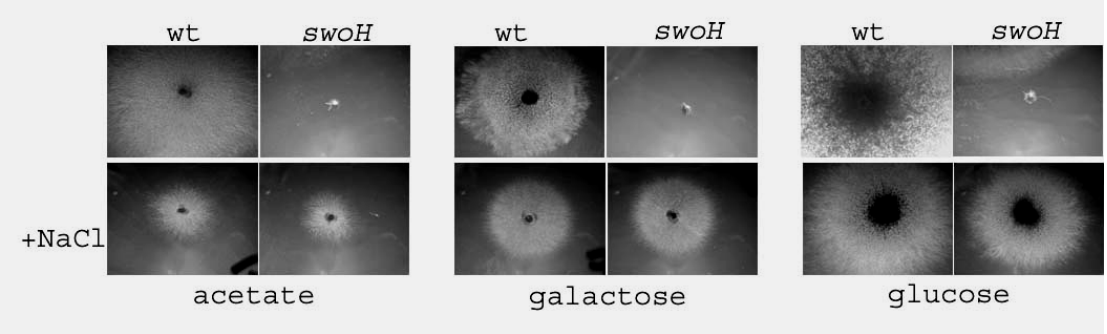
wt
swoH
wt
swoH
wt
swoH
+NaCl
acetate
galactose
glucose

Figure 4.6. SwoHp working model. Red indicates new growth, black indicates cell wall. Left to right: from original spore to apical cell.

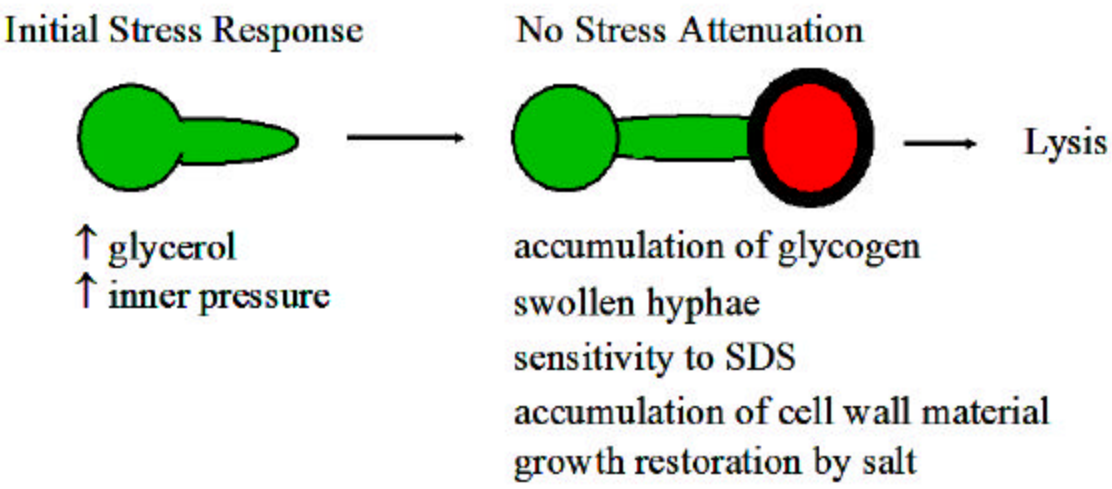
Initial Stress Response
No Stress Attenuation
Lysis
↑ glycerol
↑ inner pressure
accumulation of glycogen
swollen hyphae
sensitivity to SDS
accumulation of cell wall material
growth restoration by salt

REFERENCES

Agarwal, R. P., B. Robison and R. E. Parks, Jr., 1978 Nucleoside diphosphokinase from human erythrocytes. Methods Enzymol **51:** 376-386.

Agou, F., S. Raveh and M. Veron, 2000 The binding mode of human nucleoside diphosphate kinase B to single-strand DNA. J Bioenerg Biomembr **32:** 285-292.

Barbosa, J. A., J. Sivaraman, Y. Li, R. Larocque, A. Matte *et al.*, 2002 Mechanism of action and NAD+-binding mode revealed by the crystal structure of L-histidinol dehydrogenase. Proc Natl Acad Sci U S A **99:** 1859-1864.

Blomberg, A., 1997 Osmoresponsive proteins and functional assessment strategies in *Saccharomyces cerevisiae*. Electrophoresis **18:** 1429-1440.

Carsiotis, M., and R. F. Jones, 1974 Cross-pathway regulation: tryptophan-mediated control of histidine and arginine biosynthetic enzymes in *Neurospora crassa*. J Bacteriol **119:** 889-892.

Carsiotis, M., R. F. Jones and A. C. Wesseling, 1974 Cross-pathway regulation: histidine-mediated control of histidine, tryptophan, and arginine biosynthetic enzymes in *Neurospora crassa*. J Bacteriol **119:** 893-898.

Chatterjee, M. T., S. A. Khalawan and B. P. Curran, 2000 Cellular lipid composition influences stress activation of the yeast general stress response element (STRE). Microbiology **146 (Pt 4):** 877-884.

Choi, G., H. Yi, J. Lee, Y. K. Kwon, M. S. Soh *et al.*, 1999 Phytochrome signalling is mediated through nucleoside diphosphate kinase 2. Nature **401:** 610-613.

Cuello, F., R. A. Schulze, F. Heemeyer, H. E. Meyer, S. Lutz *et al.*, 2002 Activation of heterotrimeric G proteins by a high-energy phosphate transfer via nucleoside

diphosphate kinase (NDPK) B and Gbeta subunits I. Complex formation of NDPK B with Gbeta gamma dimers and phosphorylation of His266 in Gbeta. J Biol Chem.

da-Silva, M. M., M. L. Polizeli, J. A. Jorge and H. F. Terenzi, 1994 Cell wall deficiency in "slime" strains of *Neurospora crassa*: osmotic inhibition of cell wall synthesis and beta-D-glucan synthase activity. Braz J Med Biol Res **27:** 2843-2857.

Fillinger, S., G. Ruijter, M. J. Tamas, J. Visser, J. M. Thevelein *et al.*, 2001 Molecular and physiological characterization of the NAD-dependent glycerol 3-phosphate dehydrogenase in the filamentous fungus *Aspergillus nidulans*. Mol Microbiol **39:** 145-157.

Fournier, H. N., S. Dupe-Manet, D. Bouvard, M. L. Lacombe, C. Marie *et al.*, 2002a ICAP-1alpha interacts directly with the metastasis suppressor nm23-H2 and both proteins are targeted to newly formed cell adhesion sites upon integrin engagement. J Biol Chem **27:** 27.

Fournier, H. N., S. Dupe-Manet, D. Bouvard, M. L. Lacombe, C. Marie *et al.*, 2002b Integrin cytoplasmic domain-associated protein 1alpha (ICAP-1alpha) interacts directly with the metastasis suppressor nm23-H2, and both proteins are targeted to newly formed cell adhesion sites upon integrin engagement. J Biol Chem **277:** 20895-20902.

Galvis, M. L., S. Marttila, G. Hakansson, J. Forsberg and C. Knorpp, 2001 Heat stress response in pea involves interaction of mitochondrial nucleoside diphosphate kinase with a novel 86-kilodalton protein. Plant Physiol **126:** 69-77.

Garcia-Rodriguez, L. J., A. Duran and C. Roncero, 2000 Calcofluor antifungal action depends on chitin and a functional high-osmolarity glycerol response (HOG) pathway: evidence for a physiological role of the *Saccharomyces cerevisiae* HOG pathway under noninducing conditions. J Bacteriol **182:** 2428-2437.

Georgopapadakou, N. H., 2001 Update on antifungals targeted to the cell wall: focus on beta-1,3-glucan synthase inhibitors. Expert Opin Investig Drugs **10:** 269-280.

Goossens, A., T. E. Dever, A. Pascual-Ahuir and R. Serrano, 2001 The protein kinase Gcn2p mediates sodium toxicity in yeast. J Biol Chem **276:** 30753-30760.

Guest, G., and M. Momany, 2000 Analysis of cell wall sugars in the pathogen *Aspergillus fumigatus* and the saprophyte *Aspergillus nidulans*. Mycologia **92:** 1047-1050.

Han, K. H., and R. A. Prade, 2002 Osmotic stress-coupled maintenance of polar growth in *Aspergillus nidulans*. Mol Microbiol **43:** 1065-1078.

Harris, S. D., J. L. Morrell and J. E. Hamer, 1994 Identification and characterization of *Aspergillus nidulans* mutants defective in cytokinesis. Genetics **136:** 517-532.

Harvey, C., and P. W. French, 2000 Effects on protein kinase C and gene expression in a human mast cell line, HMC-1, following microwave exposure. Cell Biol Int **23:** 739-748.

Hinnebusch, A. G., and K. Natarajan, 2002 Gcn4p, a master regulator of gene expression, is controlled at multiple levels by diverse signals of starvation and stress. Eukaryot Cell **1:** 22-32.

Hippe, H. J., S. Lutz, F. Cuello, K. Knorr, A. Vogt *et al.*, 2002 Activation of heterotrimeric G proteins by a high-energy phosphate transfer via nucleoside

diphosphate kinase (NDPK) B and Gbeta subunits II. Specific activation of Gsalpha by a NDPK B-Gbeta gamma complex in H10 cells. J Biol Chem.

Ho, Y., A. Gruhler, A. Heilbut, G. D. Bader, L. Moore *et al.*, 2002 Systematic identification of protein complexes in *Saccharomyces cerevisiae* by mass spectrometry. Nature **415:** 180-183.

Hoffmann, B., O. Valerius, M. Andermann and G. H. Braus, 2001 Transcriptional autoregulation and inhibition of mRNA translation of amino acid regulator gene *cpcA* of filamentous fungus *Aspergillus nidulans*. Mol Biol Cell **12:** 2846-2857.

Ito, T., T. Chiba, R. Ozawa, M. Yoshida, M. Hattori *et al.*, 2001 A comprehensive two-hybrid analysis to explore the yeast protein interactome. Proc Natl Acad Sci U S A **98:** 4569-4574.

Jia, M. H., R. A. Larossa, J. M. Lee, A. Rafalski, E. Derose *et al.*, 2000 Global expression profiling of yeast treated with an inhibitor of amino acid biosynthesis, sulfometuron methyl. Physiol Genomics **3:** 83-92.

Kafer, E., 1977 Meiotic and mitotic recombination in Aspergillus and its chromosomal aberrations. Adv Genet **19:** 33-131.

Lee, I. H., S. I. Chang, K. Okada, H. Baba and H. Shiku, 1997 Transcription effect of nm23-M2/NDP kinase on c-myc oncogene. Mol Cells **7:** 589-593.

Leung, S. M., and L. E. Hightower, 1997 A 16-kDa protein functions as a new regulatory protein for Hsc70 molecular chaperone and is identified as a member of the Nm23/nucleoside diphosphate kinase family. J Biol Chem **272:** 2607-2614.

Levit, M. N., B. M. Abramczyk, J. B. Stock and E. H. Postel, 2002 Interactions between *Escherichia coli* nucleoside-diphosphate kinase and DNA. J Biol Chem **277:** 5163-5167.

Mager, W. H., and A. J. De Kruijff, 1995 Stress-induced transcriptional activation. Microbiol Rev **59:** 506-531.

Marbach, I., R. Licht, H. Frohnmeyer and D. Engelberg, 2001 Gcn2 mediates Gcn4 activation in response to glucose stimulation or UV radiation not via GCN4 translation. J Biol Chem **276:** 16944-16951.

Martin-Yken, H., A. Dagkessamanskaia, P. De Groot, A. Ram, F. Klis *et al.*, 2001 *Saccharomyces cerevisiae* YCRO17c/CWH43 encodes a putative sensor/transporter protein upstream of the BCK2 branch of the PKC1-dependent cell wall integrity pathway. Yeast **18:** 827-840.

Matsumoto, T. K., A. J. Ellsmore, S. G. Cessna, P. S. Low, J. M. Pardo *et al.*, 2002 An osmotically induced cytosolic Ca2+ transient activates calcineurin signaling to mediate ion homeostasis and salt tolerance of *Saccharomyces cerevisiae*. J Biol Chem **277:** 33075-33080.

Mendoza, I., F. Rubio, A. Rodriguez-Navarro and J. M. Pardo, 1994 The protein phosphatase calcineurin is essential for NaCl tolerance of *Saccharomyces cerevisiae*. J Biol Chem **269:** 8792-8796.

Momany, M., E. A. Richardson, C. VanSickle and G. Jedd, 2002 Mapping Woronin body position in *Aspergillus nidulans*. Mycologia.

Momany, M., P. J. Westfall and G. Abramowsky, 1999 *Aspergillus nidulans swo* mutants show defects in polarity establishment, polarity maintenance and hyphal morphogenesis. Genetics **151:** 557-567.

Nakamura, T., Y. Liu, D. Hirata, H. Namba, S. Harada *et al.*, 1993 Protein phosphatase type 2B (calcineurin)-mediated, FK506-sensitive regulation of intracellular ions in yeast is an important determinant for adaptation to high salt stress conditions. Embo J **12:** 4063-4071.

Natarajan, K., M. R. Meyer, B. M. Jackson, D. Slade, C. Roberts *et al.*, 2001 Transcriptional profiling shows that Gcn4p is a master regulator of gene expression during amino acid starvation in yeast. Mol Cell Biol **21:** 4347-4368.

Nickerson, J. A., and W. W. Wells, 1984 The microtubule-associated nucleoside diphosphate kinase. J Biol Chem **259:** 11297-11304.

Ogura, Y., Y. Yoshida, N. Yabe and K. Hasunuma, 2001 A point mutation in nucleoside diphosphate kinase results in a deficient light response for perithecial polarity in *Neurospora crassa*. J Biol Chem **276:** 21228-21234.

Ohkura, N., M. Kishi, T. Tsukada and K. Yamaguchi, 2001 Menin, a gene product responsible for multiple endocrine neoplasia type 1, interacts with the putative tumor metastasis suppressor nm23. Biochem Biophys Res Commun **282:** 1206-1210.

Orlov, N., T. G. Orlova, Y. K. Reshetnyak, E. A. Burstein and N. Kimura, 1997 Interaction of recombinant rat nucleoside diphosphate kinase alpha with bleached bovine retinal rod outer segment membranes: a possible mode of pH and salt effects. Biochem Mol Biol Int **41:** 189-198.

Orlov, N. Y., and N. Kimura, 1998 Interaction of nucleoside diphosphate kinase with membranes of bleached bovine retinal rod outer segments. Effects of pH, salts, and guanine nucleotides. Biochemistry (Mosc) **63:** 171-179.

Otsuki, Y., M. Tanaka, S. Yoshii, N. Kawazoe, K. Nakaya *et al.*, 2001 Tumor metastasis suppressor nm23H1 regulates Rac1 GTPase by interaction with Tiam1. Proc Natl Acad Sci U S A **98:** 4385-4390.

Pascual-Ahuir, A., R. Serrano and M. Proft, 2001 The Sko1p repressor and Gcn4p activator antagonistically modulate stress-regulated transcription in Saccharomyces cerevisiae. Mol Cell Biol **21:** 16-25.

Posas, F., J. R. Chambers, J. A. Heyman, J. P. Hoeffler, E. de Nadal *et al.*, 2000 The transcriptional response of yeast to saline stress. J Biol Chem **275:** 17249-17255.

Postel, E. H., 1999 Cleavage of DNA by human NM23-H2/nucleoside diphosphate kinase involves formation of a covalent protein-DNA complex. J Biol Chem **274:** 22821-22829.

Postel, E. H., B. A. Abramczyk, S. K. Gursky and Y. Xu, 2002 Structure-based mutational and functional analysis identify human NM23-H2 as a multifunctional enzyme. Biochemistry **41:** 6330-6337.

Postel, E. H., S. J. Berberich, J. W. Rooney and D. M. Kaetzel, 2000 Human NM23/nucleoside diphosphate kinase regulates gene expression through DNA binding to nuclease-hypersensitive transcriptional elements. J Bioenerg Biomembr **32:** 277-284.

Quail, P. H., 2000 Phytochrome-interacting factors. Semin Cell Dev Biol **11:** 457-466.

Reymond, A., S. Volorio, G. Merla, M. Al-Maghtheh, O. Zuffardi *et al.*, 1999 Evidence for interaction between human PRUNE and nm23-H1 NDPKinase. Oncogene **18:** 7244-7252.

Richard, M., S. Ibata-Ombetta, F. Dromer, F. Bordon-Pallier, T. Jouault *et al.*, 2002 Complete glycosylphosphatidylinositol anchors are required in *Candida albicans* for full morphogenesis, virulence and resistance to macrophages. Mol Microbiol **44:** 841-853.

Rodriguez-Pena, J. M., V. J. Cid, J. Arroyo and C. Nombela, 2000 A novel family of cell wall-related proteins regulated differently during the yeast life cycle. Mol Cell Biol **20:** 3245-3255.

Roymans, D., R. Willems, D. R. Van Blockstaele and H. Slegers, 2002 Nucleoside diphosphate kinase (NDPK/NM23) and the waltz with multiple partners: possible consequences in tumor metastasis. Clin Exp Metastasis **19:** 465-476.

Roymans, D., R. Willems, K. Vissenberg, C. De Jonghe, B. Grobben *et al.*, 2000 Nucleoside diphosphate kinase beta (Nm23-R1/NDPKbeta) is associated with intermediate filaments and becomes upregulated upon cAMP-induced differentiation of rat C6 glioma. Exp Cell Res **261:** 127-138.

Santos, B., and M. Snyder, 2000 Sbe2p and sbe22p, two homologous Golgi proteins involved in yeast cell wall formation. Mol Biol Cell **11:** 435-452.

Schurch, A., J. Miozzari and R. Hutter, 1974 Regulation of tryptophan biosynthesis in *Saccharomyces cerevisiae*: mode of action of 5-methyl-tryptophan and 5-methyl-tryptophan-sensitive mutants. J Bacteriol **117:** 1131-1140.

Serre, V., H. Guy, B. Penverne, M. Lux, A. Rotgeri *et al.*, 1999 Half of *Saccharomyces cerevisiae* carbamoyl phosphate synthetase produces and channels carbamoyl phosphate to the fused aspartate transcarbamoylase domain. J Biol Chem **274:** 23794-23801.

Song, E. J., Y. S. Kim, J. Y. Chung, E. Kim, S. K. Chae *et al.*, 2000 Oxidative modification of nucleoside diphosphate kinase and its identification by matrix-assisted laser desorption/ionization time-of-flight mass spectrometry. Biochemistry **39:** 10090-10097.

Talloczy, Z., W. Jiang, H. W. t. Virgin, D. A. Leib, D. Scheuner *et al.*, 2002 Regulation of starvation- and virus-induced autophagy by the eIF2alpha kinase signaling pathway. Proc Natl Acad Sci U S A **99:** 190-195.

Tanaka, N., M. Konomi, M. Osumi and K. Takegawa, 2001 Characterization of a *Schizosaccharomyces* pombe mutant deficient in UDP-galactose transport activity. Yeast **18:** 903-914.

Tanaka, N., T. Ogura, T. Noguchi, H. Hirano, N. Yabe *et al.*, 1998 Phytochrome-mediated light signals are transduced to nucleoside diphosphate kinase in *Pisum sativum* L. cv. Alaska. J Photochem Photobiol B **45:** 113-121.

Thines, E., R. W. Weber and N. J. Talbot, 2000 MAP kinase and protein kinase A-dependent mobilization of triacylglycerol and glycogen during appressorium turgor generation by *Magnaporthe grisea*. Plant Cell **12:** 1703-1718.

Tsuchiya, K. S., T. Kanbe, M. Hori, Y. Uehara, Y. Takahashi *et al.*, 1993 Distinct effects of clinically used anthracycline antibiotics on ras oncogene-expressed cells. Biol Pharm Bull **16:** 908-911.

Weber, R. W. S., D. Pitt and J. Webster, 1998 Teaching techniques for mycology. 3. Amylase secretion by *Aspergillus oryzae*. Mycologist **12:** 8-9.

Wolfner, M., D. Yep, F. Messenguy and G. R. Fink, 1975 Integration of amino acid biosynthesis into the cell cycle of *Saccharomyces cerevisiae*. J Mol Biol **96:** 273-290.

Zaborina, O., N. Misra, J. Kostal, S. Kamath, V. Kapatral *et al.*, 1999 P2Z-Independent and P2Z receptor-mediated macrophage killing by *Pseudomonas aeruginosa* isolated from cystic fibrosis patients. Infect Immun **67:** 5231-5242.

Zhang, D., and K. Chang, 1995 The regulatory effect of nucleoside diphosphate kinase on G-protein and G-protein mediated phospholipase C. Chin Med Sci J **10:** 25-29.

Zhang, D., J. G. Li, C. Chen and L. Y. Liu-Chen, 1999 Nucleoside diphosphate kinase associated with membranes modulates mu-opioid receptor-mediated [35S]GTPgammaS binding and agonist binding to mu-opioid receptor. Eur J Pharmacol **377:** 223-231.

Zimmermann, S., A. Baumann, K. Jaekel, I. Marbach, D. Engelberg *et al.*, 1999 UV-responsive genes of arabidopsis revealed by similarity to the Gcn4-mediated UV response in yeast. J Biol Chem **274:** 17017-17024.

CHAPTER 5

CONCLUSION

Polar growth is a separate process from nuclear division but is correlated with nuclear distribution in *A. nidulans*. In the work described here, we support the idea that nuclear division and polar growth are separate processes based on the continued nuclear replication in the isotropically growing *swoC1* mutant at restrictive temperature. The molecular markers that tag the sites of polarity establish are likely to be accumulated and dispersed during isotropic growth due to an endocytosis defect, which leads to multiple germ tube emergence upon temperature block release. We found that nuclear distribution or positioning is correlated with polar growth. In the *swoC1* mutant, even a slight delay in polarity establishment during early vegetative growth affects later compartmentation and conidiation caused by improper nuclear distribution, suggesting that these two processes are correlated. We also observed that clusters of branches are tightly coupled with cluster of nuclei in the branching mutant *ahbA* (unpublished observation), suggesting that nuclear distribution may affect new tip growth initiation (polarity establishment). Also it has been shown that a nuclear migration defect can cause isotropic growth in *A. nidulans* (Chiu *et al.* 1997). In yeast, worms, plants and mammals correct nuclear positioning is crucial for polarity establishment (Huang and Sheridan 1994; Huang and Sheridan 1996; Suzuki *et al.* 1999; Chang 2001; Tsou *et al.* 2002)

SwoCp has functions other than rRNA pseudouridine synthase activity. The *swoC* gene encodes the rRNA pseudouridine synthase and is essential in *A. nidulans*.

Based on the fact that we failed to detect any changes in ? levels or rRNA processing in the mutant, we think that the *swoC1* mutation might affect some other essential functions of SwoCp other than pseudouridine synthase activity. While the C-terminus is dispensable for growth, the conserved PUA RNA-binding domain upstream of the C-terminus where the *swoC1* mutation occurs seems important for this essential function. The V338F mutation may structurally disrupt specificity or the ability of SwoCp to bind certain RNA or DNA substrates, while retaining the pseudouridine synthase enzyme activity. Yeast CBF5p has been shown to bind centromeres and human DKC1p can bind human telomerase RNA suggesting that this protein has the potential to bind strands of polynucleotides. It is likely that in *A. nidulans* SwoCp has a substrate other than box H/ACA snoRNA for rRNA pseudouridine synthesis and this substrate may be involved in nuclear positioning and act as a polarity establishment marker.

Nucleoside diphosphate kinase is essential for growth in *A. nidulans*. The *swoH* gene encodes the nucleoside diphosphate kinase in *A. nidulans* and the *swoH1* mutation caused reduced NDK activity in the mutant cells. Although reduced activity was also found in unicellular organisms with NDK deletions, these organisms appear phenotypically normal. Surprisingly, the *swoH1* mutant cells were swollen and lysed at restrictive temperature and SwoHp is essential in *A. nidulans*. We proposed that NDK might not be essential for unicellular organisms such as *S. cerevisiae, S. pombe, E. coli* and *P. aeruginosa*, but important for multicellular organisms such as plants, animals, filamentous fungi and even bacteria with a multicellular life style such as *M. xanthus*.

Nucleoside diphosphate kinase is involved in specific stress responses attenuation in *A. nidulans*. The phenotype of the *swoH1* mutant could result from

changes to SwoHp function other than the nucleoside diphosphate kinase activity. Results presented in chapter 4 suggest that NDK may be involved in specific stress response attenuation in *A. nidulans.* Failure to attenuate stress response at restrictive temperature in the *swoH1* mutant might lead to increased glycerol level, swollen hyphae and cell lysis. However, in conditions such as saline stress, where stress response need not relax, the *swoH1* mutant could be rescued.

Mutations in "Nonpolarity genes" can perturb polarity establishment and maintenance. Many different mutations have been reported to result in a nonpolar phenotype. In yeast, defects in a 60S ribosomal subunit protein QSR1 (Eisinger *et al.* 1997), a C53 subunit of RNA polymerase (Mann *et al.* 1992) and a ubiquitin ligase SCF (Patton *et al.* 2000), result in formation of large unbudded cells. In *A. nidulans*, defects in the alpha subunit of mitochondrial phenylalanyl--tRNA synthase and transcription factor IIF interacting component of the CTD phosphatase give two polarity-defective mutants, *podG* and *podH* (Osherov *et al.* 2000). Defects in protein modification also affect polarity establishment and maintenance (Shaw *et al.* 2002; Shaw and Momany 2002). This evidence suggests that polar growth requires coordination of multiple processes. In this dissertation we showed that a defect in nuclear distribution caused by *swoC1* mutation in rRNA pseudouridine synthase and a defect in stress response attenuation caused by *swoH1* mutation in nucleoside diphosphate kinase also lead to the swollen phenotype, suggesting that perturbation of one or more processes can perturb polarity establishment and maintenance. This may be especially appropriate in filamentous fungi since their growth is typically a polar tip growth and perturbation of growth in general may lead to a polar tip growth defect.

REFERENCES

Chang, F., 2001 Studies in fission yeast on mechanisms of cell division site placement. Cell Struct Funct **26:** 539-544.

Chiu, Y. H., X. Xiang, A. L. Dawe and N. R. Morris, 1997 Deletion of nudC, a nuclear migration gene of *Aspergillus nidulans*, causes morphological and cell wall abnormalities and is lethal. Mol Biol Cell **8:** 1735-1749.

Eisinger, D. P., F. A. Dick and B. L. Trumpower, 1997 Qsr1p, a 60S ribosomal subunit protein, is required for joining of 40S and 60S subunits. Mol Cell Biol **17:** 5136-5145.

Huang, B. Q., and W. F. Sheridan, 1994 Female Gametophyte Development in Maize: Microtubular Organization and Embryo Sac Polarity. Plant Cell **6:** 845-861.

Huang, B. Q., and W. F. Sheridan, 1996 Embryo Sac Development in the Maize indeterminate gametophyte1 Mutant: Abnormal Nuclear Behavior and Defective Microtubule Organization. Plant Cell **8:** 1391-1407.

Mann, C., J. Y. Micouin, N. Chiannilkulchai, I. Treich, J. M. Buhler *et al.*, 1992 RPC53 encodes a subunit of *Saccharomyces cerevisiae* RNA polymerase C (III) whose inactivation leads to a predominantly G1 arrest. Mol Cell Biol **12:** 4314-4326.

Osherov, N., J. Mathew and G. S. May, 2000 Polarity-defective mutants of *Aspergillus nidulans*. Fungal Genet Biol **31:** 181-188.

Patton, E. E., C. Peyraud, A. Rouillon, Y. Surdin-Kerjan, M. Tyers *et al.*, 2000 SCF(Met30)-mediated control of the transcriptional activator Met4 is required for the G(1)-S transition. Embo J **19:** 1613-1624.

Shaw, B. D., C. Momany and M. Momany, 2002 *Aspergillus nidulans swoF* encodes an N-myristoyl transferase. Eukaryot Cell **1:** 241-248.

Shaw, B. D., and M. Momany, 2002 *Aspergillus nidulans* polarity mutant *swoA* is complemented by protein O-mannosyltransferase *pmtA*. Fungal Genet Biol **37:** 263-270.

Suzuki, H., T. Azuma, H. Koyama and X. Yang, 1999 Development of cellular polarity of hamster embryos during compaction. Biol Reprod **61:** 521-526.

Tsou, M. F., A. Hayashi, L. R. DeBella, G. McGrath and L. S. Rose, 2002 LET-99 determines spindle position and is asymmetrically enriched in response to PAR polarity cues in *C. elegans* embryos. Development **129:** 4469-4481.